Design of robot systems with self-healing function utilizing melting-solidification phenomenon

溶融凝固現象を用いた自己修復機能を持つロボットシステムの設計に関する研究

February, 2023

Shota MIYAKE
三宅　章太

Design of robot systems with self-healing function utilizing melting-solidification phenomenon

溶融凝固現象を用いた自己修復機能を持つロボットシステムの設計に関する研究

February, 2023

Waseda University Graduate School of Creative Science and Engineering

Department of Modern Mechanical Engineering, Research on Intelligent Machines

Shota MIYAKE
三宅　章太

Abstract

The number of robots in operation around the world continues to increase, and this trend is expected to continue in the future as the population of people engaging in the robotics industry increases. Therefore, in order for robots to continue to expand their activities around the world, they must be able to operate without human involvement. The aim of this dissertation on self-healing robot systems has been to achieve robot systems that can continue to operate without human intervention, eliminating the need for periodic maintenance and other performance maintenance actions. Despite extensive research into self-healing materials and methods, few have been adapted to robots due to a lack of mechanical properties, although a lot of self-healing materials and methods have been studied. As a result, this dissertation proposes melting-solidification phenomena as a self-healing method capable of both strength and self-healing efficiency. In order to incorporate self-healing employing melting-solidification phenomena into the robot system, mechanical design requirements such as sealing the healing material inside the mechanism and using two types of materials to maintain the structure are proposed. Moreover, a linear-acting type transmission element and a rotating type transmission element are developed based on the proposed requirements for the transmission element that transmits the output of the actuator and an external force, and their self-healing performance is evaluated. Furthermore, this dissertation introduces these self-healing transmission elements into the robot joints and shows that the robot joints acquired self-healing performance in evaluation experiments.

Because the self-healing process requires actuation, a self-healing transmission element capable of transmitting linear motion is developed as a self-healing linear actuator unit. The healing material in this actuator unit is thermoplastic resin, which has a high viscosity during melting, but evaluation experiments show that the healing material must be sealed inside the mechanism using a thermal gradient to maintain a high self-healing efficiency. In addition, evaluation experiments are conducted by mounting the developed linear actuator unit on a single-joint, tendon-driven robot joint. As a result, it is confirmed that the self-healing transmission element prevents the wire from being broken because the thermoplastic resin breaks down when overloaded and that the broken robot joint can be self-healed. Therefore, it has been shown that the self-healing performance of a robot can be improved by equipping it with a self-healing linear motion transmission element.

The transmission elements capable of transmitting rotational motion are made of low-melting-point metal as the healing material. The healing material is completely sealed inside the mechanism, and induction heating is used to simplify the mechanism structure by allowing non-contact heating during the self-healing process. In the performance evaluation experiment, the self-healing efficiency of nearly 100% is maintained even after 30 self-healing cycles. For evaluation experiments, the newly developed rotatory self-healing transmission element is mounted on a motor-driven single-joint robot. As a result, it has been confirmed that when an overload occurs in the joint, the low-melting-point metal part of the transmission element breaks down, preventing damage to critical parts of the robot such as the motor and reduction gear. Furthermore, it has been confirmed that self-healing enables the broken robot joint to re-operate. Therefore, incorporating a self-healing transmission element into a robot improves its reliability.

The mechanical design theory of a self-healing robotic system using melting solidification phenomena is presented at the end of this dissertation by dividing the design requirements into structural and material properties based on the results of evaluation and demonstration experiments. According to the findings of this research, the structural design requirement is that the healing material can be sealed inside the mechanism, and the material property design requirement is that the healing material can re-form broken bonds between molecules or atoms via the melting-solidification phenomena and self-heal, and that the healing material can bond with the structural materials. Prospects include the realization of self-healing robot systems in combination with other self-healing methods and robot systems that can adapt to the operating environment and target tasks by focusing on the fact that the shape of parts can be freely changed due to the melting and solidification phenomena.

Contents

List of Figures

List of Tables

Symbol table

Symbol table

Symbol	Meaning
f_{S-H}	Self-healing efficiency
F_{S-H}	Tensile strength after self-healing
F_{virgin}	Tensile strength at first fracture
E	Young's modulus
F	Transmission force of linear transmission elements
A_t	Area in the tensile direction of a structural part coupled with a healing material
A_s	Area in the shear direction of a structural part coupled with a healing material
σ_{max}	Maximum tensile stress
τ_{max}	Maximum shear stress
T_{all}	Transmittable torque
T_{key}	Transmimission torque by keyway structures
T_f	Transmimission torque by friction
n	Number of keyway structures
r	Radius of shaft A of a rotary transmission element
A_{key}	Area of critical cross section of a keyway structure
A_f	Contact area of low melting point metal and shaft A of a rotary transmission element except keyway structures
P	Pressure generated between low melting point metal and shaft A of a rotary transmission element
μ'	Coefficient of kinetic friction
θ_b	Slip angle when keyway structures of a rotary transmission element is completely destroyed
Q	Amount of energy absorbed when a rotary transmission element shuts off torque

Chapter 1

Exordium

1.1 Research Background

As shown in Figure 1 [1], the number of robots working in society is increasing year by year. The number of operating robots in 2020 has tripled compared to 2010, and the trend of increasing operating robots around the world is expected to continue. However, current robots require periodic maintenance, and when robots are damaged, they need to be repaired by humans. Therefore, it can be said that human intervention is necessary for robots to continue their operation. In addition, human resources required to maintain robots as they become more widespread in the world will only increase in the future [2]. Many approaches to overcome this limitation have been investigated and can be divided into two main categories.

1. Multiple robot systems complement each other and become independent of humans.

2. Complete with a single stand-alone robot system and independent of humans.

The independence of a robot system from humans means reducing the need for repair and periodic maintenance, and ultimately, a robot system that can continue to operate in an unmanned environment can be said to be completely independent of humans. The major difference between the two categories is whether multiple robot systems are involved and independent of humans or whether a single robot system is independent of humans.

Research in which robots build robots [3] and research in which robots are modularized [4–6] are examples of the first type, in which various robot systems are involved

in a complementary manner and are independent of humans. Although humans are still involved in some tasks at present, robots are being produced by robots in several factories, and robots are becoming increasingly independent of humans [7]. In addition, modularization of robots can reduce the number of human maintenance tasks [4], which is synonymous with less human intervention. Finally, when all robots consist only of modules [5] and robot systems even removes and replaces the modules [6, 8], it can be said to be independent of humans. Other ideas include a system in which robots are repaired and maintained by dedicated robots that fix other robots, just as humans have doctors [9, 10]. The first approach is to make robot systems independent from humans by having multiple robot systems mutually complement each other.

Research on self-healing materials and robot systems [11, 12] falls into the second area of research that aims to establish independence from humans using only a single robot system. Self-healing means that when some damage occurs in the system and the system cannot operate, it repairs the damage by itself and restores the system to a state where it functions normally. If a material has a self-healing function, it can heal cracks and scratches that occur in the material so that robot systems are not affected [11]. In addition, if a robot system has a self-healing function, it restores its own functionality by repairing the cause of inoperability by itself [12]. When humans are not involved in this self-healing process, the robot system can be said to be independent of humans. The second approach is to attempt independence from humans through its own functions alone, without intervention from other robot systems, by combining self-healing capabilities.

Although the two approaches have been described as independent with respect to the methods by which robot systems become independent of humans, they can coexist. For example, self-healing capability can improve the module's ability to continue operating. By adding self-healing capabilities to non-modularized pieces, a system can also continue to operate for a long period of time without maintenance. As a result, the robot system requires less frequent maintenance and refurbishment of parts, reducing the frequency of human intervention. Alternatively, the number of robot systems that can be managed by a single maintenance-only robot system can be increased, allowing more robot systems to operate independently of humans. Thus, it can be said that the realization of robot systems that continue to operate independently of humans will require research on both systems in which multiple robot systems complement each other and systems that aim for independence on their own. Based on this background,

this dissertation focuses on the self-healing of robot systems.

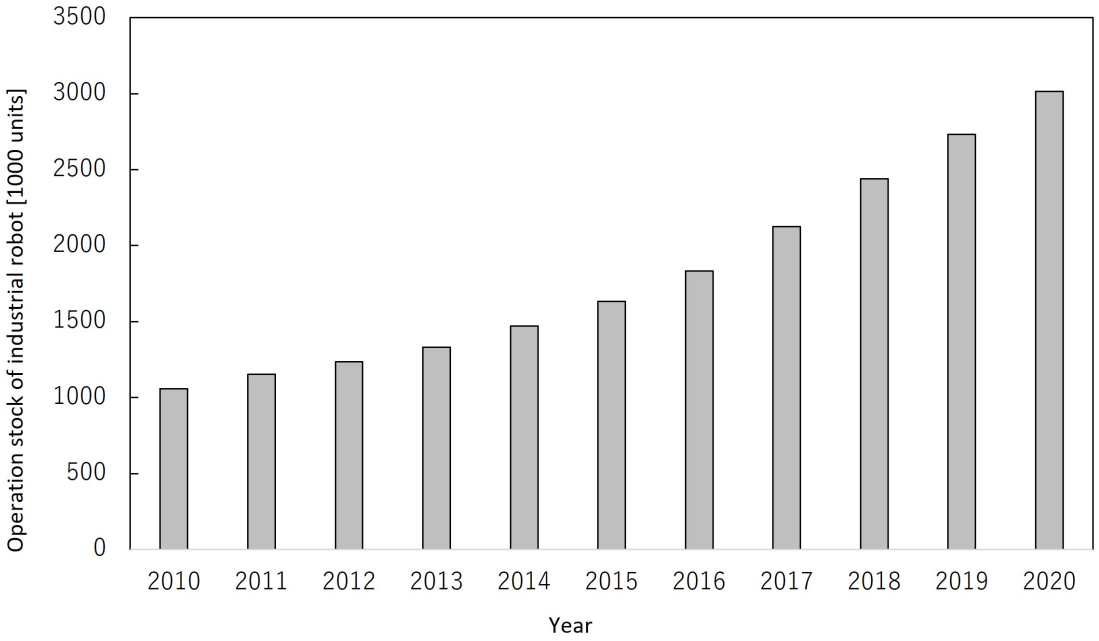

Figure 1.1 Total number of robots in operation worldwide [1]. The number of robots in operation around the world is increasing each year.

1.2 Related research

1.2.1 Self-healing methods of materials

Self-healing utilizing intermolecular forces

Self-healing using reversible reaction and intermolecular forces, such as hydrogen bonds and van der Waals forces, is one of the most studied methods of self-healing materials. In these methods, the chemical bonds are modified simply by bringing the cut surfaces into contact with each other, allowing for self-healing. Dingwei Zhao et la., at the Beijing Institute of Technology, for example, developed a self-healing gel with high-strength for a material mainly based on intermolecular forces, using the layered structure of PAMSA hydrogels produced by mixing polyacrylamide (PAM) hydrogel with sodium alginate (SA) solution. The stable cross-linked network by dynamic hydrogen bonds was produced by mixing PAM hydrogels with an aqueous SA solution, and the gels had high-strength and self-healing ability as materials mainly using intermolecular forces [13]. In addition, there was some research on self-healing films as a practical application of self-healing materials using hydrogen bonding [14, 15]. These

studies concluded that it was possible to make thin films transparent again by self-healing through the formation of hydrogen bonds, even if the films became cloudy due to cuts and scratches.

However, self-healing materials that use only intermolecular forces have limited mechanical properties. Therefore, research on self-healing gels forming other bonds in addition to hydrogen bonds has been actively conducted to improve the mechanical properties and self-healing performance. For example, hydrogels based on hydrogen bonding and dual metal-carboxylate coordination bonds have achieved both a self-healing rate of over 90% and high mechanical strength [16]. In addition, self-healing materials using hydrogen bonding and physical cross-linking induced by crystalline polymers have also been studied, and the polymer can withstand stresses of up to nearly 10 MPa has been developed, although the self-healing rate is about 40% [17]. Moreover, various researches on self-healing materials using intermolecular forces have been conducted [18–21].

Self-healing utilizing microstructures built-in the material

One of the approaches of healing strengths of materials is to construct microstructures in the materials [22]. In many methods, the microstructures are capillary structures, and one or two types of liquid self-healing agents are flowed into the capillaries. The principle is shown in Figure 1.2. When the capillary structures break down and healing agents inside the capillaries flow out, the healing agents mix and react with each other or with catalysts inside a material to self-heal the broken part. There are several methods for constructing capillary structures inside materials. For example, there are methods in which the shapes of capillaries are formed using a macro-nozzle like a 3D printer, the main material of the resin is hardened together with the formed structure, and the capillary structures are constructed by removing the resins that are initially formed [23], or in which capillary structures are formed by placing tubes in grooves dug in the material and sandwiching it with the other materials [24]. Another example is the study of self-healing materials by embedding tubes in the material to construct capillary structures and flowing healing agents through it [25, 26].

However, multiple cycles of self-healing cannot be achieved with these methods because the inside of the capillaries is solidified by the healing agents due to the previous fracture if the exact same location as previous fracture is occurred is fractured again.

Recently, research has been conducted on materials with a three-dimensional arrangement of capillary structures to complicate the supply path of healing agents [27, 28], and on materials with capillary structures with multiple suppling paths for self-healing materials [29, 30] in order to improve self-healing performance. In addition to the research discussed here, there has been research on self-healing using capillary structures, including research on membranes with self-healing performance [31], research on materials that self-heal even after a large hole is made [32], research on increasing the number of self-healing cycles by supplying healing agents into the capillaries by applying a load to the material [33], and research on adding self-healing performance to materials other than resin [34].

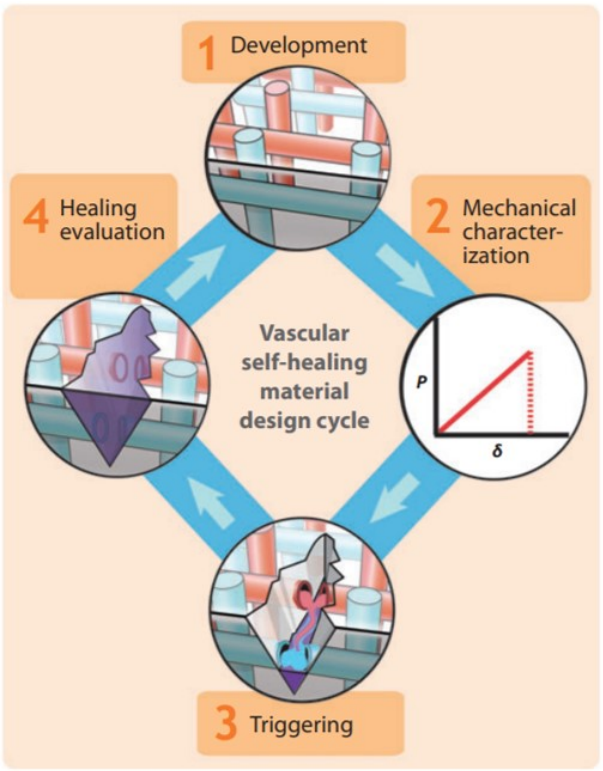

Figure 1.2 Principles of self-healing materials by capillary structure adapted from B. J. Blaiszik, et la., 2011 [11]. 1) A self-healing material including capillary structures; 2) Overload added to the material; 3) Failure of the material and outflow of the healing agent in the capillaries; 4) Self-healing by the healing agents.

Self-healing utilizing microstructures built-in the material

One method of adding a self-healing capability to materials is to place microcapsules in them. The principle is shown in Figure 1.3. The microcapsules contain liquid-type healing agents or microorganisms that produce healing agents, and when the

material breaks down, the microcapsules also break down and release the healing agents or microorganisms (Figure 1.3, (ii)), and the fractured part of the material is then self-healed by the released healing agents (Figure 1.3, (iii)). Research on self-healing materials using microcapsules can be divided into research on the generation method of microcapsules [35,36] and research on the evaluation of the self-healing performance of the material that has microcapsules inside [37,38].The research on self-healing materials itself is focused on here. The development of self-healing coating materials is one of the research area utilizing the characteristics of microcapsules [39, 40]. The diameter of the microcapsules is very small, approximately tens to hundreds of micrometers, allowing the self-healing material to be applied thinly to the surface of other materials, which cannot be done with other types of self-healing methods. In addition, research on self-healing by mixing microcapsules inside materials to self-heal cracks inside the material and the strength of the material itself has also been actively conducted. For example, there were research on materials that self-healing by the reaction between healing agents in microcapsules and catalysts in the material [41–43], materials that self-heal by placing microcapsules with multiple types of healing agents and by using the reaction of these different healing agents [44, 45], and self-healing concretes using microorganisms encapsulated in microcapsules that produce calcium carbonate [46,47]. Furthermore, there was also research on self-healing materials using microcapsules with multiple cores to improve the continuity of their self-healing ability [48].

Self-healing with added energy

This section focuses on methods for self-healing by adding energy. In comparison to other approaches, these methods can produce self-healing materials with relatively high strengths. However, unlike previous ways, these self-healing methods do not automatically self-heal in response to material failure, but instead self-heal by adding energy to the fractured area after the fracture. Electrical energy, light energy, and thermal energy make up the bulk of the energy load for self-healing.

The electric and magnetic fields generated by electricity are used when harnessing electrical energy for self-healing. For example, there were studies of self-healing using dielectrophoresis generated by a non-uniform electric field between electrodes [49, 50]. These studies were on the self-healing of flexible or stretchable electrical wiring, which enabled conductive self-healing by collecting metal particles near the broken wiring by

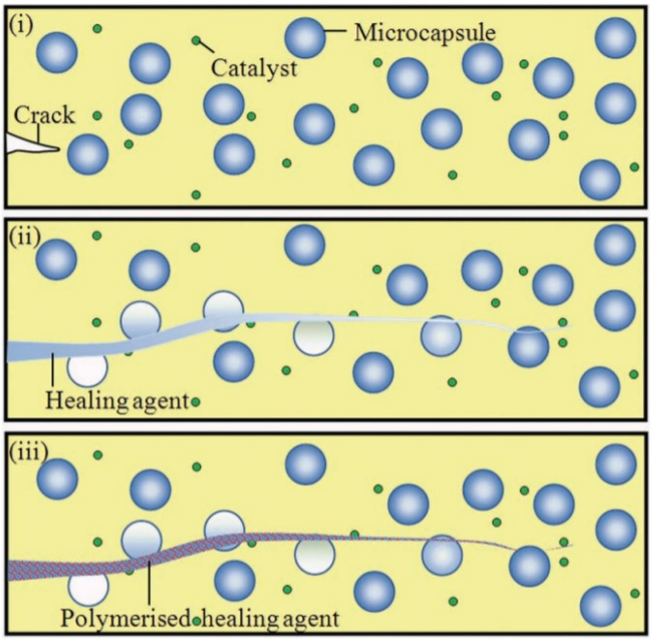

Figure 1.3 A principles of self-healing materials using microcapsules, adapted from Tim S. Coope, et la. 2011 [42]. (i) a crack beginning to appear in a material, (ii) a crack in the material propagates and destroys the microcapsules, causing the healing agents inside the capsules to flow out, (iii) Self-healing by the spilled healing agents.

dielectrophoresis. There was also research on the self-healing of strength by adding electrical energy [51, 52]. In these studies, an aqueous solution containing ions of a metal is placed around the metal to be self-healed, and electricity is applied to the metal and the aqueous solution to generate a metallic plating on the fractured surface for self-healing. This method is mainly used for self-healing of metallic materials and could heal up to 96% of the original strength [51].

UV light is used in the majority of self-healing treatments that use light energy. This is because of the enormous energy contained in UV light. By irradiating the material with UV light when the fracture surfaces are in contact with each other, the chemical reaction near the fracture surfaces is promoted, and self-healing occurs. In addition, most of the self-healing materials in this method are polymeric materials. For example, self-healing methods and materials that respond to UV light using coumarin [53], cinnamic acid [54], anthraquinone [55], thymine [56], disulfide bond material [57] have been studied. In addition, self-healing elastic materials of polyurethane with fracture strength of about 27 MPa was studied [58]. Furthermore, in combination with the aforementioned self-healing method of placing microcapsules in materials, research has been conducted on self-healing materials that are effective even in extreme

environments such as space environments [59, 60], and on concrete that self-heals by UV light or sunlight [61].

When thermal energy is used, the chemical reaction of the material is accelerated by adding energy while the fracture surfaces of the material are in contact, as when light energy is used. Among the polymers that self-heal using thermal energy, self-healing materials using the Diels-Alder reaction ofent have high strength [62, 63]. A number of materials have been studied for their self-healing performance by the Diels-Alder reaction upon heating. For example, Pengfei Du et al. of Shanghai Jiao Tong University synthesized a self-healing material that can recover 80% of its strength [64]. Other research on self-healing epoxy resins using the Diels-Alder reaction has enabled self-healing with even higher strength than the previously described methods, and the self-healing of fiber-reinforced resin materials have also been discussed [65]. Other methods of self-healing using thermal energy has also been used to self-heal metallic materials. For example, shape-memory alloys were placed in the metallic material to allow contact with the fracture surfaces even when large deformation occurs during fracture, and when the microcapsules containing the low-melting-point alloy placed inside the metallic material were heated in the destroyed state, the melting low-melting-point metal was released only around the destroyed surface, enabling the metallic material to self-heal [66, 67]. Moreover, many studies have been carried out on such things as 3D printer materials in the form of photolithography that combine both shape-memory and thermal self-healing properties [68], and self-healing materials using heat generated from microwaves, IR light, electromagnetic radiation, and electricity, etc. [69–72].

1.2.2 Research on self-healing robot systems

Research on self-healing actuators and mechanisms is still limited. However, there are three kinds of studies, and these are introduced

Hydraulically amplified self-healing electrostatic (HASEL) actuator

The structure and operating principle of the HASEL actuator are shown in Figure 1.4, and the principle of self-healing is shown in Figure 1.5. The HASEL actuator consisted of electrodes, elastomeric shells, and liquid dielectrics. When several tens [kV] were applied to the electrodes (Figure 1.4a), the electrodes were attracted to each other

and the liquid dielectric between the electrodes was pushed out (Figure 1.4b). When the electrodes were completely attracted to each other, the thickness of the actuator itself increased (Figure 1.4c), and the actuator operated. However, the electrodes of the HASEL actuator approached each other in close proximity and were subjected to a high voltage, which caused a short circuit between the electrodes (Figure 1.5a). At this time, the elastomeric shell was broken, and the electrodes became conductive, but liquid dielectric flowed into the broken part (Figure 1.5b), which insulated the electrodes and restored the function of the actuator (Figure 1.5c). Research on robots using HASEL actuators have been also underway. Research on a gripper of HASEL actuators [73] and actuators with complex structures [74], on mimicking biological shapes [75], and on creating HASEL actuators and sensors using 3D printing technology [76] have been conducted until now.

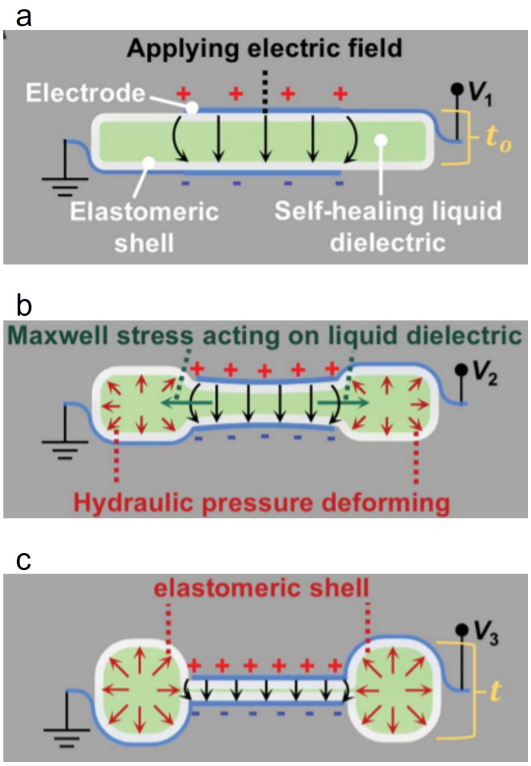

Figure 1.4 Structure and principle of operation of HASEL actuators adapted from E. Acome, et la, 2018 [1]. a) the state when no voltage is applied to the HASEL actuator; b) the state when voltage is added to the actuator and it starts to deform; and c) the state when the actuator is fully deformed.

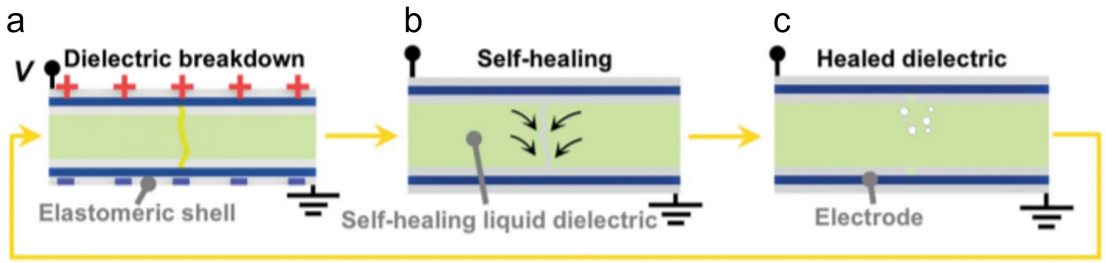

Figure 1.5 Self-healing principle of the HASEL actuator is adapted from E. Acome, et la., 2018 [1]. a) A short circuit occurs between the electrodes, destroying the elastomeric shell of the HASEL; b) Liquid dielectric flows into the destroyed area; and c) The liquid dielectric insulates the short-circuited area, causing the actuator to self-heal.

Self-healing for fluid leakage

One of the research on self-healing adapted to robot systems is to prevent fluid leakage by self-healing [77–79]. Leakage is defined as the release of internal fluid through holes that occur in the tire or in the fluid circulation path, and self-healing is defined as the automatic healing of the holes that caused the leakage. The principle of self-healing of tires is shown in Figure 1.6.a, and the principle of self-healing of liquid circuits is shown in Figure 1.6.b. Both are similar self-healing methods. The liquid installed in the tire or the circulating liquid in the circulation path seeped out through the hole formed in the tire or the circulation channel. These leakage liquids had the property of solidifying when they came into contact with air, thus plugging the holes that were the source of the leakage. As a result, fluid outflow could be prevented. Research on self-healing pump systems has also discussed robots that use these self-healing liquid circulation systems, and demonstrations of robots with built-in actuators that use liquid movement have been conducted.

Robots and mechanisms using self-healing materials based on the Diels-Alder reaction

Among self-healing materials, materials based on the Diels-Alder reaction have a high-strength. Therefore, there is research on robots and mechanisms using self-healing materials according to this principle [12, 80–83]. These materials using Diels-Alder reaction for self-healing are elastic. Hence, when the polymer was molded into a hollow structure and air was pumped into the interior, it expanded to enable actuation. The self-healing material itself could be used as the structures and actuators of the robot

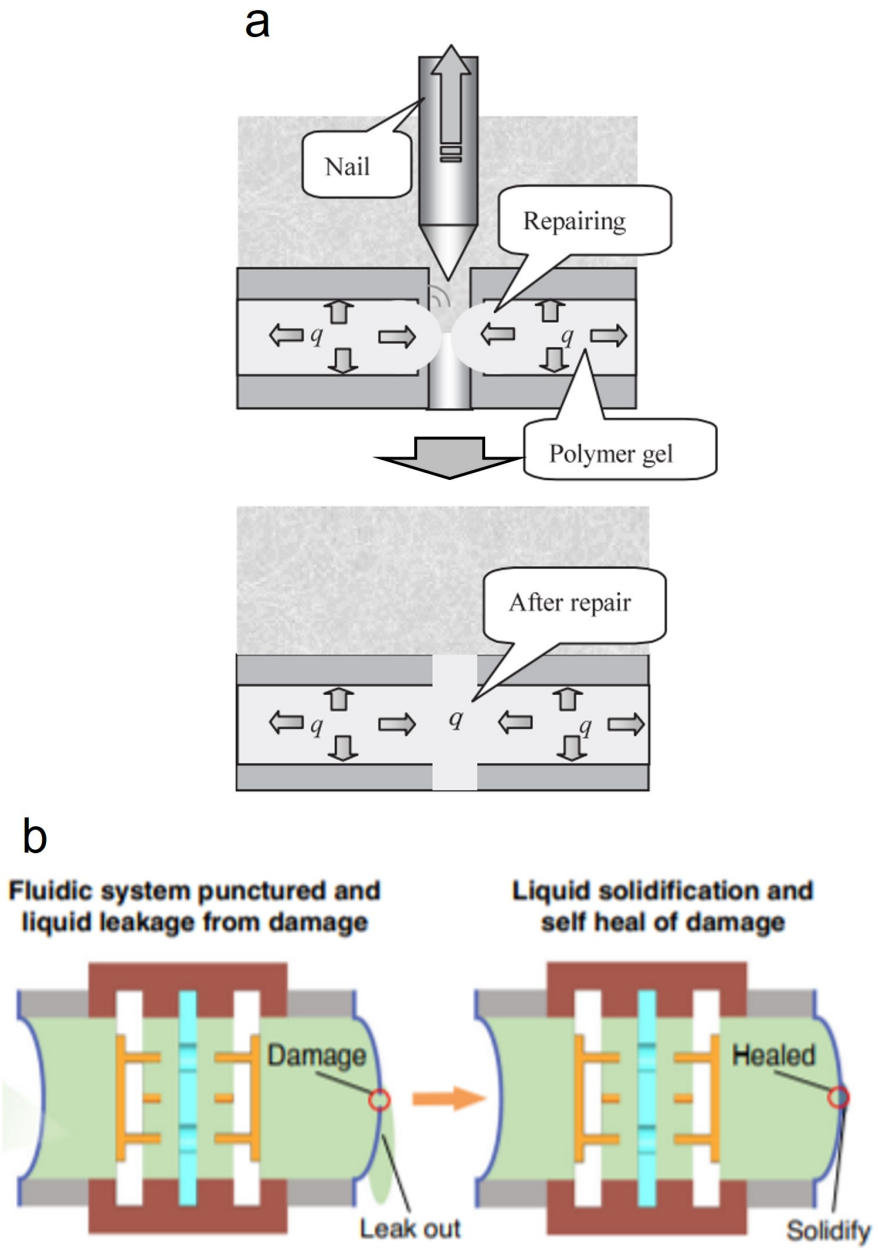

Figure 1.6 a) A principle of self-healing tires adapted from Kosuke Nagaya, et la., 2006 [77]. Polymer gel installed in the tire leaks out through the hole and seals the hole, which self-heals by solidification when the gel comes into contact with air. b) A principle of self-healing adapted from Wei Tang, et la, 2018 [79]. Circulating liquid leaks out of the holes in the circulation path and comes into contact with air and self-heal by solidification.

to add self-healing performance to the entire robot [12, 80]. In addition, there were several studies that made it possible to provide self-healing performance for some of the functions by placing self-healing materials inside the robot [81,82]. The mechanism was not equipped with heaters or other heating devices, and the surrounding air was heated to promote the chemical reaction that allowed the material to heal itself. Materials that can undergo the Diels-Alder reaction in a greenhouse have recently been developed, and research has been conducted on robots that can self-heal without the healing process [83].

1.3 Self-healing of materials and robot systems

There are various self-healing methods, as described in the related research section, and self-healing materials have the following two points in common.

1. The self-healing process reconstitutes the broken bonds between atoms or molecules and restores the fractured area.

2. During the self-healing process, the fracture surface is in contact with another fracture surface or healing material.

Self-healing of materials chemically reconnects broken bonds between atomic molecules. The self-healing processes by which bonds are reformed are varied and include self-healing by the addition of energy such as heat or electricity to a material to promote chemical reactions or phase changes [52, 62, 63], and self-healing by releasing healing agents contained in the material at the fracture site and causing chemical reactions when the healing agents contact other healing agents or catalysts to create new bonds in the fracture site [42, 43]. There are also self-healing materials in which the fracture part is healed by bonds different from those of the base material because the healing agents and those base materials are different [41, 84]. In any self-healing process, the chemical reactions required for self-healing occur when atoms and molecules collide with each other with sufficient energy. Therefore, for a material to self-heal, the fracture surface to be healed must be in contact with another fracture surface or healing agents. All self-healing materials are characterized by the fact that they eventually regain their strength by reforming the atomic and molecular bonds at the fracture site.

On the other hand, two things are common in self-healing methods for robot systems.

1. Self-healing by utilizing the properties of materials used in the system.

2. The structure of the robot systems is used for self-healing.

Self-healing robot systems utilize some material properties, but do not necessarily require re-formation at fracture sites. For example, the HASEL actuator self-heals its actuation function by utilizing the insulating nature of the operating oil inside the mechanism and a mechanism shape that allows the operating oil to flow into the broken parts [73]. Research on self-healing pumps has made it possible for the pumping function to self-heal by utilizing the property of the circulating liquid to solidify when exposed to air and the structural feature that the circulating liquid does not come into contact with air except at the point of breakage [79]. In this case, the circulating fluid can be regarded as healing agents and the air as a catalyst that promotes the chemical reaction. However, the self-healing principle of the pumping system is that healing agents are solidified by exposure to air through plug holes created in the circulation channel. This means that the mechanical properties of the system have not been healed. These self-healing robot systems that do not re-form bonds between atoms and molecules like self-healing materials, can functionally repair, but they do not restore the strength and durability of the destroyed area. The number of destructive locations in the robot system increases with the number of self-healings, and eventually the system becomes inoperable. On the other hand, there are robot systems that heal themselves by reconstructing bonds in the fracture site, similar to self-healing materials. Studies using self-healing materials based on the Diels-Alder reaction as actuators appear to rely solely on the properties of the material for self-healing [12]. However, if reversible reactions such as the Diels-Alder reaction are used for self-healing, adhesion can occur when materials remain in contact with each other and undergo a self-healing process [80, 85]. Therefore, the independently operating parts must be structurally non-contact, and the fracture surfaces to be self-healed must be structurally in contact with each other. Thus, whatever material properties are used, both material properties, such as self-healing performance and insulation, and structural properties of the system must be exploited in order to achieve self-healing robot systems.

1.4 Research Purpose

A lot of research on self-healing has been conducted and has recently gained momentum [86–90]. However, few have been applied to mechanical and robot systems. This is because the elemental components of a robot system require strength and rigidity that are difficult to achieve with conventional self-healing methods, or the self-healing process and conditions are special and difficult to incorporate into robot systems. In addition, previous studies on self-healing robot systems have focused on systems related to soft actuators or flexible robot system elements [12,73,79].In these studies, instead of providing the entire robot system with self-healing capability, only a couple of elements of the system are given self-healing capability to recover their functions and strength in the event of damage, thereby improving the ability of the system to continue to operate.

No previous studies have applied self-healing performance to the actuation of robot systems that require strength and rigidity because conventional self-healing methods are difficult to adapt due to a lack of mechanical properties. However, the operation continuity of robots can be greatly improved by adding self-healing capability to parts subjected to large loads. Robot systems can always collide with people or objects and be destroyed by unexpected overloads when operating in a complex environment, such as a human living environment, since a robot cannot avoid all collisions with objects or humans by its own sensing alone [91]. The self-healing robot systems that have been studied in the past have only added self-healing capability to some parts, and they cannot self-heal when an overload occurs and a part that requires strength is destroyed. In addition, many self-healing methods cannot fully recover the strength of the fracture after self-healing. Hence, a self-healing robot system cannot perform as well after self-healing as it did before the fracture. Furthermore, the self-healing soft actuator systems that have been studied are difficult to control precisely, have a small output, and have a small range of adaptability. On the other hand, self-healing performance can be provided to structural components and actuation parts for which self-healing has not been applicable at present by establishing a high-strength self-healing method. This means that self-healing performance can be added to high-power robots such as industrial robots, leading to an expansion of the range of self-healing application.

Therefore, this dissertation has the following three objectives.

1. Proposal of high-strength self-healing method applicable to robot systems.

2. Development of self-healing robots using the proposed method.

3. Proposal of uniform requirements for the design of robot systems that can self-heal by the proposed method.

Conventional self-healing methods lack mechanical properties in terms of stiffness and strength, and some self-healing processes are difficult to adapt to robot systems. Hence, a self-healing method that is adapted to the robot system while referring to the research on conventional self-healing methods is proposed. This proposal discusses methods with high-strength and high rate of recovery of strength after self-healing by considering the self-healing performance of materials and robot systems and self-healing methods that are easy to adapt to robot systems. Furthermore, two self-healing mechanisms that can be adapted to linear motion and rotational motion, respectively are proposed, since many robot systems operate in both directions. The self-healing performance of the proposed method is evaluated by focusing on three factors: self-healing efficiency, self-healing time, and strength of the self-healing. Self-healing efficiency means the percentage of strength recovered after self-healing compared to before self-healing. Self-healing time means the time required for the self-healing process, and the strength of the self-healing process means the maximum tension of a linear motion mechanism or the maximum transmission torque of a rotational mechanism. After evaluating the performance of each mechanism, the proposed mechanism is mounted on a single-joint robot to evaluate the robot system's self-healing performance. The evaluations of the self-healing performance of robot systems verify that single-joint robot arms that are destroyed due an overload and rendered inoperable can self-heal and operate again. Furthermore, this dissertation finally summarizes the unified requirements for the design of self-healing robot systems based on the self-healing evaluation experiments.

1.5 Paper organization

Chapter 2 proposes self-healing robot systems that can self-heal actuation parts by adding self-healing performance to the transmission elements. In addition, the melting-solidification phenomenon is proposed as a self-healing method with high-strength and

high self-healing efficiency for self-healing transmission elements. Designs for transmission elements with self-healing using melting-solidification phenomena are also presented at the end of this chapter.

Chapter 3 summarizes research on the development of a linear motion mechanism equipped with a transmission mechanism that can self-heal using the melting-solidification phenomenon of thermoplastic resin. Details of the mechanical design of using thermoplastics for self-healing are described. The method to achieve a higher self-healing efficiency by simulating the temperature change of the self-healing transmission element where the resin is placed is discussed. After that, the self-healing efficiency and the strength of the self-healing mechanism are investigated to evaluate the self-healing performance.

Chapter 4 summarizes the research on the adaptation of the linear motion mechanism developed in Chapter 3 to a robot joint. This chapter shows that the use of the melting-solidification phenomenon of the resin gives the robot self-healing capability and that a joint that becomes inoperable due to overload can be made to operate again.

Chapter 5 summarizes research on self-healing torque transmission mechanisms using the melting-solidification phenomenon in low-melting-point metals developed as a rotary self-healing transmission element. The principle and mechanism of using low-melting-point metals for self-healing are described, followed by a discussion of the theoretical transmission torque of the mechanism. After that, the self-healing efficiency and strength are investigated to evaluate the self-healing performance and torque transmission capability.

Chapter 6 summarizes the research on adapting the torque transmission mechanism developed in Chapter 5 to a robot joint. A method of incorporating a self-healing torque transmission mechanism using the melting-solidification phenomenon of low-melting-point metals into a robotic joint is shown. The joint that have become inoperable by overload are confirmed to be able to re-operate through self-healing process at the end of this chapter.

Chapter 7 summarizes results obtained in this dissertation, unified requirements for the design of robot systems that can self-heal using the phenomena of melting and solidification, and future works. Figure 2 shows the organization of this paper.

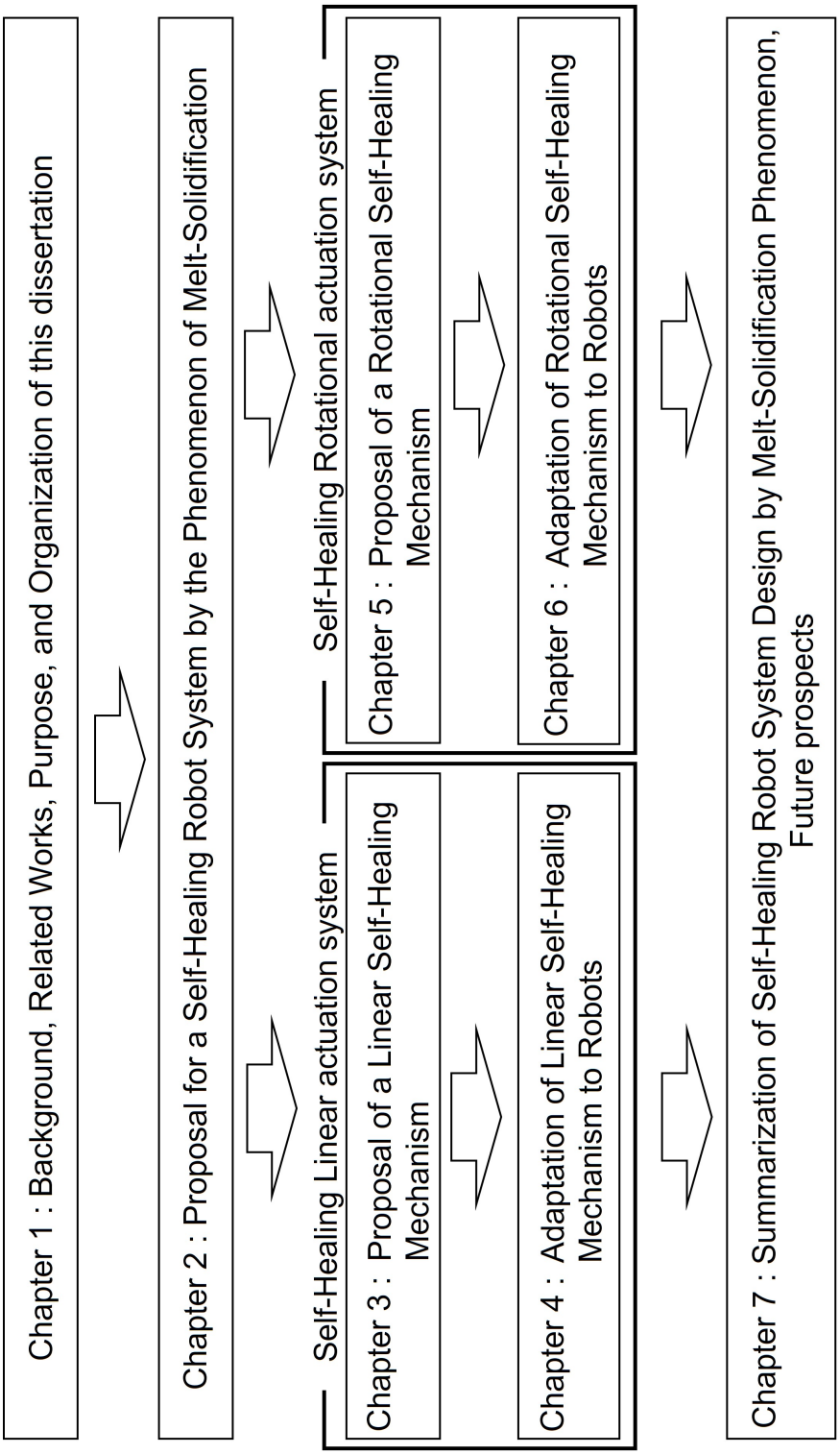

Figure 1.7 Paper organization

Chapter 2

Self-healing for robot systems

2.1 Self-healing robot systems in this dissertation

At first, the self-healing that this dissertation aims to achieve is discussed. Self-healing means that a system repairs damage by itself and restores the functions normally. Related research on self-healing robot systems uses both material and structural properties to restore functionality after a fracture renders them inoperable. According to related research, the system is self-healing if only the functional failure is healed and the function of the system is restored, even if the strength deterioration of some parts is not restored. Therefore, there is no need to recombine the broken bonds between atoms or molecules. However, this definition of self-healing means functional recovery and ignores the degradation of the mechanical properties of the robot system after the function is restored. Therefore, these self-healing robot systems that only restore function eventually fail due to the degradation of the mechanical properties of the structures. The final goal of a self-healing robot system is to continue to operate independently of humans, and functional recovery alone is not an essential solution to the problem. Hence, the damage to be healed by self-healing is not only functional damage but also strength damage to components, and both function and durability of the robot system should be restored after self-healing by restoring atomic or molecular bonds, as in self-healing materials.

This dissertation aims to create robot systems that can self-heal the broken bonds of atoms and molecules and the function of the robot, but it is difficult to provide all components of the robot system with self-healing functions. For example, motors have a complex structure and require material properties that cannot be achieved by conventional self-healing methods, and gears require machinability in addition to the

strength and rigidity of self-healing materials. Therefore, in order to build self-healing robot systems, this dissertation focused on the transmission element. This is because transmission elements have the role of transmitting many forces, such as transmitting the output from an actuator to a driving part or transmitting external loads to an actuator that is the end point for receiving forces. Hence, it is suitable for the transmission element to have the high strength self-healing function. In addition, in the event of an overload condition caused by high output or external forces, the transmission element breaks and interrupts the load, preventing losses to critical and non-self-healing components such as actuators. This performance is known to be obtained by placing a torque limiter or clutch between the actuator and output section [91]. Furthermore, the breakdown of the transmission element can be healed by the self-healing function, although the broken transmission element is not able to transmit the load and the robot system can't operate. In other words, the self-healing function of the transmission element allows the robot to re-operate without human intervention even after it has been destroyed and is inoperable. Moreover, because transmission elements are employed in many robots, it is easy to adapt a self-healing function to robot systems if self-healing performance can be added to only one transmission element. Thus, the aim of this dissertation is to make a self-healing robot system by adding self-healing capability to a transmission element.

In summary, the transmission elements with self-healing functions are used to provide self-healing performance to robots in this dissertation. Robots can self-heal because of self-healing capability of transmission elements that can recover the transmission function and the strength of the broken part, respectively, by self-healing after the transmission function is lost because of overload. This self-healing process aims to restore the broken atoms' or molecules' bonds, enabling the transmission of the same load as before the breakdown. The reason for providing self-healing performance to transmission elements is that they connect the actuation and output sections, and that most loads, such as robot output and external forces, are transmitted through the transmission element. Transmission elements with self-healing capability prevent the destruction of components that are fatal to the system because the transmission elements are broken preferentially and the destroyed transmission element can self-heal, allowing the system to re-operate independently of humans.

2.2 Comparison of self-healing transmission elements, clutchs and mechanical fuses

Clutches and mechanical fuses are conventional mechanisms used in robot systems to connect and disconnect transmission forces. These mechanisms and elements work similarly to self-healing transmission elements. Therefore, the possibility using self-healing to overcome problems with these conventional mechanisms are shown. Clutches can be classified into five types based on how they transmit force: Positive contact, friction, magnetic overrunning, and fluid coupling [92]. Positive contact, friction, and magnets are used to connect and disconnect power transmissions. Overrunning and fluid coupling are not compared here because they are both commonly used for one-way rotating transmissions and as torque converters. Positive contact refers to a claw clutch that uses mechanical coupling, is smaller than the clutches used by the friction and magnetic methods, and can achieve a larger transmission force. However, power disconnection and reconnection require a dedicated linear actuator, such as a solenoid or hydraulic pressure, which limits the miniaturization of the system as a whole. The necessity to detect overloads and actively cut power further complicates the control system. On the other hand, the friction and magnetic methods are more reliable as overload prevention devices than positive contact because slip occurs on its own if power transmission is not interrupted during overloading. However, when the transmission force grows, these methods tend to increase the size and complexity of the mechanism, making it difficult to achieve both a high transmission force and a small mechanism. Mechanical fuses are also categorized according to how they break: tensile [93], bending [94], and shear [95]. Because all mechanical fuses are designed to absorb energy due to fuse breakage when power is interrupted, they have the effect of interrupting overloads and reducing the damage generated by overloads to the structure around the fuse. However, each time an overload is prevented, the fuse components are damaged, resulting in the need to replace parts. In particular, robot structures tend to be complex, and fuse replacement maintenance can be a hassle for robots. Furthermore, designing the robot so that fuse components are exposed on the robot's surface to reduce maintenance effort may limit the robot's performance.

As described above, the conventional mechanism has the following problems: (1) it is complicated, (2) it is large, and (3) it requires part replacement at each fracture. However, a self-healing transmission element, like positive contact clutch, can transmit

force by the strength of the material itself, and the mechanical structure can be simplified because the element can use the bonding between atoms and molecules of the material as the transmitting force. Therefore, self-healing transmission elements can be smaller and have a greater transmitting force than clutches that rely on friction or magnetism for transmitting force. In addition, unlike a positive-contact clutch, self-healing transmission elements do not require an actuator to disconnect or reconnect the power because the power is disconnected by breaking the self-healing material and reconnected by self-healing. Hence, transmission elements smaller than conventional clutches can be achieved. Furthermore, energy absorption occurs due to the breakdown of self-healing materials, which can be expected to reduce damage to the surrounding structure in the same way that mechanical fuses do when power is interrupted, and the self-healing capability allows the system to continue to operate without the need for maintenance in the event of a fracture.

2.3 High-strength self-healing methods for robot systems

Many self-healing methods have been studied, but only a few of them are relevant to transmission elements. Internal capillary structures or microcapsules in self-healing materials offer better strength and stiffness than previous techniques [11, 37]. This is because the healing system breaks down the internal microstructure of the material and releases the healing agents in the fracture area, which requires a strong and hard foundation material. However, self-healing using the microstructure of the material makes it difficult to heal fractures in the same location because a single self-healing uses most of the healing agents around the fracture area. All the healing agents in the fracture zone is used in a single fracture in the case of self-healing materials that encapsulate microcapsules [37]. Self-healing via capillary structures seems to replenish the healing agents many times. However, throughout the self-healing process, the microstructure of the fracture zone is destroyed, and the self-healing performance for the same area is reduced. Some research has studied materials having microcapsules with multiple nuclei inside [48] or has studied the deformation of the material to fill healing agents [33] in order to increase the number of self-healing cycles, but the effect has been limited. Therefore, self-healing materials based on microstructures are unreliable because multiple self-healing cycles make the material fragile and impossible to self-

heal. Furthermore, materials with capillary structures cannot be processed, limiting the shapes of the parts [11].

On the other hand, self-healing methods that use the base material property of a reversible reaction without using microstructures can self-heal multiple times, but many of these methods are inferior in terms of mechanical properties such as strength and stiffness compared to self-healing methods that use microstructures [37]. However, some research is being conducted to increase the strength of self-healing materials. Table 2.1 summarizes the research of self-healing methods with a strength of 20 MPa or greater that re-form the bonds of the base material without using microstructures. For each self-healing material, this table lists the self-healing mechanism (S-H mechanism), fracture strength (Strength), strain at failure (Fracture Strain), Young's modulus (E), self-healing process (S-H process), self-healing efficiency (S-H efficiency), and the number of self-healing cycles performed in the paper (S-H cycle) for each self-healing material. Because some of these publications contain viscoelastic materials, young's modulus values are only summarized in the papers where they are mentioned. The self-healing efficiency is expressed by the following equation (2.1).

$$f_{S-H} = \frac{F_{S-H}}{F_{virgin}} \tag{2.1}$$

f_{S-H} is the self-healing efficiency, F_{versin} is the strength of the material before self-healing, and F_{S-H} is the strength after self-healing. When multiple cycles of self-healing experiments are conducted in a paper, the self-healing efficiency is referred to F_{S-H} at the time of the last self-healing cycle. Strength refers to F_{virgin}, and the S-H cycle is indicated when self-healing is performed two or more times. The materials listed in Table 2.1 have a wide range of properties, from 21 to 89 MPa in strength and 1.6 to 1600% in strain, and most of them are ductile materials. In addition, there is only one case in which the self-healing efficiency exceeded 90% and multiple cycles of self-healing were conducted [114], while the other research with a self-healing efficiency exceeding 90% only performed self-healing once. Furthermore, strength decreased with increasing self-healing cycles in most of the research in which multiple self-healing cycles were performed. However, the exceptions are found in some research [110, 112, 114]. What these studies have in common is that they are all self-healing using phase change, especially through the phenomena of melting and solidification. Sang-Hyub Lee, et la., at Chonbuk National University used disulfide and imine bonds for the self-healing mechanism of the material, and the bonding of the material was re-formed at 170°C,

well above the glass transition temperature of 50℃ of the proposed material, during the self-healing process [114]. Shen Yu, et la., at Nankai University did not describe the self-healing efficiency in the paper and Table 2.1 did not have the value of self-healing efficiency, but the self-healing efficiency in which the material was indicated completely melted and re-formed showed the self-healing efficiency of almost 100% of its strength [112]. Pengfei Du, et la., at Shanghai Jiao Tong University, conducted 5 self-healing cycles with a self-healing efficiency of 61%, but this was self-healing under conditions where melting-solidification phenomena were not used, and the strength of the material recovered before self-healing when the material was melted and re-formed. [110]. Thus, melting-solidification phenomena can be used to achieve both many self-healing cycles and high self-healing efficiency.

When the melting-solidification phenomenon is exploited for self-healing, thermal energy must be added to the self-healing material. This means that self-healing does not occur automatically, and that when self-healing using melting-solidification phenomena is applied to a robot system, it is necessary to recognize the destruction and undertake self-healing. Although this appears to be a defect in the self-healing system, the materials that have automatic self-healing functions, such as room temperature self-healing, will bond to each other if the self-healing materials remain in contact with each other for an extended period of time [85]. Therefore, unexpected points may become glued if the robot continues to maintain the same posture. However, the possibility of self-healing working in an unintended location is low when a self-healing process is executed after detecting a breakdown. Hence, the feature to specify the points of self-healing can be an advantage for systems such as articulated robots in which contact between mechanical elements inside the mechanism or contact with the outside change by the robot's posture.

Therefore, the self-healing mechanism applied to the transmission element in this dissertation is the melting-solidification phenomenon. The most important reason for this is that it is possible to achieve both a high self-healing efficiency and a high number of self-healing cycles. Because the transmission element can be destroyed several times by overwhelming or overloading, it is important to be able to perform multiple self-healing cycles in a stable manner. In addition, it is important to designate self-healing during the self-healing process.

Table 2.1 Summary of mechanical properties of self-healing materials above 20 MPa

S-H mechanism	Strenght [MPa]	Fracture strain [%]	E [MPa]	S-H process	S-H efficiency [%]	S-H cycle	ref
Hydrogen bonds	44	600	-	100 °C, 48 h	90	-	[96]
Hydrogen bonds Metal–ligand coordination	21	800	-	80 °C, 24 h	73	-	[97]
Hydrogen bonds Ionic interactions	27	800	-	RT, 48 h	92	-	[98]
Hydrogen bonds Disulfide bonds	20	550	112	90 °C, 24 h	94	-	[99]
Hydrogen bonds Disulfide bonds	25	1400	-	100 °C, 2 h	92	-	[100]
Hydrogen bonds Disulfide bonds	25	1600	56	70 °C, 24 h	85	-	[101]
Hydrogen bonds Diels–Alder chemistry	37	700	-	130 °C, 30 min 60 °C, 8 h	92	-	[102]
Diels–Alder chemistry	47	250	-	130 °C, 5 min 55 °C, 24h	65	3	[103]
Diels–Alder chemistry	32	190	-	130 °C, 10 min	88	-	[104]
Diels–Alder chemistry	89	-	2570	135 °C, 4.5 h 90 °C, 3 h 70 °C, 3 h	74	3	[105]
Diels–Alder chemistry	26	1100	-	100 °C, 5 d	46	-	[106]
Diels–Alder chemistry	21	1.6	1755	80 °C, 24 h 25 °C, 3 d	70	30	[80]
Diels–Alder chemistry	28	1600	290	HIFU, 60 min	92	-	[107]
Diels–Alder chemistry	23	1360	247	NIR, 60 s	96	-	[108]
Diels–Alder chemistry	26	1050	-	NIR, 90 s	98	-	[109]

Continue to the next page

Continuation of Table 2.1

S-H mechanism	Strenght [MPa]	Fracture strain [%]	E [MPa]	S-H process	S-H efficiency [%]	S-H cycle	ref
Diels–Alder chemistry	40	240	-	120 °C, 1.5 min 55 °C, 24 h	61	5	[110]
Diels–Alder chemistry	51	320	-	120 °C, 1.5 min 55 °C, 24h	76	2	[111]
Diels–Alder chemistry Phase change	50	300	230	180 °C, 10 min	-	-	[112]
Disulfide bonds Shape memory	26	630	9.7	70 °C, 1 h	98	-	[113]
Disulfide bonds Imine bonds	35	9.4	500	170 °C, 10 MPa, 30 min	95	5	[114]
Ionic interactions	48	860	93	RT	70	3	[115]
Oxime–carbamate	49	680	-	120 °C, 10 MPa, 30 min	70	4	[116]
C=C double bonds	27	890	2.26	UV, 40 min	71	-	[58]

When multiple lines are listed in S-H process, it indicates that multiple S-H processes are required.
RT: Room temperature
HIFU: High Intensity Focused Ultrasound
NIR: Near InfraRed light
UV: Ultraviolet

2.4 Mechanical Design for self-healing using melting-solidification phenomena

It is impossible to construct the entire mechanism out of healing materials because they melt throughout the self-healing process and do not maintain mechanism structure. Thus, a mechanism with a self-healing function that employs the melting-solidification phenomenon must be composed of healing materials for self-healing and structural materials to maintain the mechanism's structure, and the healing materials and structural materials need to be bonded. There are two methods to join healing materials and structural materials.

1. Utilize the atomic and molecular bonds that occur between healing materials and structural materials.

2. Utilize mechanical bonds that occur between healing materials and structural materials.

Utilizing atomic and molecular bonding means using chemical bonds, such as intermolecular forces that occur between materials. By using the melting-solidification process, self-healing can repair the fractured parts of the healing materials while simultaneously healing the atomic and molecular bonds between the healing materials and the structural materials. This method can also be used for metal-to-metal and resin-to-metal bonds [119], but it is not applicable to all materials because bonding may not occur depending on the material to be bonded. On the other hand, mechanical bonding is a method that utilizes mechanical coupling between parts, such as fastening with screws or transmitting torque with mechanical keyways. This method is expected to have high transmission forces because the strength of the material can be used as the force and can be adapted to a lot of materials. However, while utilizing this procedure, the healing material should be metal since the bond strength depends on the strength of the material [120].

The molten healing material is fluid during the self-healing process, even if the mechanism can be composed of structural and healing materials. Therefore, when the melting-solidification phenomenon is applied to robot systems, it is necessary to take measures to prevent molten healing material from flowing out of the mechanism. Here are two possible measures to prevent leakage.

1. Materials with high viscosity when melted are used as healing materials.

2. healing materials are structurally sealed inside the mechanism.

Outflow Measure 1: it is expected that using a material with high viscosity when melted prevents material from dripping due to gravity. Although the viscosity value varies depending on the material, if the viscosity is approximately $10^7\ Pa \cdot s$ or higher, the material does not drip under its own weight, thus preventing the healing material from spilling [117]. However, most thermoplastic resins become viscosity value below $10^7\ Pa \cdot s$ as temperature increases. In addition, the viscosity of the liquid metal is very small, ranging from 6.16×10^{-3} to 4.76×10^{-4} [118]. If the viscosity of the molten healing material is low, structural sealing (Outflow Measure 2) is necessary to maintain the self-healing efficiency.

2.5 Design for Self-healing Transmission element

The majority of robot systems are driven by two types of motion: linear motion and rotational motion. Therefore, design overviews of linear and rotary self-healing transmission elements are shown in Figure 2.1. The linear and rotatary transmission elements have one component made of healing material and two transmission partts made of structural material in common. The structural material's strength is higher than that of the healing material. In addition, common is that the healing material joins two structural materials. The two transmission parts are the transmission parts A and B shown in Figure 2.1. These transmission parts are assumed to be connected to an actuator or an output. The healing material bonds the two transmission parts in order to enable the transmission of force between the transmission parts, and the bond by the healing material is destroyed and the transmitting ability is lost in the event of overload. Self-healing repairs the ability of the two transmission portions to transfer force by repairing these fractures and reconnecting them.

2.5.1 Self-healing linear transmission element

Linear motion type "Fracture" in Figure 2.1 shows that the bond between the healing material and the transmission part B breaks down, separating the fracture surfaces. Even if the transmission performance is lost due to the failure of the healing material

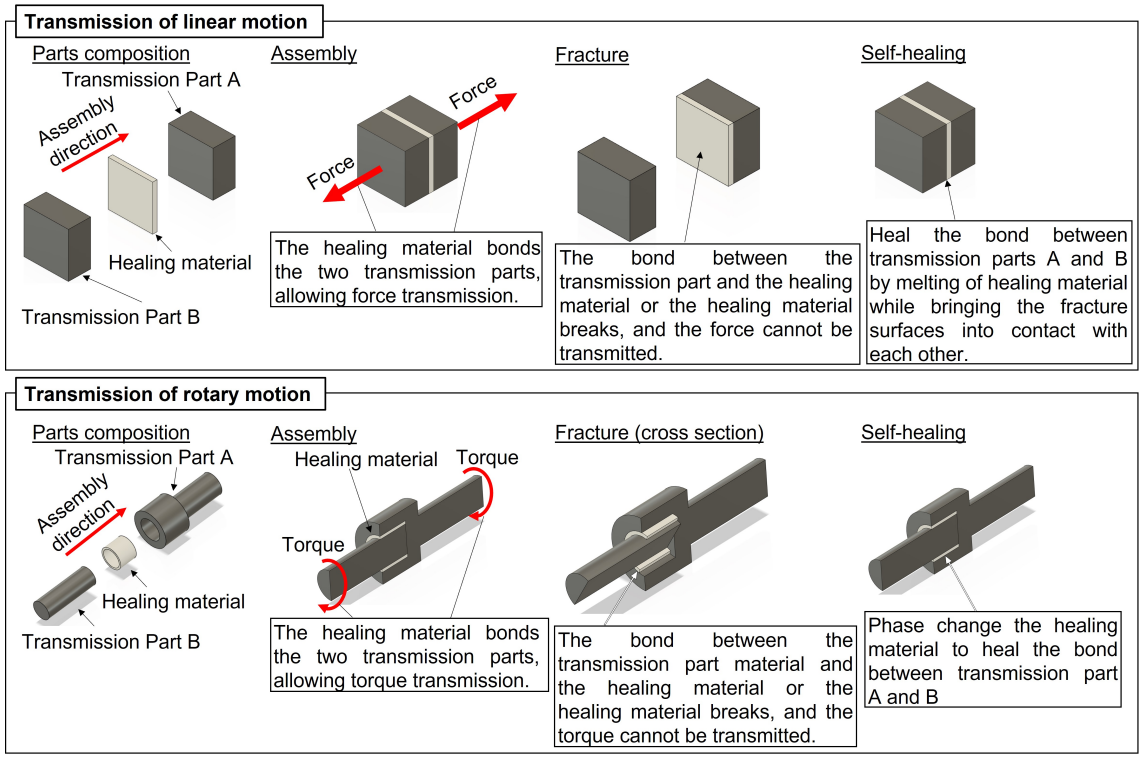

Figure 2.1 Overview of self-healing linear and rotary motion transmission elements.

rather than the bond between the healing material and the transmission parts, the failure surfaces are separated from each other in the linear type. The healing material loses its original shape due to plastic deformation caused by fracture of the healing material or breaking of the bond between the melted healing material and the transmission parts. Therefore, even if the mechanism has a sealed structure to prevent the healing material from leaking out, the seal function cannot be maintained due to the healing material after the fracture, and the material leaks out during the self-healing process. Hence, it is necessary to use a healing material made of resin that has a high viscosity when it melts and does not easily flow out during a self-healing process in a linear transmission element (Outflow Measure 1). In addition, when mechanical bonding is utilized to combine healing material and transmission parts, the clearance between the healing material and the transmission parts needs to be very small to eliminate play. Consequently, the deformation of the healing material during fracture prevents the spatial connection of the transmitting portions and healing material from being restored to its pre-fracture state. Hence, the linear self-healing mechanism does not use mechanical bonds but rather utilizes the atomic and molecular bonding that occurs between the healing material and the transmitting parts.

A heat source, such as a heater, can be used by the linear self-healing mechanism to provide thermal energy for the melting phenomenon during self-healing. The heat source can supply energy by wire since linear motion has a fixed range of movement. Therefore, the healing material melts and self-heals using a heat source installed in the structural material.

2.5.2 Self-healing rotary transmission element

The rotary motion type "Fracture" in Figure 2.1 shows that the bond between the healing material and the transmission parts B and A breaks down, but the fracture surfaces makes contact with each other. Furthermore, the positional relationship between the healing material and transmission parts A and B between before and after the fracture changes only in the torsional direction relative to the axis of the transmitted rotational motion. Therefore, the healing material can be sealed by using machine components, such as an oil seal that can be sealed against the spinning shaft (Outflow Measure 2). In addition, because the transmission parts are stronger than the healing material, they can remain sealed within the sealed structure even if the healing material plastically deformed during fracture. Hence, a sealing structure can prevent leakage of the healing material, which has low viscosity during the self-healing process, and a metal material with greater strength than resin can be used as the healing material. The availability of high-strength healing materials also makes it suitable for mechanically connecting the healing material to the transmission parts.

It is difficult to install a wire-powered heat source in the transmission part of rotary transmission elements, as is the case with linear motion type, in order to provide energy for self-healing. This is because the installation of a wired heat source on the transmission part limits the rotation of the self-healing transmission element. Power is delivered to the rotating shaft by several connectors, such as slip rings, but their use limits the amount of power supplied to the heat source and complicates the mechanism. Therefore, the healing material is heated by induction heating because it is a non-contact heating method that does not limit the number of rotations of the self-healing mechanism. In addition, induction heating can be used to directly heat the healing material since it is metal. Furthermore, induction heating requires only the installation of a coil around the periphery of the mechanism, simplifying its structure and enabling it to be reduced.

Chapter 3

Linear actuator with self-healing transmission element

3.1 Introduction

This chapter designed and tested a linear motion transmission element with self-healing capability based on the melting-solidification phenomenon. A linear self-healing mechanism requires that the fracture surfaces come into contact with each other before the self-healing process. When the transmission element includes an actuator only to bring the fracture surfaces into contact, the transmission element structure becomes more complex and larger. Therefore, the same actuator was used for the linear motion and actuation for contact with the fracture surface, resulting in the development of a small linear actuator unit. After that, the value of the transmission force, self-healing time, and self-healing efficiency of the linear self-healing transmission element were evaluated using the developed actuator unit.

3.2 Concept of self-healing using thermoplastic resin

Figure 3.1 shows the concept of thermoplastics' self-healing. Figure 3.1 A is the structural parts, C is the thermoplastic, and B is the boundary between A and C, respectively. When structural parts are subjected to a considerable load (Figure 3.1 STEP 1), the lowest strength point, such as B or C, will fail (Figure 3.1 STEP 2). After fracture, the fractured parts are reconnected by heating and melting the thermoplastic resin while contacting the fractured surfaces (Figure 3.1 STEP 3), and self-healing is completed (Figure 3.1 STEP 4).

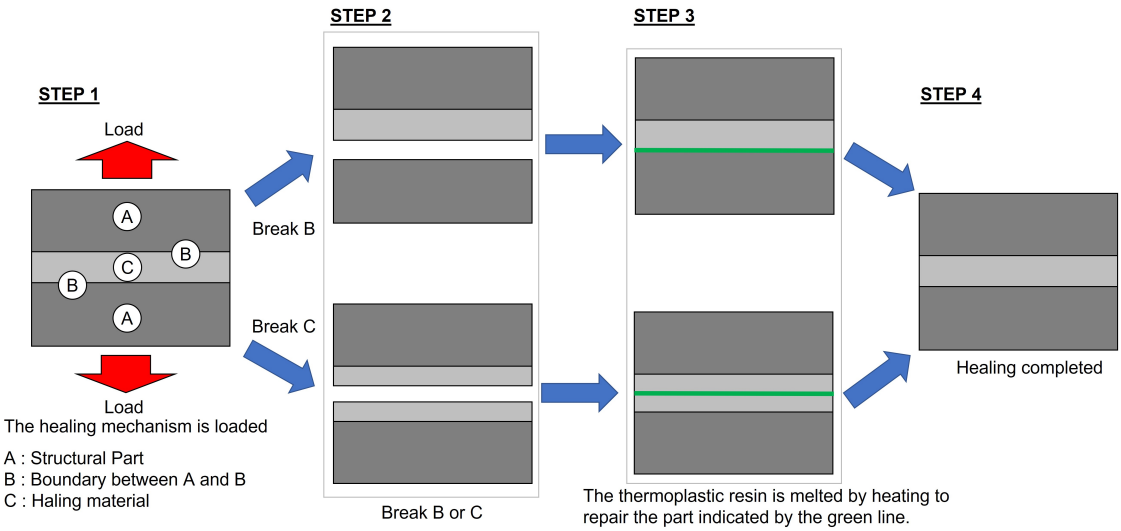

Figure 3.1 Conceptual diagram of self-healing using thermoplastic resin

3.3 Self-healing actuator unit

3.3.1 Structure of self-healing actuator unit

Figure 3.2 shows a schematic diagram of a linear actuator unit developed in this dissertation. The developed mechanism is about 211 mm × 31 mm × 35 mm. in size. The proposed mechanism is a linear actuator mechanism that connects in series a motor, a ball screw, and a self-healing linear transmission element. To stabilize the linear motion and prevent the ball screw from generating a moment, the linear transmission element is coupled to a linear guide. In addition, by using a ball screw as the motor's reduction gear, a large thrust force and high positioning accuracy are obtained for the linear motion mechanism. It is necessary to make contact between the fractured surfaces when they are self-healing. However, if actuators are installed in order just to contact the fractured surfaces, the mechanism becomes complicated and large. Therefore, a compact actuator unit is achieved by using a single actuator for performing linear motion and contacting the fracture surfaces.

The assembly diagram of the linear transmission element is shown in Figure 3.3. During the self-healing operation, structural parts bonded to the thermoplastic resin in the mechanism need to be heated to a high temperature in order to melt the thermoplastic resin. Therefore, a separating part with a heat-insulating effect is used between the structural part and the rest of the parts to prevent the entire mechanism from becoming hot and to efficiently use the thermal energy for melting the thermoplastic

resin. The thermoplastic resin is heated using a ceramic via a structural part. The heater is equipped with a thermocouple to control the temperature of the heater so that it does not exceed the specified value. To measure the load created in the actuator portion, a load cell is connected between the ball screw and the linear transmission element.

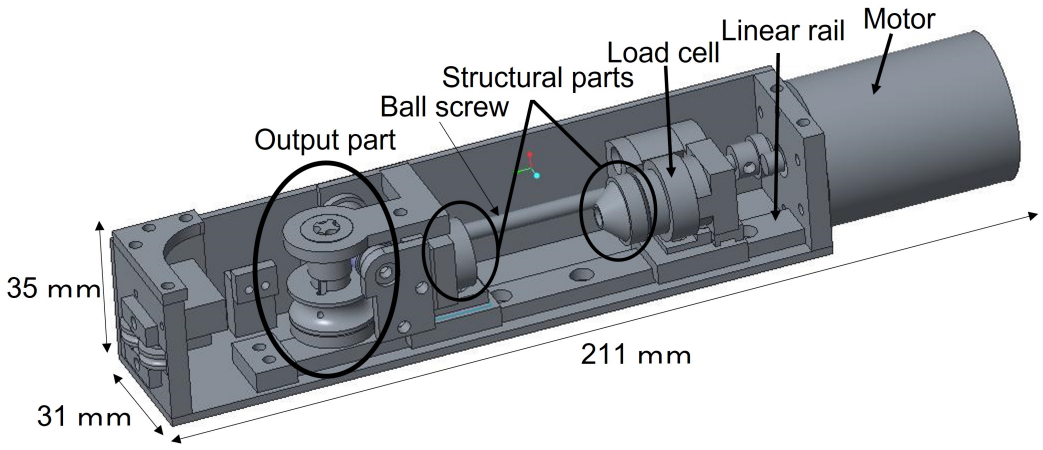

Figure 3.2 An overview diagram of the self-healing linear actuator unit. The mechanism is 35 x 31 x 211 mm in size. A motor and a ball screw are connected via gears in this actuator unit, and the ball screw is connected to the linear transmission element on the motor side. A thermoplastic resin connects the structural part on the motor side and the structural part on the output side.

3.3.2 Self-healing of linear actuator unit

The flow of the self-healing process from the state in which the proposed mechanism is working normally to the state in which it reoperates after breaking due to overload is described in three stages (Figure 3.4 states A to C). This section also explains the operation of the mechanism and the self-healing process in each stage.

Step A Self-healing actuator unit can operate normally (Figure 3.4A)

In state A, the thermoplastic resin joins the two structural parts (motor side and output side) into one. Therefore, the motor's power is transmitted to the output part via the ball screw and linear transmission element, enabling linear motion.

Step B Self-healing actuator unit is broken by overload (Figure 3.4B)

The linear transmission element receives the overload generated by the robot system. The linear transmission element's thermoplastic resin breaks down due to the transmitted overload, absorbing the impact load's energy. In addition, the

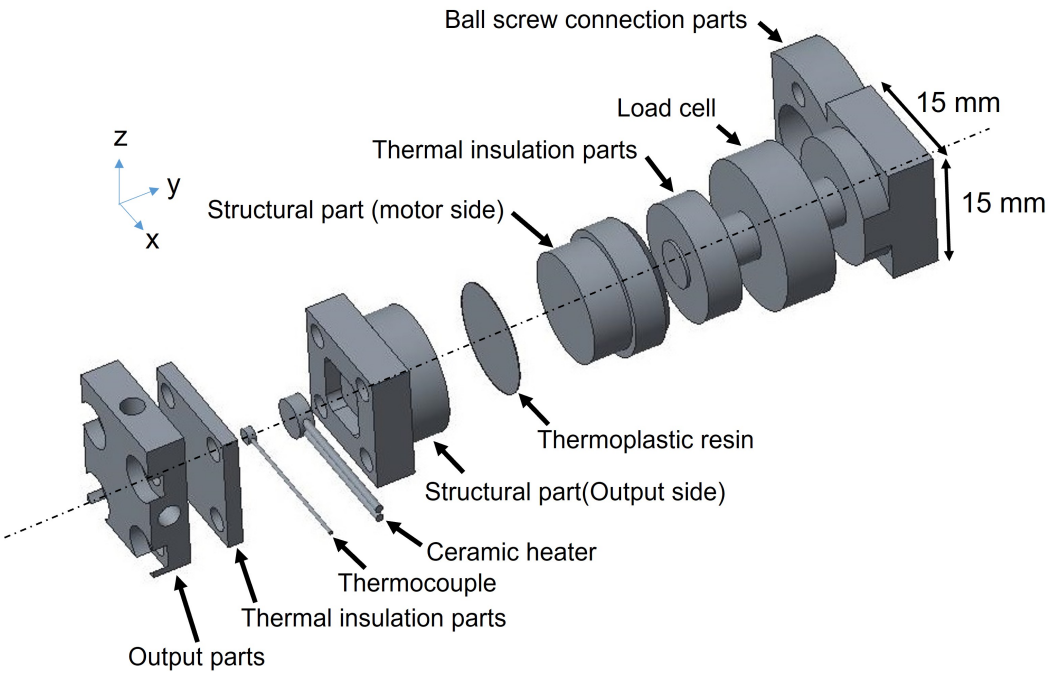

Figure 3.3 Assembly of a linear transmission element. A load cell is installed between a part that connects to a ball screw and a part that connects to the thermoplastic. Insulation material is inserted between the load cell and a structural part. Between a structural part on the other side and an output part, a heater and a thermocouple are incorporated. In addition, a heat insulator is inserted between the heater and the output part.

structural parts of the linear transmission element are physically separated into two parts to relieve the load on the actuator and mechanical elements other than the linear transmission element. In order to create a fracture at the thermoplastic bonding site, the resin's bonding strength is set to be smaller than that of the other points. The proposed mechanism is equipped with a load cell that detects the failure of the linear transmission element and starts the self-healing process.

Step C Self-heal of broken actuator unit (Figure 3.4C)

The fracture surfaces are first brought into contact with each other. Since the proposed mechanism's linear motion is constrained by the linear guide, the fractured surfaces can be positioned by simply touching them with the motor. After contacting the fractured surfaces, the linear transmission element is heated by a heater to melt the thermoplastic resin and heal the fracture. The heating is performed using the thermocouple feedback control of a ceramic cartridge heater. In addition, crimping the fractured surfaces together with a motor during heating enables the thermoplastic resin to contact the fractured surfaces evenly, thereby attempting to achieve a high self-healing efficiency. Because the self-healing ef-

ficiency varies depending on the time required to melt the resin, it is necessary to verify the appropriate heating time through experiments. After heating, the temperature of the thermoplastic decreases with time, and the bonds are reconstituted when the temperature drops below the softening point. The actuator unit returned to state A when the thermoplastic resin reached room temperature (25 °C).

3.4 Performance evaluation of the linear transmission element

3.4.1 Design and healing performance of structural parts

The design of structural parts and the self-healing process (heating time) are considered important for improving the following three criteria for the performance of the self-healing linear transmission element in this dissertation:

- Self-healing efficiency
- Required healing time (healing time)
- Fracture strength of thermoplastic resin bonds of the linear transmission element

There are two reasons why the self-healing efficiency of the linear transmission element using thermoplastic resin is not stable. As shown in Figure 3.5, one is insufficient heating of the thermoplastic resin during self-healing, and the other is overheating. The thermoplastic resin cannot be completely melted, and the bonding area between the resin and the structural parts becomes smaller than normal if the heating time is not sufficient. On the other hand, in the case of overheating, the thermoplastic resin remains in the liquid state longer during self-healing. This causes the resin to flow out of the linear transmission element, resulting in a shortage of the resin required for healing and defects in the thermoplastic portion of the healing mechanism. In both cases, the fracture strength is lower than the normal state, which directly leads to a decrease in the self-healing efficiency. Therefore, the heating time during self-healing and the shape of the structural parts are important to prevent the flow of thermoplastic resin.

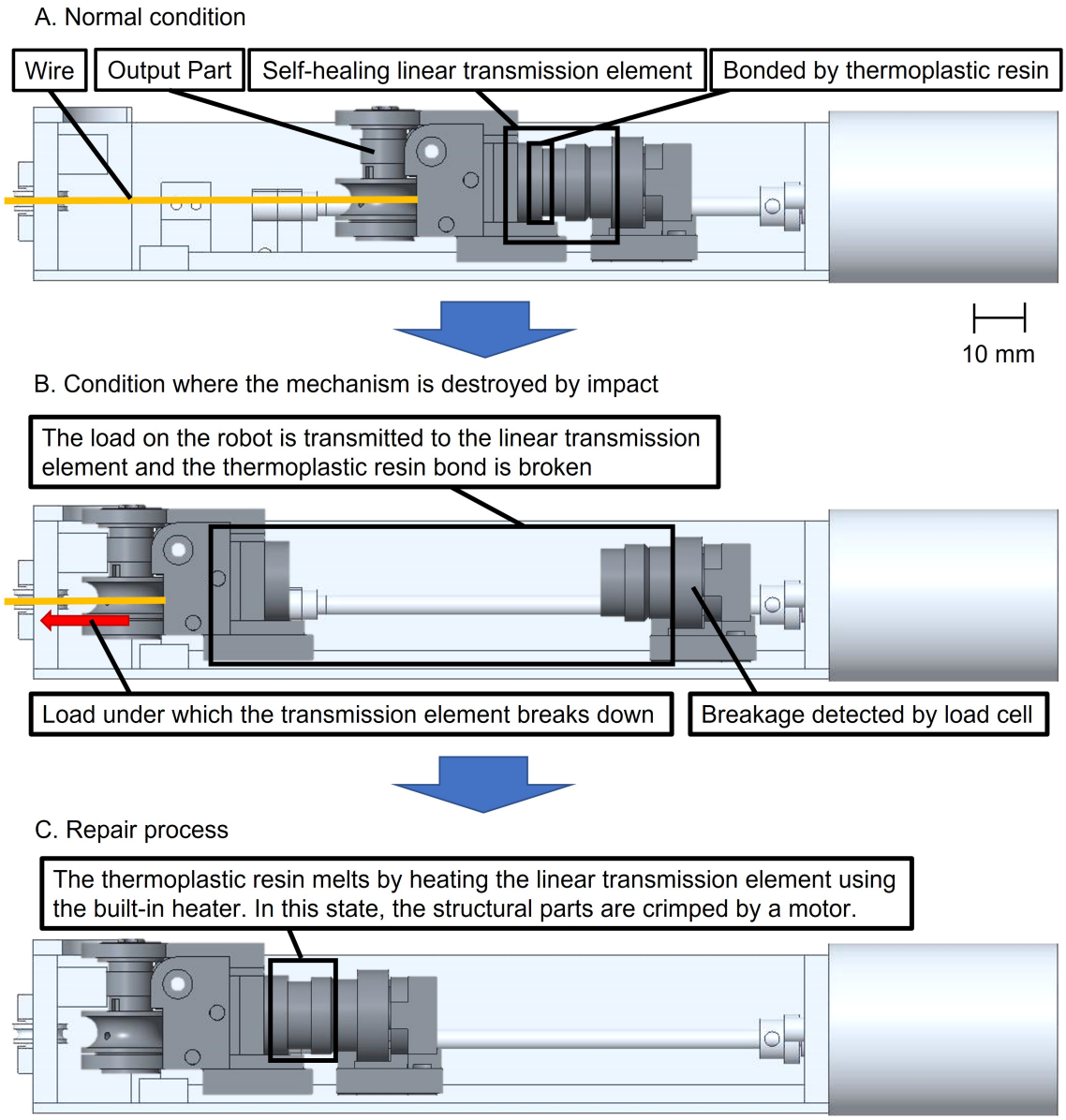

Figure 3.4 Self-healing procedure of the proposed mechanism. The towing of a wire is depicted in this illustration as an example of the use of the proposed mechanism. In state A, the thermoplastic resin binds the structural parts together so that the power of the motor can be transmitted to the output part to which the wires are connected. When a substantial load is applied to the output portions through wire, the thermoplastic bond breaks, reducing the load on the robot in state B. In state C, the fractured part is healed by heating and melting the thermoplastic resin, with the fractured surface crimped by a motor.

The healing time is the time required for all thermoplastics involved in the self-healing process to reach the softening point. When the proposed mechanism is mounted on a robot, the healing time is synonymous with the time required for the robot to resume normal operation. Therefore, the healing time should be as short as possible. The cause of the change in the healing time is considered to be the difference in the amount of heat transferred to the resin depending on the shape of the structural parts and the contact area between the structural parts and the thermoplastic resin. As a result, the healing time depends on the design of the structural parts.

It tends to be less strong than metal parts since the linear transmission element is bonded with thermoplastic resin. The small strength of the linear transmission element contribute to a reduction in the adaptive application range of the proposed mechanism because various robotic systems are composed of metal. Therefore, the strength of the linear transmission element should be as high as possible. The linear transmission element's fracture strength is considered to vary depending on the bonding area between the structural parts and the thermoplastic resin. Hence, structural parts are important in order to achieve a linear transmission element with higher strength.

This dissertation evaluates the aforementioned three items for various structural parts with different shapes and discusses the design of the structural parts for self-healing mechanisms.

3.4.2 Design of structural parts

This dissertation compared the self-healing performance of three different shapes of structural parts shown in Figure 3.6, Shapes A through C in order to evaluate the change in self-healing performance depending on the shape of the structural parts. Figure 3.7 shows the diagram when each structural part is bonded by the thermoplastic resin. The thermoplastic resin contact point is a cylinder with a diameter of 16mm and a height of 4mm for the structural part on the output side and a cylinder with a diameter of 13mm and a height of 5mm for the structural part on the motor side, which is a fixed parameter for each part. Shape A is the reference shape for comparison with others (Figure 3.7 Shape A). Therefore, the part to be bonded to the thermoplastic resin is flat. Shape B focuses on increasing the contact area between the thermoplastic and the structural parts (Figure 3.7 Shape B). The thermal resistance can be reduced and the healing time can be shortened by increasing the contact area. Simultaneously,

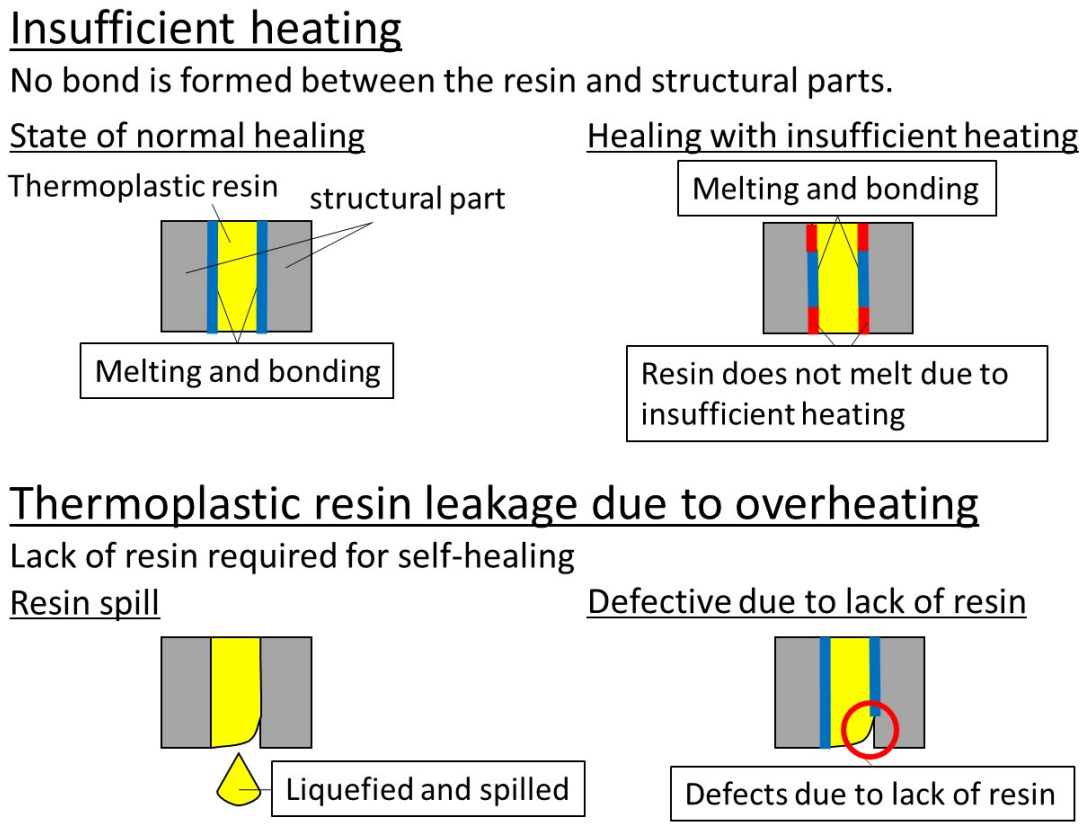

Figure 3.5 Causes of non-reproducibility in self-healing strength. Insufficient heating results in incomplete bonding. Overheating results in defects due to outflow of resin.

the fracture strength is expected to increase due to the increase in the bonding area between the thermoplastic and the structural parts. Shape C is attempted to prevent the thermoplastic resin from flowing out during self-healing (Figure 3.7 Shape C). In this design, the thermal gradient generated by heating a heater causes the melted thermoplastic to be sealed by the unmelted resin, and it is possible to achieve a high self-healing efficiency by preventing the resin from flowing out. However, since this design uses more thermoplastic than the other two shapes, it is projected that self-healing will take longer.

3.4.3 Thermal simulation experiment

The performance of self- healing using thermoplastic resin varies greatly depending on the resin's heating time. Therefore, before the performance evaluation experiment utilizing actual mechanisms, thermal simulation experiments were conducted for each structural part's configuration to estimate the healing time. Based on the experimental

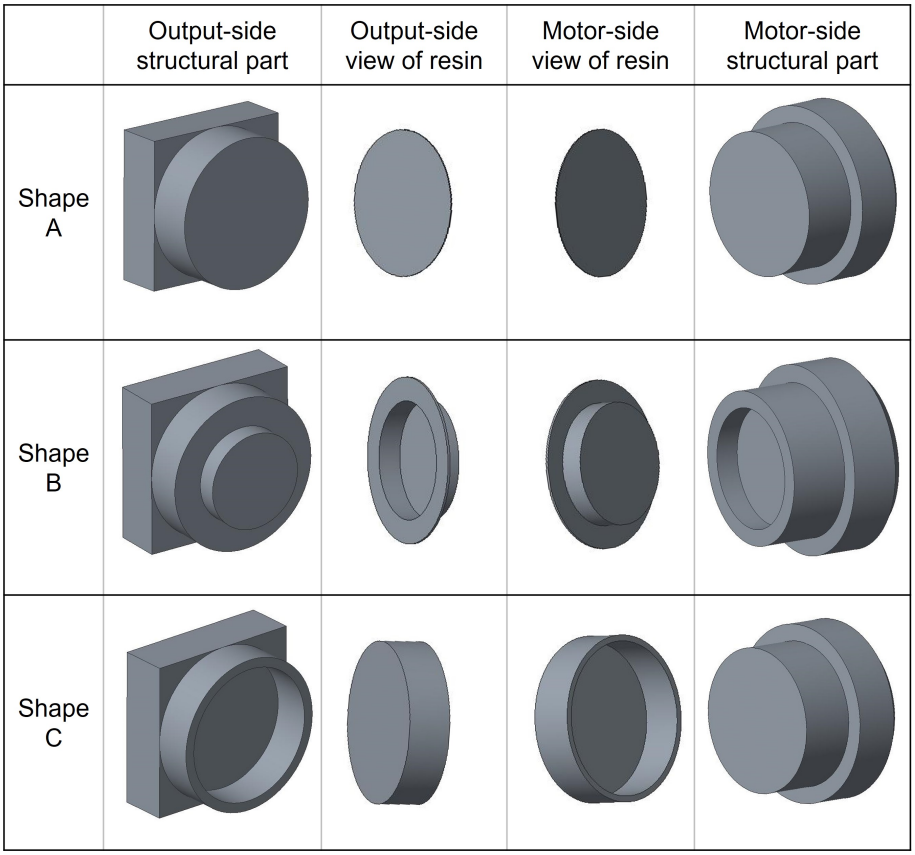

Figure 3.6 Shapes of structural parts. This figure shows 3D views of each structural part and the 3D shape of the thermoplastic resin when sandwiched between the structural parts as viewed from the output side and motor side.

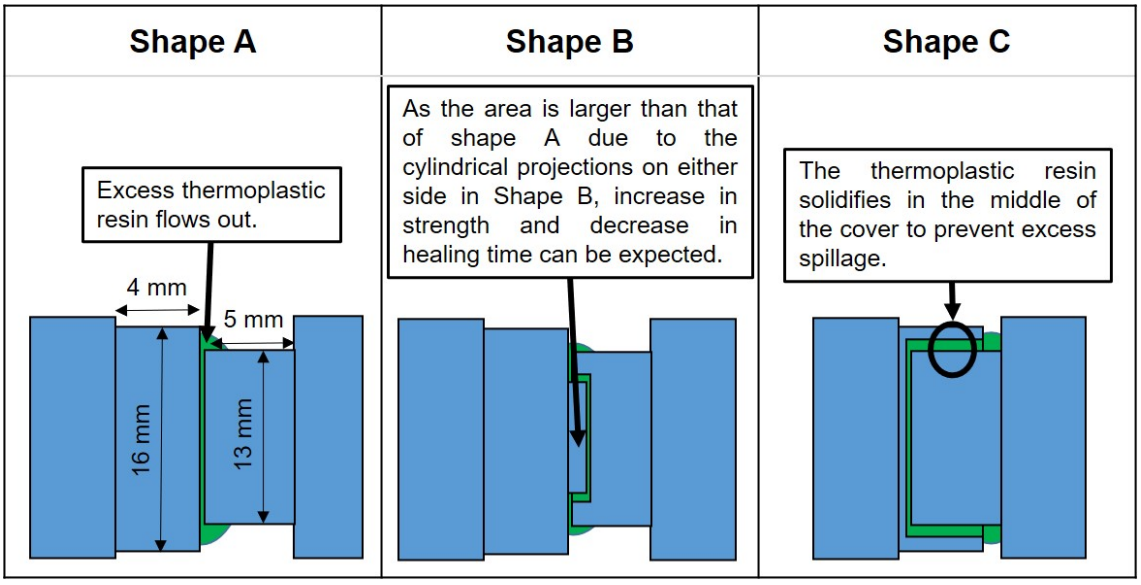

Figure 3.7 Sectional view of bonding structural parts to thermoplastic resin. The fixed parameters of the connected parts are shown for shape A.

results, this dissertation compared the temperature change between Shapes A and B and discussed the shape of the structural parts that required less time for self-healing. This dissertation also confirmed that a thermal gradient occurred for Shape C that could prevent the thermoplastic resin from flowing out.

The simulations were performed on only four elements: a heater, two structural parts, and thermoplastic resin sandwiched between the structural parts, as shown in Figure 3.8, assuming that heat conduction was completely blocked by the insulation material. The part that contacted the outside air was calculated as the heat dissipation when the temperature was 25 °C. PPET1008 of Toa Gosei Co., Ltd. was used as the thermoplastic resin, and its softening point is 95 °C. The output of the heater was set to 7.6 [W] which was the output of the heater mounted on the actual mechanism when 13 V was applied, and the material information of silicon was set to carbide which was the main component of the heater. The material information of A6063 used in the actual machine was set for the structural parts. In addition, a quarter-symmetric model was used in this simulation to reduce the calculation time.

The simulations started at 25°C which was the same as the room temperature, and this dissertation measured the time that it took for the temperature of all thermoplastics involved in fracture strength to exceed the softening point and the time which it took for the temperature of all components to reach a steady state upon heating. The time when the temperature of all thermoplastics exceeds the softening point was also measured in order to estimate the time when the resin flow prevention effect will perform for Shape C.

The results of the thermal simulation for each coupling part are shown in Figure 3.9. A-1, B-1, and C-1 of Figure 3.9 are the results immediately after the start of simulation, and A-2, B-2, and C-2 are the results when self-healing is completed after the healing time of each shape has elapsed. The healing time was shorter for Shapes B, A, and C, in that order. It could be seen that a thermal gradient occurs inside the thermoplastic resin in C-5, which was an enlargement of C-2. C-3 is the result of the time when all the thermoplastic resin inserted in Shape C reached a softening point, and C-6 is an enlarged view of the resin part at this time. A-3, B-3, and C-4 are the results of the time when the heating by the heater is balanced with the heat radiation to the outside and the simulation reaches steady state. Therefore, the thermal simulation was terminated because no change in the temperature state occurred after this time.

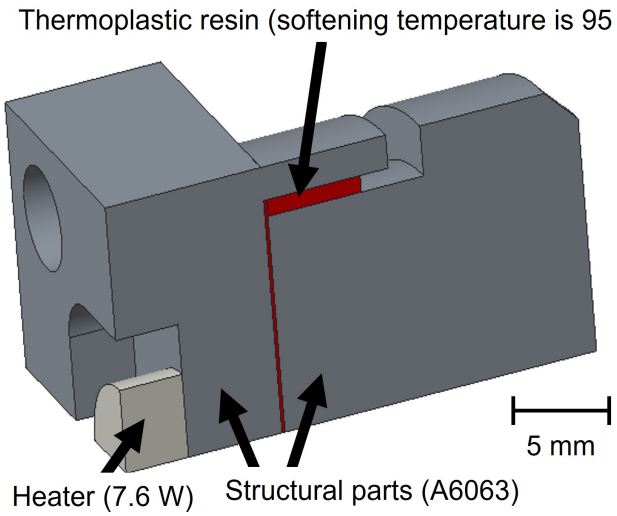

Figure 3.8 Thermal simulation settings. The simulation model was a 1/4 model to reduce calculation time. The output power of the heater was 7.6 [W], and the set values of each material were the physical properties of A6063 for the structural parts and silicon carbide for the heater. The room temperature was 25 ˚C.

3.4.4 Self-healing performance evaluation experiment

Experiments were conducted to evaluate the self-healing performance of the developed linear actuator unit in order to confirm the relationship between the healing time confirmed by the simulation and the actual healing efficiency and fracture strength of the linear transmission element. Based on the results of this experiment, the relationship between the fracture strength and the contact area of the resin and the structural parts was discussed by comparing Shapes A and B. In addition, this dissertation confirms whether the healing efficiency of Shape C has improved.

Fracture strength measurement and self-healing were repeated with the healing time as a fixed parameter in this experiment. The experiment procedure is described based on the self-healing procedure of Figure 3.4. To begin with, a thermoplastic resin was inserted into the actuator unit without material in the linear transmission element, and the linear transmission element was heated during the healing time to bond the structural parts, thus putting the actuator in state A. Heating was performed by applying 13[V] to the ceramic heater, and feedback control by thermocouples was used to prevent the heater from exceeding the maximum usable temperature of 300°C. The amount of thermoplastic resin to be inserted was 0.15 g for Shapes A and B and 0.25 g for shape C. The system shifted to state B by generating a load on the wire connected to the actuator unit in state A and overloading the output side structural part. The

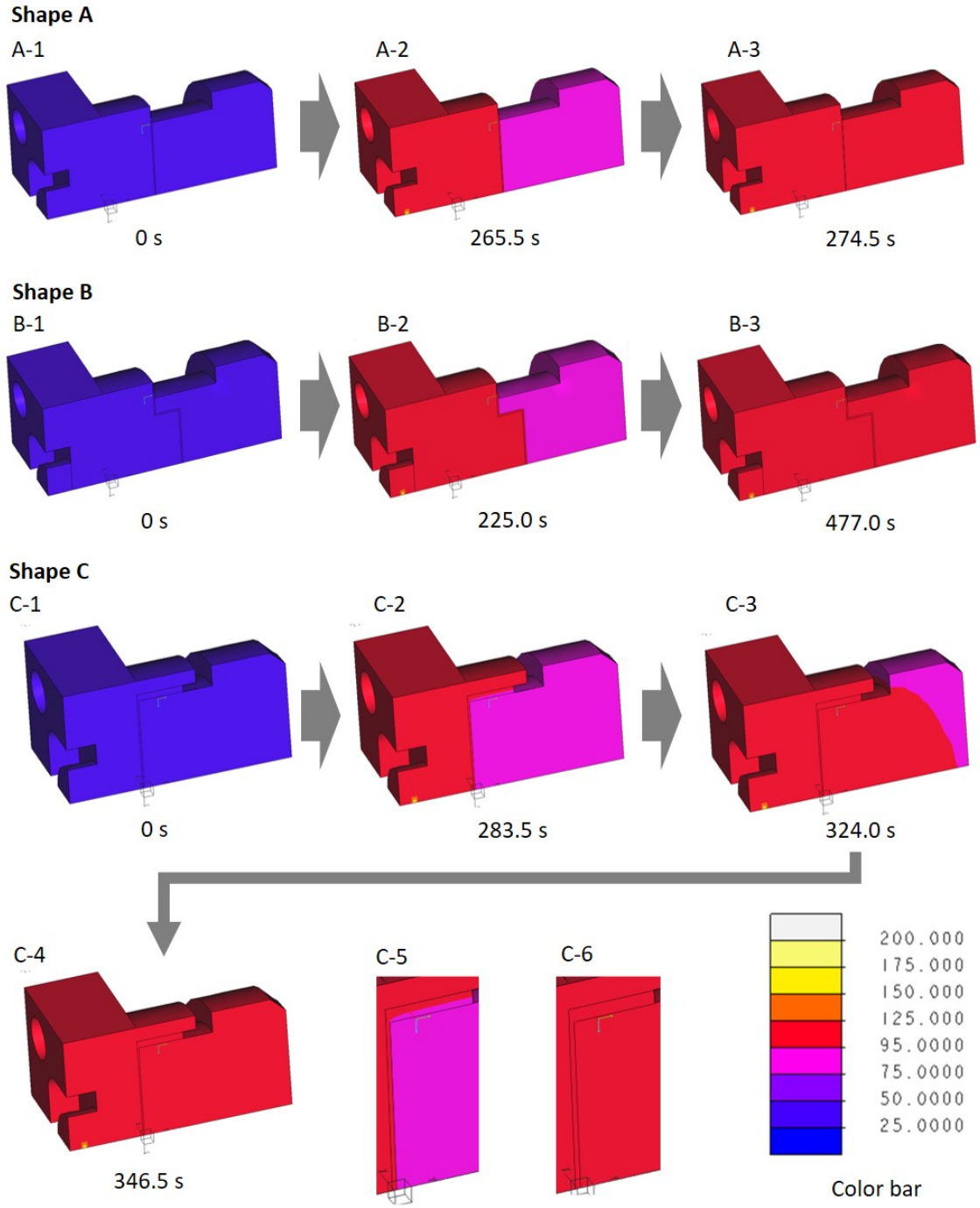

Figure 3.9 Results of the thermal simulation experiment. The color bar indicates the temperature of the structural parts and the thermoplastic resin. The simulation environment was PTC Creo Simulate 3.0, and the solver was a direct solver.

load was gradually increased until the healing mechanism was broken. The load applied to the actuator during this procedure was measured by a load cell to detect the fracture strength of the linear transmission element. Self-healing was performed before this measurement, so it was treated as the 0th self-healing. Following the devastation, the system moved to the self-healing process of state C. The healing time and heating conditions in state C were the same as when state A was first created. When the thermoplastic resin returned to room temperature after the healing time had elapsed and stopped heating, the self-healing process was complete, and it was shifted to state A to measure the fracture strength. The total number of measurements was five at each healing time since the measurements at the time of self-healing and fracture strength measurement were performed four times in succession.

The relationship between the healing time, the number of self-healing cycles, and the fracture strengths for Shapes A, B, and C is shown in Figures 3.10, 3.11, and 3.12 respectively. Table 3.1 also shows the mean fracture strength and standard deviation for each shape and each heating time. Fracture strength fundamentally tends to decrease with each self-healing cycle. However, even after repeated self-healing, the fracture strength of Shape C, whose healing time was 6 minutes, did not become smaller than that of the 0th measurement. The average fracture strength after self-healing was the highest for Shape C, with a healing time of 6 minutes. The heater temperature was controlled to interrupt heating when it exceeded 300°C, but it never exceeded 300°C during the experiment. Therefore, the heating condition was constant at 7.6 W for any healing time.

3.5 Discussion

3.5.1 The design of the structural parts and healing time

The design of the structural parts that reduces the healing time is discussed based on the results of the thermal simulation experiment in this section. It can be seen that the healing time of Shape B was shorter by comparing the results of the thermal simulation of Shape A and Shape B. There was no difference in the shapes except that the contact area of Shape B was 47% larger than that of Shape A. This suggests that the increased contact area led to an increase in the amount of heat flowing into the thermoplastic resin and shortened the healing time. Next, Shape C is considered to have a shorter

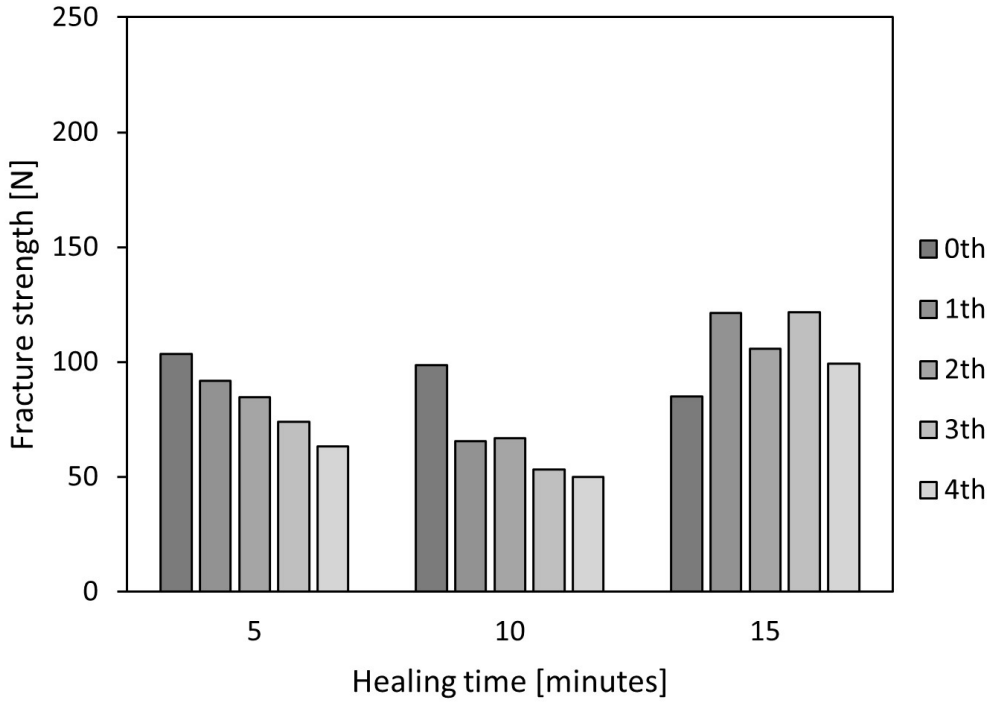

Figure 3.10 Results confirming healing performance (Shape A)

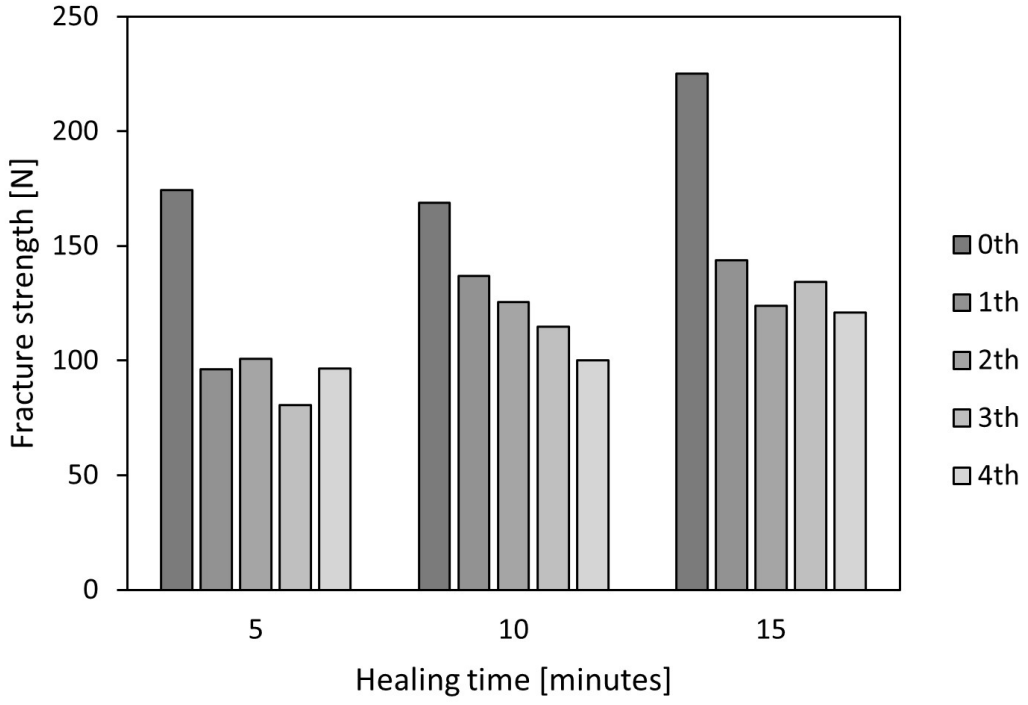

Figure 3.11 Results confirming healing performance (Shape B)

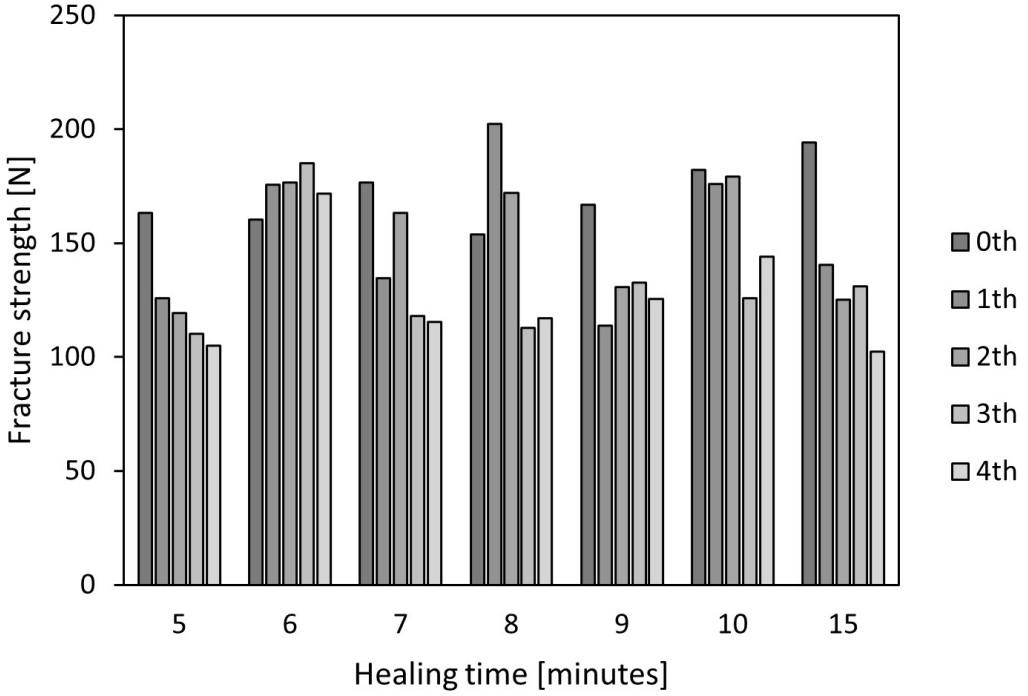

Figure 3.12 Results confirming healing performance (Shape C)

Table 3.1 Mean and standard deviation of fracture strength for each heating time and of each shape

Shape	Heating time [min]	Mean value [N]	Standard deviation [N]
A	5	83.5	13.9
A	10	66.8	17.2
A	15	106.7	13.9
B	5	109.7	33.0
B	10	129.3	23.2
B	15	149.6	38.6
C	5	124.8	20.5
C	6	173.8	8.1
C	7	141.6	24.5
C	8	151.6	33.8
C	9	134.0	17.8
C	10	161.5	22.6
C	15	138.6	30.5

healing time because it has a 154% larger area in terms of the contact area between the resin and the structural parts when comparing Shape A and Shape C. However, the simulation results show that the healing time was shorter for Shape A. This is because the effect of the increase in the amount of resin required by the mechanism was larger than the effect of the increase in heat influx in the contact area with the resin. The thermoplastic resin used in this dissertation had a lower thermal conductivity and a higher specific heat capacity than the structural parts (A6063). Therefore, the healing time is prolonged because the heat transfer time and the amount of heat required for melting the resin increase. Therefore, it is considered necessary to design the structural parts so that the amount of thermoplastic resin used in the linear transmission element is reduced and the contact area between the structural parts and the thermoplastic resin is increased in order to shorten the healing time.

3.5.2 The design of the structural parts and fracture strength

A comparison between Shapes A and B is discussed by using the result of the self-healing evaluation experiment of an actual mechanism in this section. Tables 3.2 show the contact area, average fracture strength, and average fracture stress of the structural parts and thermoplastic resin for Shapes A and B. The increase in contact area with resin and the average fracture strength of Shape B over A were 47 % and 51 %, respectively. The direction of the surface of the increasing contact area was the direction in which the adhesive surface between the thermoplastic and the structural parts broke down in the shear direction when the linear transmission element was loaded. Therefore, the fracture strength of the linear transmission element using thermoplastic resin can be increased by increasing the contact area between the structural parts and the thermoplastic resin, regardless of the direction of the load.

Table 3.2 Comparison of the structural parts of Shapes A and B

Parameter	Shape A	Shape B
Contact area [mm^2]	132.7	195.6
Average strength [N]	85.7	129.5
Average fracture stress [kPa]	645.6	662.1

3.5.3 Causes of unstable fracture strength

The causes of unstable self-healing efficiency in self-healing evaluation experiments using an actual mechanism are discussed in this section. Figure 3.13 shows the states of the healing mechanism before fracture and the fracture surface after fracture for each design. Shapes A and B show images of the 15-minute healing time, whereas Shape C shows images of the 6-minute and 15-minute healing times in Figure 3.13, respectively. The photographs of each shape before fracture in Figure 3.13 show that the resin melts in a hanging state at 15 minutes for Shapes B and C and completely melts down for shape A. When the condition following the fracture was confirmed, no bubbles were observed at 6 minutes for Shape C, while bubbles were observed at 15 minutes for Shapes A, B, and C when the condition following the fracture was confirmed. As a result, the outflow of resin during self-healing and the inclusion of air bubbles may be the causes of the decrease in strength. According to Figure 3.10, 3.11, and 3.12, the fracture strength values of the proposed mechanism fluctuated. Except for the condition with a 15-minute healing time for Shape A and the condition with a 6-minute healing time for Shape C, the fracture strength values exhibited a declining trend. The cause of this strength reduction trend is that the thermoplastic resin liquefied due to heating during self-healing, and the resin flowed out to areas not related to fracture strength, resulting in an insufficiency of resin and air bubbles inside the linear transmission element, as can be seen in the 15-minute photographs of Shape A, Shape B, and Shape C in Figure 3.13.

In contrast, the fracture strength might increase after the 1rt or more self-healing rather than the 0th as the heating time increases, and this situation was noticeable in the 15-minute condition of Shape A in Figure 3.10. The reason for this is because during the initial heating of the evaluation experiment, the thermoplastic resin adhered to the periphery of the structural parts in the opposite direction of gravity, resulting in state A. Due to gravity, liquid resin flows into the gap between the structural parts during self-healing. Therefore, the fracture strength increases. The photograph of Shape B before fracture in Figure 3.13 shows that the resin also existed on the opposite side of the gravity direction. When this resin flowed into the healing mechanism due to overheating and bubbles were expelled to the outside, an unexpected increase in strength may occur.

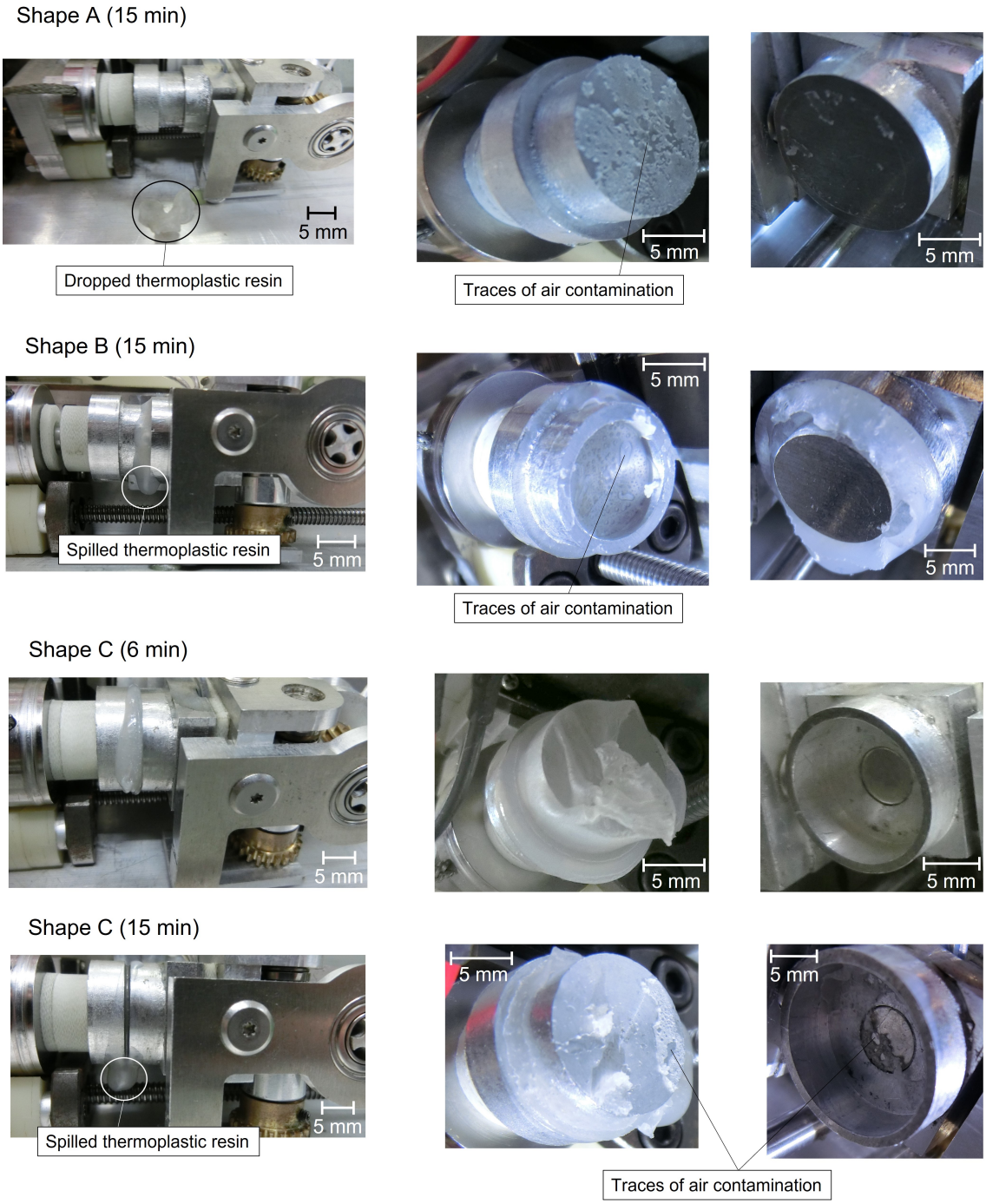

Figure 3.13 Images of structural parts before fracture and images of fracture surfaces. The structural parts before breaking are shown on the left, the broken surfaces on the motor side are shown in the middle, and the broken surfaces on the output side are shown on the right.

3.5.4 Design of the structural parts and self-healing efficiency

This section discusses whether Shape C can prevent the flow of dissolved resin and lead to stable fracture strengths based on the results of thermal simulation experiments and self-healing performance evaluation experiments using actual equipment. During self-healing, the liquid thermoplastic resin generally flows out through the gaps between the structural parts, resulting in strength loss. However, in the state of C-5 in Figure 3.9 which is the result of the thermal simulation experiment, the thermoplastic resin in the part that was related to the fracture strength was completely melted, but the other parts of the resin were not completely melted, and there were parts that were a mixture of liquid and solid due to the occurrence of a thermal gradient. In addition, in order for the entirely liquid resin to flow out of the linear transmission element in this condition, the liquid resin must pass through the mixture of solid and liquid resin. Therefore, the resin, which is a mixture of solid and liquid, such as the state of C-5, has a sealing effect that prevents the liquid resin from flowing out. Furthermore, by minimizing liquid resin leakage, the fracture strength can be stabilized. However, at the state of C-6, 60 seconds after C-5, all of the thermoplastic resin is liquid, and the outflow of the melted resin cannot be prevented. Hence, if the heating time is unsuitable, the repeatability of fracture strength is likely to suffer.

The results of the self-healing evaluation of Shape C by the actual machine in Figure 3.12 show that stable self-healing was performed when the healing time was 6 minutes. During the four self-healing cycles in this experiment, the healing efficiency never fell below 100% with an average self-healing efficiency of 110% and the highest self-healing efficiency of 115% during the third cycle. No resin leakage occurred in the 6 minutes of Shape C in Figure 3.13, and the clean formation of the resin film indicates that there were no air bubbles on the fracture surface. On the other hand, the amount of heating was not sufficient, and the bond between the resin and the structural parts was not sufficiently reformed when the healing time was 5 minutes, so that the fracture strength decreased with each repetition of self-healing. In addition, the outflow of the thermoplastic resin could not be prevented at healing times of 7 minutes or longer, and the fracture strength tended to decrease with repeated self-healing. It is observed that the resin flowed out and bubbles were mixed in the resin, confirming the 15-minute time of Shape C in Figure 3.13. In other words, it is confirmed that the fracture strength is not stable when the healing time is not appropriate, even for Shape C.

3.5.5 Fracture strength of the linear transmission element

The physical properties of the thermoplastic resin used in this dissertation are shown in Table 3.3, and the theoretical fracture strength and the measured strength of the healing mechanism are shown in Table 3.4. Shape C(1) in Table 3.4 is calculated assuming that the resin is bonded to the entire surface of the coupling part without considering the thermal gradient, while Shape C(2) is calculated assuming that the resin is not bonded in the shear direction due to the thermal gradient. The theoretical fracture strength is calculated according to Equation (3.1), assuming that there are no bubbles in the thermoplastic resin.

$$F = A_t \sigma_{max} + A_s \tau_{max} \tag{3.1}$$

A_t and A_s are the areas of the coupling parts loaded to forces in the tensile and shear directions, and σ_{max} and τ_{max} are the maximum tensile stress and maximum tensile stress of the thermoplastic resin, respectively. Table 3.4 shows that the measured strength of Shapes A and B is only approximately 60% to 80% of the theoretical strength. This is because of the presence of bubbles as well as the occurrence of adhesion failure in the healing mechanism. The failure principle of the healing mechanism is explained as follows. The healing mechanism consists of two coupling parts joined by a thermoplastic resin. The failure modes of the joint can be divided into four categories [121] when two materials are joined by a material that is different from the two materials. Explanations of these fracture modes are shown in Figure 3.14. The first type of failure is adhesive failure, shown in Figure 3.14 (a), in which the boundary between the coupling parts and the thermoplastic resin is torn off and fractures. The second type of failure is cohesion failure, shown in (b), in which the thermoplastic breaks down. The third is a mixture of adhesive failure and cohesive failure, shown in (c). The fourth is substrate failure, shown in (d), in which the coupling parts break. Confirming the fracture surfaces in Figure 3.13, the fractures of the healing mechanisms of Shapes A and C are a mixture of adhesive failure and cohesion failure, as shown in Figure 3.14(c). Fracture surfaces of the healing mechanisms of Shape B are adhesive failures. The reason substrate failure does not occur is that the coupling parts are made of A6063, which has greater strength than thermoplastic resin. A mixture of adhesive/cohesion fractures indicates that the bond strength between the coupling parts and the thermoplastic resin is not sufficient. Therefore, The values are

expected to be close to the theoretical strengths shown in Table 3.4 by increasing the bond strength between the coupling parts and the thermoplastic resin through surface treatment that can be expected to have an anchoring effect and by ensuring that only cohesive failure occurs when the healing mechanism breaks down.

The measured strength values exceeded the theoretical strength of Shape C(2) from Table 3.4. This is because the theoretical strength of Shape C(2) assumed that only the resin in the tensile direction was bonded due to the thermal gradient, but some of the resin in the shear direction was bonded to the structural parts when the strength was measured. The strength of Shape C(1) should be reached when the resin is completely bonded to the structural parts of the shape. However, the measured strength is lower than this value. Therefore, it is considered that the structural parts and the resin were partially bonded to the part subjected to shear force.

Table 3.3 Physical Properties of Thermoplastic Resin

Melt viscosity [Pa·s]	4
Softening temperature [°C]	95
Hardness [Shore D]	40
Tensile strength [MPa]	1.4
Tensile shear strength [MPa]	0.8
Peeling strength [N/25mm]	70

Table 3.4 Fracture strength without bubbles

Parameter	Shape A	Shape B	Shape C(1)	Shape C(2)
Theoretical fracture strength [N]	185.8	261.2	283.8	185.8
Measured strength[N]	121.8	225.2	202.4	202.4

3.5.6 Thermal simulation and actual healing time

In the thermal simulation experiment, the healing time to reach a state where spillage could be prevented is 283.5 seconds. However, the actual tranismission element required 6 minutes, which was longer than the simulation results. This is because the simulation does not consider the outflow of heat from the insulation part in order to shorten the simulation time. The heat insulator used this mechanism was a mixture of silicate binder and glass fiber, and had a heat transfer coefficient of 0.24 W/m·k. The heat outflow was calculated to be 1.5 W when the thermoplastic resin temperature reached 100°C, which reliably softens the thermoplastic resin. This corresponded to 20% of the

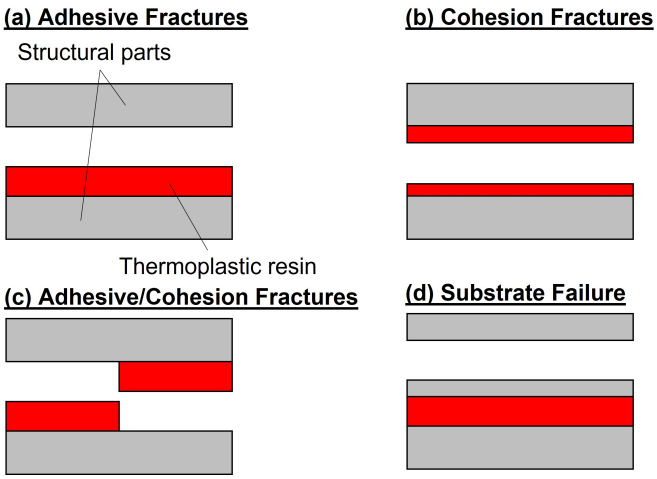

Figure 3.14 Adhesive failure modes. (a) Adhesion Failure: This occurs when the bonding surface between the structural part and the thermoplastic resin is torn off. (b) Cohesion failure occurs when the thermoplastic breaks down. (c) Adhesion/cohesion failure is a mixture adhesion failure and cohesion failure. (d) Substrate failure when the structural part breaks down.

heater's output, and heat dissipation from the insulation created the difference between simulation and reality.

3.6 Conclusion

In this chapter, a self-healing actuator unit with a linear transmission element using melting-solidification phenomenon was developed. The developed actuator unit was used to evaluate the value of the transmission force, self-healing time, and self-healing efficiency of the linear self-healing transmission element. Based on thermal simulations, the proper healing time and the design of the structural parts to reduce the healing time were discussed first because the self-healing time had a large impact on the viscosity of thermoplastic resin during self-healing. The transmission force and self-healing efficiency were evaluated for the three types of structural parts while varying the healing time. The experiment results show that the self-healing efficiency decreased if the healing time was not appropriate, such as when the heating time was 5 or 7 minutes. In addition, an average self-healing efficiency of 110 % was achieved after four self-healing cycles using structural parts that can prevent thermoplastic resin from leaking out by utilizing a thermal gradient. These results indicate that the linear self-healing transmission element based on the melting-solidification phenomenon can self-heal with no reduction in strength from that before the fracture. It was also found

that the transmission force of the linear transmission element is proportional to the contact area between healing materials and structural materials and to the strength of healing materials from the discussion of the theoretical transmission force.

Chapter 4

Robot Joint with Self-Healing Linear Actuator Units

4.1 Introduction

The self-healing linear actuator unit developed in Chapter 3 was introduced to a single-joint robot with a tendon-driven mechanism, in this chapter, to evaluate the self-healing performance. To introduce the actuator unit for the tendon-driven mechanism, the actuator unit was also provided with a mechanism that allowed wire attachment and length adjustment. An overload was generated to destroy the transmission element and render the robot joint inoperable, and it was confirmed that the broken robot joint could be reactivated by self-healing.

4.2 Self-healing for tendon-driven mechanism

The self-healing linear actuator unit that was developed was introduced in a single robot joint of the tendon-driven mechanism. Tendon-driven mechanisms are expected to be applied to a variety of fields because of their many advantages, such as flexibility in actuator placement, weight reduction, and mechanical flexibility [122]. On the other hand, tendon-driven mechanisms are mechanically fragile and have a short lifespan because the wires used to transmit power are prone to rupture. The reasons for wire rupture are mainly classified by the two types listed below.

1. A wire and the body of the mechanism rub against each other and the wire deteriorates due to friction heat or the wire's wear, resulting in a decrease in tensile strength and rupture.

2. The impact on the mechanism propagates to the wire, and the wire cannot withstand the impact load and breaks.

Mechanical and control solutions to the two causes of fracture have been studied. A wire that self-heals at the point of wear [123] and a method to suppress wire wear by liquid lubrication [124] have been proposed as wear countermeasures. If these methods can be implemented in robots, they can greatly reduce the deterioration of wires during operation by self-healing. On the other hand, to deal with shocks, a method of controlling the wire by absorbing the shocks generated by the wire using a spring [125] was proposed. However, this method decreases the robot's controllability, and there is a limit to the amount of shock that can be absorbed by the shock-absorbing mechanism, and the wire may break due to shock that cannot be fully absorbed. Therefore, if a shock is applied when the strength of the wire has decreased due to wear or thermal degradation, the wire may break even if it has sufficient strength to move the mechanism, resulting in a short life span for the tendon-driven mechanism. Therefore, the self-healing actuator unit proposed in this dissertation can be introduced as an actuator for wire traction, which is expected to solve the problem of mechanical fragility. A self-healing transmission element is inserted between the wire and the actuator by introducing the linear actuator unit into the tendon-driven mechanism. The inserted transmission element breaks before the wire breaks under overload since the transferable load of the transmission element is small in relation to the strength of the wire. The transmission element can self-heal, enabling the robot joint to resume operating. This allows the mechanism's service life to be extended until the wire wears out and is no longer strong enough to operate the mechanism.

4.3 Self-healing tendon-driven mechanism

4.3.1 Wire length adjustment mechanism

Because the tendon-driven device is powered by a wire, the wire length needs to be strictly adjusted. However, the robot itself often has a mechanism for adjusting the wire length because the wire is tied to an anchor or pulley by hand. Therefore, a mechanism to adjust the wire length is also installed in the dissertation's self-healing linear actuator unit. The adjustment mechanism is shown in Figure 4.1 along with the linear actuator unit. Figure 4.1 also shows the rack gear for driving the wire

length adjustment mechanism described below. The wire length adjustment mechanism locates between the self-healing transmission element and the wire attachment pulley (wire pulley).

The detailed and exploded views of the wire length adjustment mechanism are shown in Figure 4.2 and 4.3 respectively. The exploded view of Figure 4.2 shows the decomposition along the two linear assembly directions. The principle is explained in the following. A rack gear converts the actuator's linear action into rotating motion. At this time, the combination of a gear and a one-way clutch enables the mechanism to extract power only in the direction of wire winding, and the extracted rotation is transmitted to the worm gear. The worm gear transmits power to the worm wheel, and it is possible to wind the wire since the worm wheel is fixed to the wire pulley using a machine keyway. In addition, the use of a worm gear in the middle of the wire length adjustment mechanism eliminates back-drivability and enables the mechanical structure to receive the high tension of the wire. In order to wind the wire, the adjustment mechanism is moved back and forth near the rack gear to generate the winding power using a short rack gear installed at the end of the mechanism shown in Figure 4.1 in order to wind the wire.

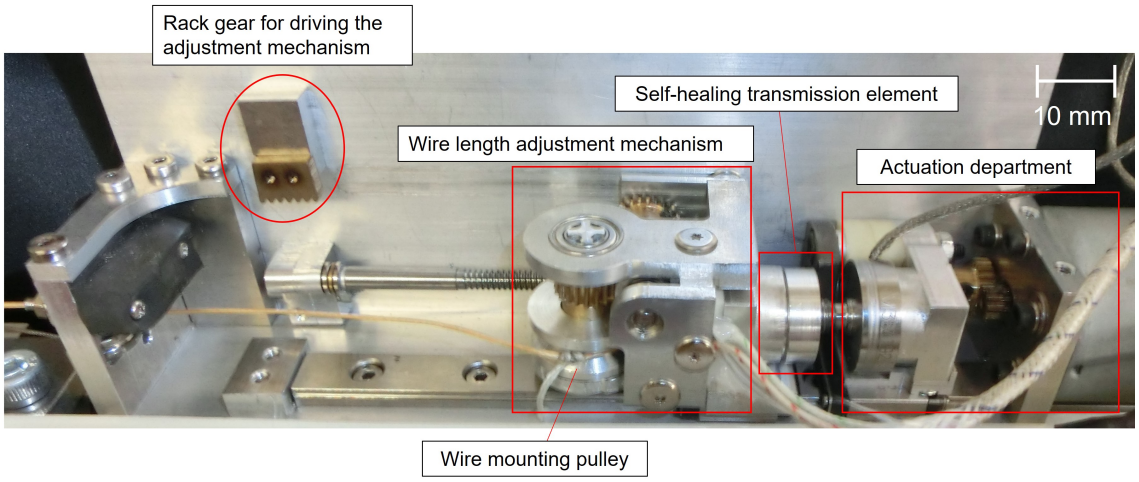

Figure 4.1 Self-healing linear actuator unit and wire length adjustment mechanism. The wire length adjustment mechanism allows fine adjustment of the wire length when mounted on the tendon-driven mechanism. To drive the adjustment mechanism, a rack gear is installed near the limit of the self-healing unit's range of motion. The adjustment mechanism is mounted adjacent to the self-healing transmission element, and the wire is applied to the transmission element through the adjustment mechanism.

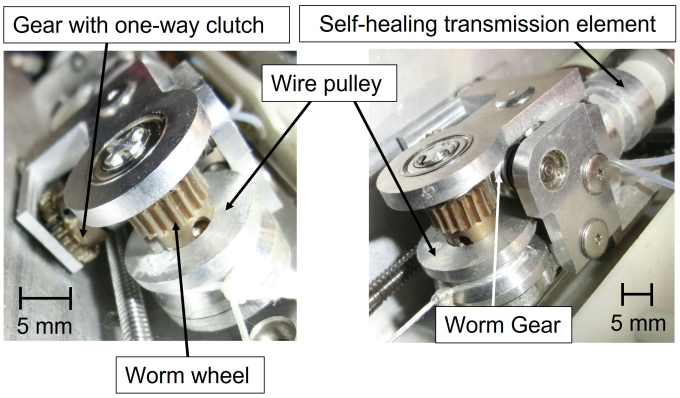

Figure 4.2 Wire length adjustment mechanism. A worm gear is attached to the wire pulley. Therefore, the gear supports the wire's tension. The wire pulley has no back-drivability, and the wire does not sag under tension.

4.3.2 Robot joint with the self-healing linear actuator unit

A robot joint with a self-healing linear actuator unit is shown in Figure 4.4. The robot joints are connected to the joint axes by long and narrow enclosures of 330 mm each, and the actuator units and wire anchors are installed in each enclosure. One side of the tendon wire is fastened to the wire pulley inside the actuator unit installed in the enclosure, and the other side of the tendon wire is fastened to the anchors installed in the enclosure on the side across the joint. Therefore, the joint can be extended by the actuator unit towing the wire. Since the purpose of this dissertation is to evaluate the self-healing performance of the robot joint, the original tendon-driven mechanism requires a pair of wires to move a single-joint; however, the actuator is installed only on the extending side of the joint and a spring is used to power the bending direction (Figure 4.5). Therefore, when the wire is loosened, the spring put into the joint can bend it. In addition, the wire of the robot joint passes through the pulleys installed in the chassis to limit the wire path.

4.4 Evaluation of self-healing tendon-driven mechanism

The evaluation experiment of the self-healing tendon-driven mechanism confirmed the joint flexion and extension movements as well as self-healing performance. During the assessment experiment, the robot joint is fixed as shown in Figure 4.6. Due to the weight of the self-healing linear actuator unit and the robot joint housing, the joint

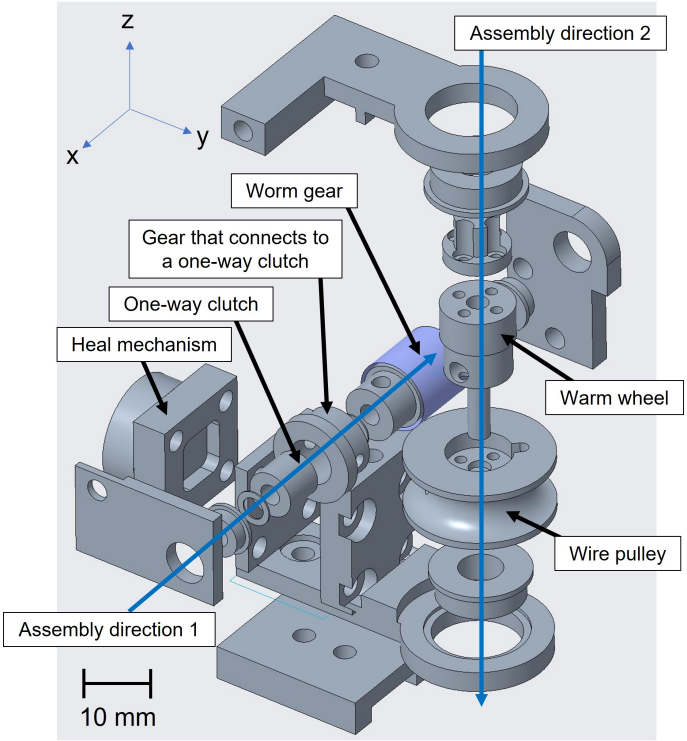

Figure 4.3 An exploded view of the wire length adjustment mechanism. The rack gear is combined with a one-way clutch to extract power only in the direction of winding the wire.

is subjected to a maximum load of 4 Nm. The evaluation experiment was conducted according to the following four procedures.

Step 1 Flex the robot joint to confirm that the actuator unit can withstand the load of flexion and extension and fix the joint in the extended position.

Step 2 Drop a 2 kg weight on the tip of the robot joint to generate an overload on the actuator unit. This load destroys the self-healing transmission element connected via wires and prevents power transmission to the joint.

Step 3 The actuator unit performs self-healing. The self-healing operation has a heating time of 6 minutes. After heating, the mechanism is left at room temperature for 15 minutes to dissipate heat.

Step 4 Confirm that the actuator unit has self-healed by performing the same operation as in Step 1 and that the robot joint can move again.

Figure 4.7 shows the bending and stretching motion in the evaluation experiment.

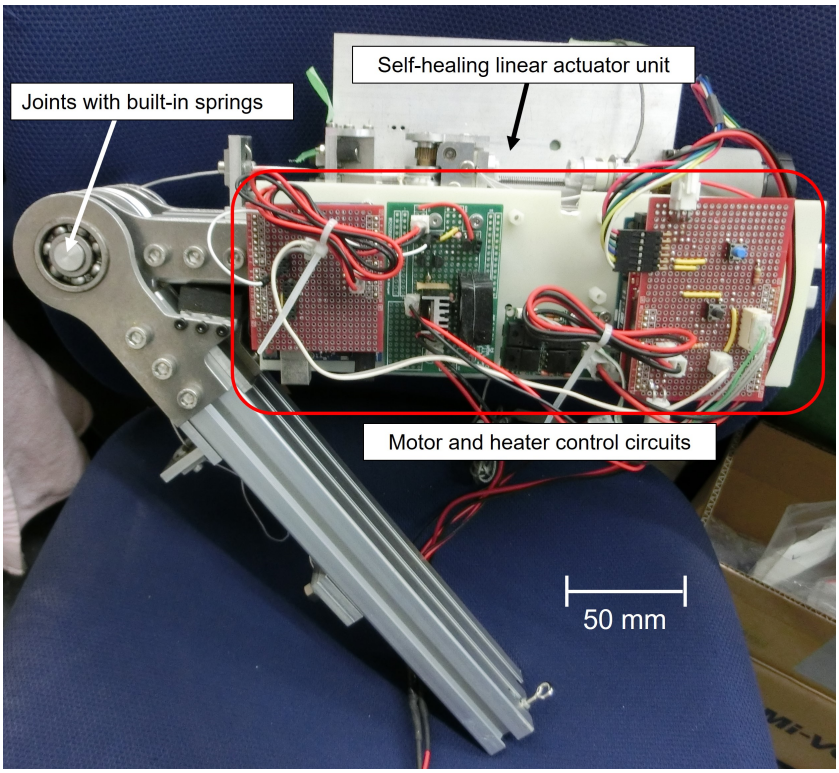

Figure 4.4 Robot joint with a self-healing linear actuator. A 330 mm frame is installed for each side of the joint. A self-healing linear actuator unit is installed on one frame, and a fastener to hold the wire is installed on the other. It weighs about 3 kg in total, and the joint has springs to assist in driving one side of the rotation. Since this mechanism is an experimental machine, it lacks a power supply and needs to be powered from an external source .

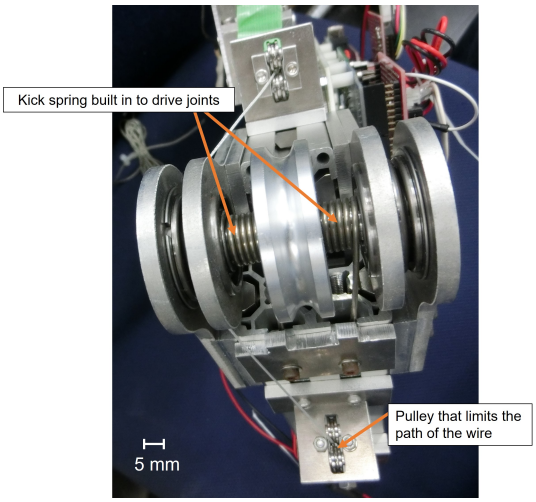

Figure 4.5 A view of the kick spring incorporated into the joint. Tendon-driven mechanisms usually require the use of a pair of wires to drive a single-joint. However, since the purpose of this experiment is to test a self-healing linear actuator unit on a robot, one of the rotations employs a spring to drive the joint. The spring consists of two kick springs that are installed on the shaft of the joint.

However, the figure for Step 4 is omitted since the movement in Step 4 was exactly the same as in Step 1. Steps 1 (a) and (b) in Figure 4.7 show the state of the joint in flexion and extension, respectively. Even during extension, when the load was greatest, the actuator unit was able to operate without destroying the transmission element.

Steps 2 of a and b in Figure 4.7 show a weight being dropped on the paw of the robot joint and the linear transmission element being destroyed by the falling weight, respectively. When a weight fell, the transmission element of the actuator unit was destroyed, and the power could not be transmitted to the wire. Step 3 shows that the linear transmission element was crimped and heated for self-healing. In this procedure, it is possible to self-heal the destroyed transmission element and tow the wire again by performing the self-healing operation described in the previous chapter. Step 4 confirmed that the robot joints could be flexed and extended as in Step 1.

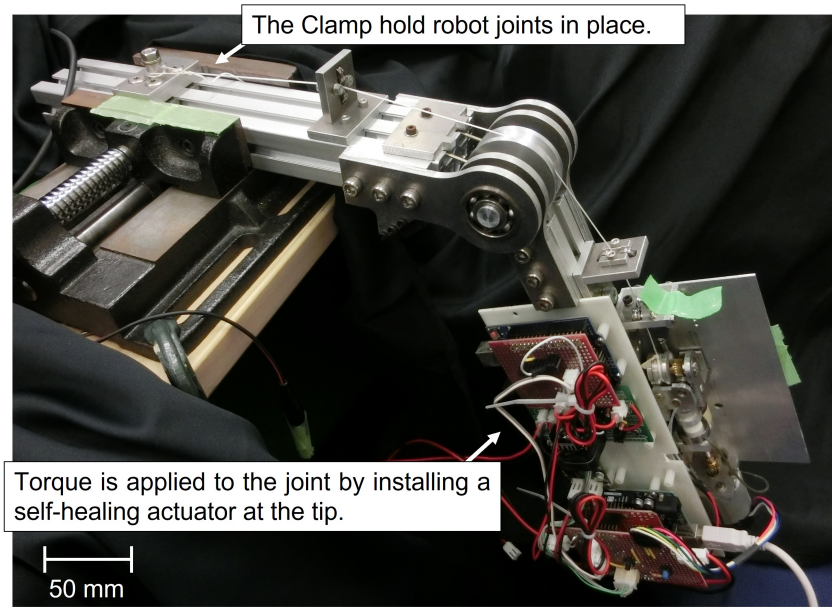

Figure 4.6 Evaluation setting of robot joint. The robot is fixed by clamping the frame, without the linear actuator unit, horizontally to the ground. Therefore, the weight of the actuator unit as well as the frame is added as a load to the joint. Therefore, the joint is subjected to a maximum load of 4 Nm.

4.5 Self-healing of a tendon-driven joint

The self-healing actuator unit mounted on the tendon-driven mechanism enabled the joint to re-operate via self-healing even when the joint was overloaded. When overloads or impact loads occur, normal tendon-driven mechanisms become inoperable due

to wire rupture. Therefore, each time an overload develops, maintenance is required to replace the wires and adjust the operation's accuracy. However, it can be re-operated without the need for manual maintenance by installing a self-healing linear actuator unit. Furthermore, actuator units equipped with self-healing capabilities based on the melting-solidification phenomenon can self-heal many times without strength degradation. Thus, self-healing actuator units enable the robot to self-heal and to continue to operate independently of humans.

4.6 Conclusion

The self-healing linear actuator unit in the previous chapter was installed in a robot joint with a tendon-driven mechanism in this chapter to evaluate the behavior of the joint under flexion, extension, and overload, as well as self-healing joint remotion. Therefore, the proposed actuator unit can operate the robot joint, as demonstrated in this chapter. This chapter also confirmed that even if an overload occurs in a joint, the transmission element in the actuator unit can protect the wires of the tendon-driven mechanism, and that self-healing enables the joint to operate again after an overload. Hence, it is shown that by mounting the self-healing linear motion transmission elements developed in Chapter 3 on robot joints, the robot can achieve self-healing performance.

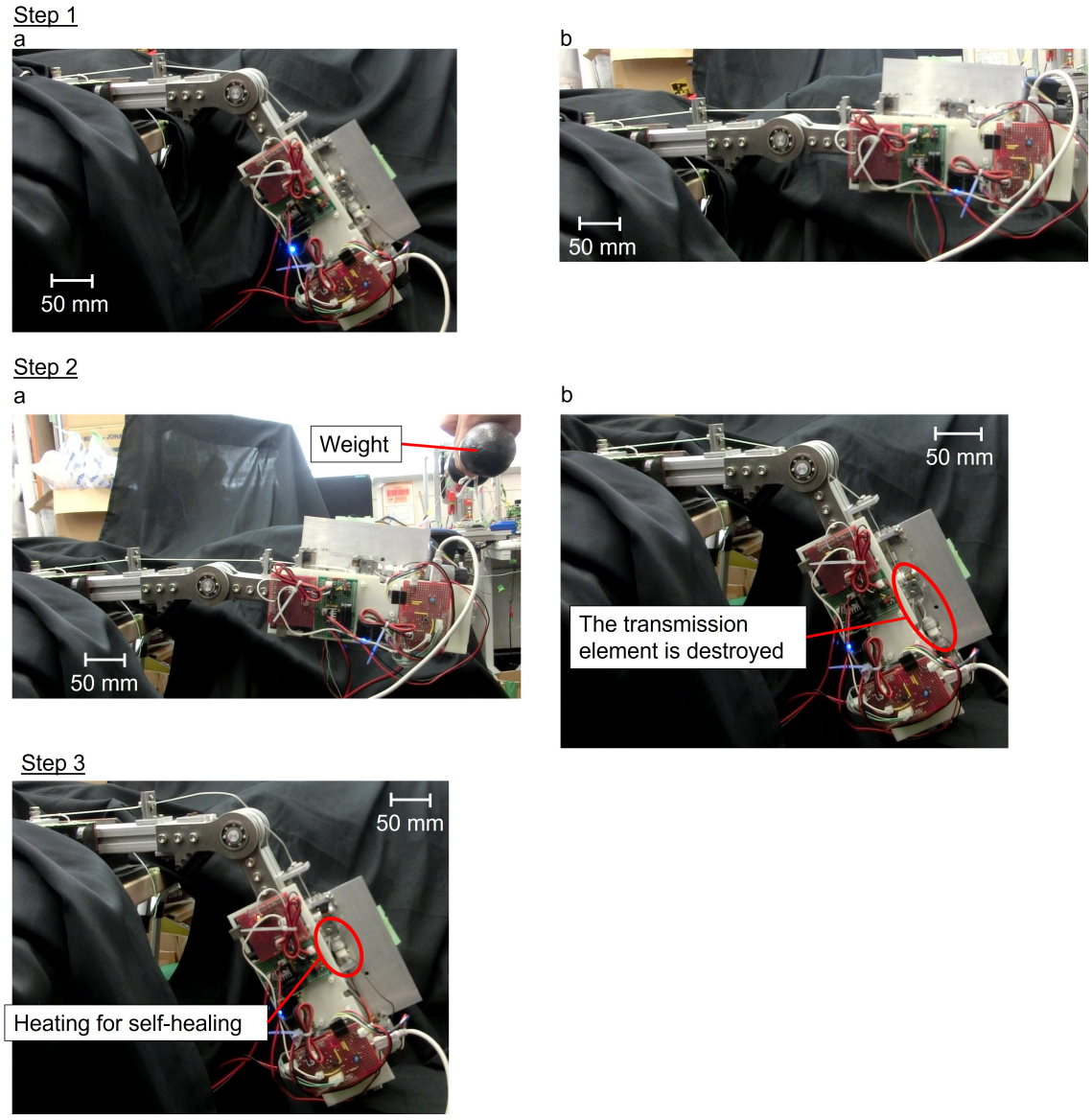

Figure 4.7 Evaluation experiment using robot joints. Step 1a shows that the actuator is bending the joint, and Step 1b shows that it is stretching it. The joint is under maximum load in Step 1b. Step2a shows the load applied to the robot joint by dropping a weight on it, and Step2b shows the destroyed actuator unit. The self-healing transmission element has been destroyed at the location highlighted in Step 2b. Step 3 shows that the actuator unit is self-healing while the motor is heating the linear transmission element while crimping it.

Chapter 5

Rotary-type self-healing transmission element

5.1 Introduction

This chapter developed and evaluated a self-healing rotary transmission element. Unlike the linear motion type, the self-healing transmission element of the rotary-type did not require an actuator for the self-healing process. Therefore, only a rotary transmission element could be developed. In addition, induction heating, which is used as an energy application method for melting, has rapid heating function and energy efficiency [126] and could reduce the healing time to tens of seconds, whereas other self-healing methods require tens of minutes or more. As a result, the self-healing time was fixed to the time when the healing material inside the transmission element completely melted, and the maximum transmission torque (transmittable torque) and self-healing efficiency were assessed in the evaluation experiment. The displacement at the torque disconnection was also used to calculate the amount of energy absorbed at the time of fracture.

5.2 Self-healing rotary transmission element

5.2.1 Design of a self-healing rotary transmission element

Figure 5.1 shows an exploded view of the self-healing rotary transmission element. The main component of the mechanism has two structural parts (shaft A and B) and a low-melting-point metal for healing material. Figure 5.2 shows the overall appearance of the complete mechanism. Figure 5.1 shows the disassembled parts of the mechanism,

and the roles of each part and the detailed internal structure will be explained in the next section on "Internal structure of the self-healing rotary transmission element". Figure 5.2 shows the assembled internal structure with three-quarter sectional views of the coil guide, the coil for induction heating, and shaft B. A coil for generating electromagnetic induction is placed on the outermost side of the proposed mechanism to melt the low-melting-point metal in the mechanism using induction heating. The mechanism is connected to a plastic coil guide for coil installation via bearings installed on shaft A and shaft B. Figure 5.2 is attached to shaft B as an example. The coil guide is made of resin because, if it were made of metal, the coil guide would be heated preferentially when induction heating was performed, and the low-melting-point metal would take time to heat. Electromagnetic induction is formed near the surface of shaft B if the coil guide is made of resin, and the time until the low-melting-point metal is heated is shortened.

The incorporation of induction heating into the suggested mechanism is intended to simplify the mechanism's construction. When using a wired heater, a slip ring or another mechanism to convey electric power is required because the suggested mechanism transmits rotational power, making the mechanism larger and more complicated. Induction heating, on the other hand, can heat the mechanism without making contact. As a result, the proposed mechanism can be simplified simply by putting a coil outside the mechanism. In addition, because the heating process uses eddy currents generated by electromagnetic induction, induction heating can heat the metal more efficiently and faster than other heaters, such as ceramic heaters.

5.2.2 Internal structure of the self-healing rotary transmission element

Figure 5.3 depicts the internal structure of the rotary transmission element. However, the coil and coil guide are omitted to show the internal structure of the proposed mechanism, and three-quarter of the mechanism is shown in cross-section in Figure 5.3. The structure has a cylindrical shape, a diameter of 13 mm, a height of 13 mm, an input shaft, and an output shaft. Shafts A or B can be used as the input and output shafts. Two bearings keep shafts A and B are kept concentric. Shaft A has four keyways that are 2 mm wide, 1 mm deep, and 3 mm long, while shaft B also has four keyways that are 3 mm wide, 1 mm deep, and 3 mm long. These keyways

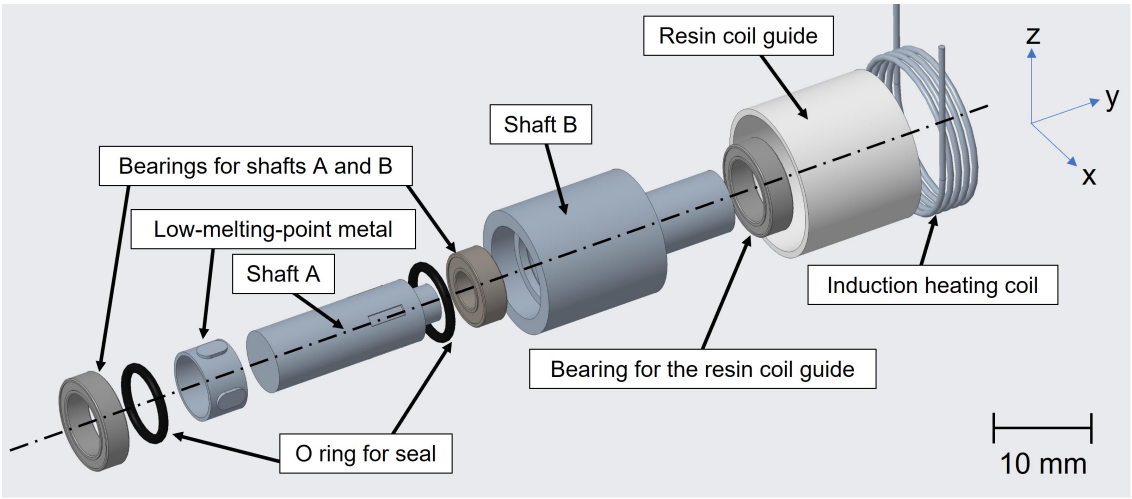

Figure 5.1 Exploded view of the self-healing rotary transmission element. Each elemental part of the proposed mechanism is disassembled and arranged in the order in which it is to be assembled.

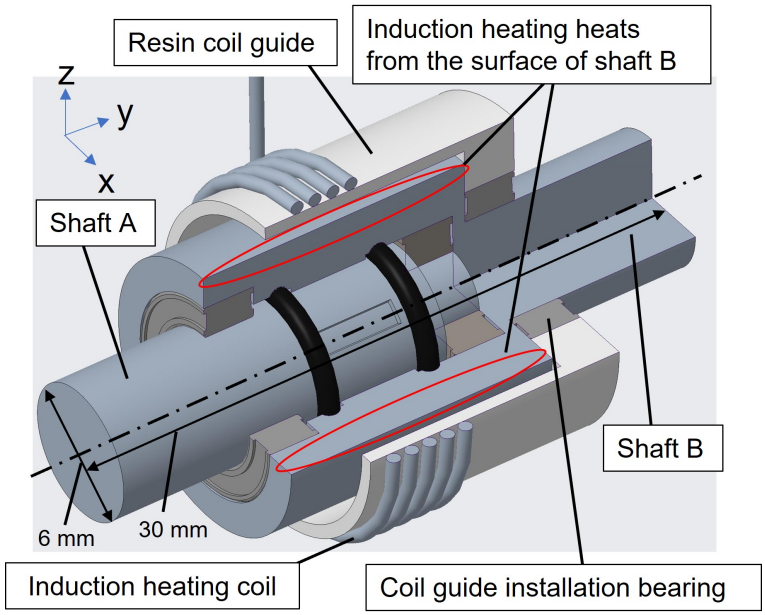

Figure 5.2 External view of the self-healing rotary transmission element. To show the intricate internal structure, the coil, coil guide, shaft B, and bearing in a three-quarter section. It also shows which sections are heated preferentially by induction heating.

are constrained by filling the space between shafts A and B with low-melting-point metal, which allows torque transmission between shafts A and B. When the proposed mechanism is subjected to an overload, the low-melting-point metal component filled between shaft A and shaft B fails and interrupts the torque transmission. After the fracture, the low-melting-point metal parts are melted and solidified by heating to self-heal and enable torque transmission again. At this time, there is a possibility that the melted metal will flow outward since the viscosity of the molten metal is low. Therefore, the space filled with the low-melting-point metal is sealed with two O-rings to prevent the molten metal from flowing out. In this dissertation, Bi-26In-17Sn (melting point 78 °C) is used as a low-melting-point metal. Although volume change usually occurs when metals melt and solidify, the proposed mechanism does not cause backlash because alloys containing more than 55% Bi have the property of expanding during solidification [127]. In addition, the pressure between the shaft A and the low-melting-point metal is created by the expansion of the low-melting-point metal. As a result, not only torque transmission by the keyway structure but also torque transmission by friction occurs between shafts A and B, making the mechanism capable of transmitting a larger torque.

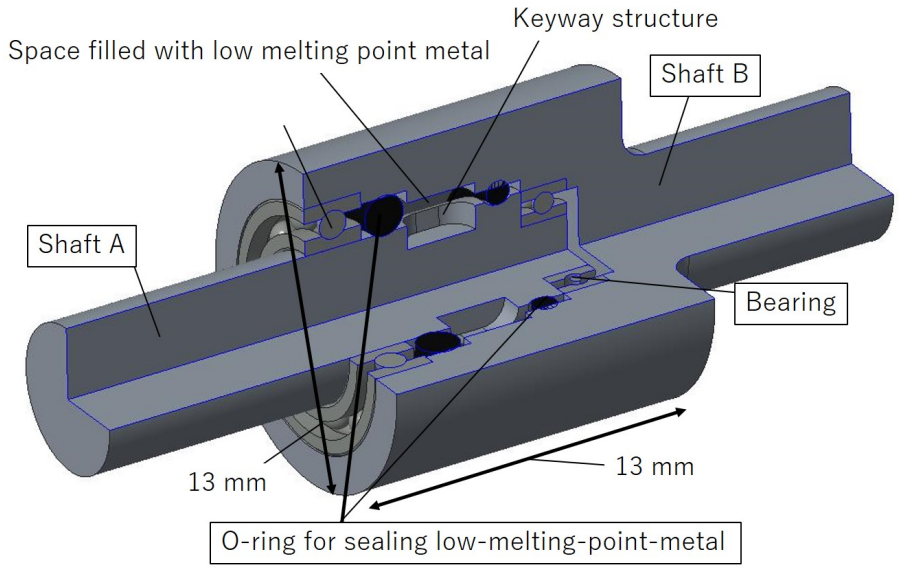

Figure 5.3 Internal structure for a self-healing rotary transmission element. The proposed mechanism is shown in the three-quarter section. The mechanism is cylindrical in shape, with a diameter of 13mm and a height of 13mm, and it contains two shafts. Two bearings keep the shafts concentric, and two O-rings prevent melted metal from leaking. There is also room for the low-melting-point metal between shafts A and B. The combination of this low-melting-point metal and the keyway structures on the shaft allows for torque transmission.

5.2.3 Assembly of self-healing rotary transmission element

Figure 5.4 shows a schematic diagram of the proposed mechanism's assembly. During assembly, the proposed mechanism needs to enclose the alloy inside the mechanism. Therefore, it is necessary to assemble the mechanism when the metal is in the molten state. Bearing 1 is first installed on shaft B and connected to shaft A. Then, O-ring 1 is inserted between shafts A and B (Process 1). The bearing 1 fixes the positional relationship between shafts A and B, and the O-ring 1 prevents the melted low-melting-point metal from entering the bearing side during assembly. Next, a thin rod-like low-melting-point metal is inserted between shafts A and B keeping shaft B heated by heater at 150 °C. This allows the space between shafts A and B to be filled with melted, low-melting-point metal (Process 2). Thereafter, O-ring 2 is inserted inside the mechanism, which is followed by the installation of bearing 2 in the mechanism (Process 3). This O-ring 2 prevents the low-melting-point metal from flowing out. Finally, the low-melting-point metal is solidified to complete the assembly of the mechanism by cooling it to a temperature of 25 °C (Process 4).

5.2.4 Self-healing process of metals using melting–solidification phenomenon

Figure 5.5 shows an overview of the operation of the proposed mechanism. Figure 5.5(a) shows the cutting plane of the cross-section shown in (b) and the direction in which the cross-section is viewed. The three figures in Figure 5.5(b) show the mechanism in cross-section and outline its operation in three different states. In all figures of Figure 5.5, the coil and coil guide are omitted as in Figure 5.3. In State A, shafts A and B are constrained by low-melting-point metal entering the keyways in each shaft, and rotary powers can be transmitted between shafts A and B. State B shows what happens when an overload occurs between shafts A and B. When an overload occurs, the low-melting-point metal that restrains the keyway portion of shaft A breaks down. Following the breakdown of the low-melting-point metal, the shaft A and the low-melting-point metal slip. At this point, there is no torque transmission between shafts A and B because shaft B and the low-melting-point metal are mechanically bonded, but shaft A and the low-melting-point metal are not. State C shows the process of self-healing for the rotary transmission element. To cure the fracture and return to State A, the fractured low-melting-point metal is heated, melted, and solidified. In other words, in State C, the

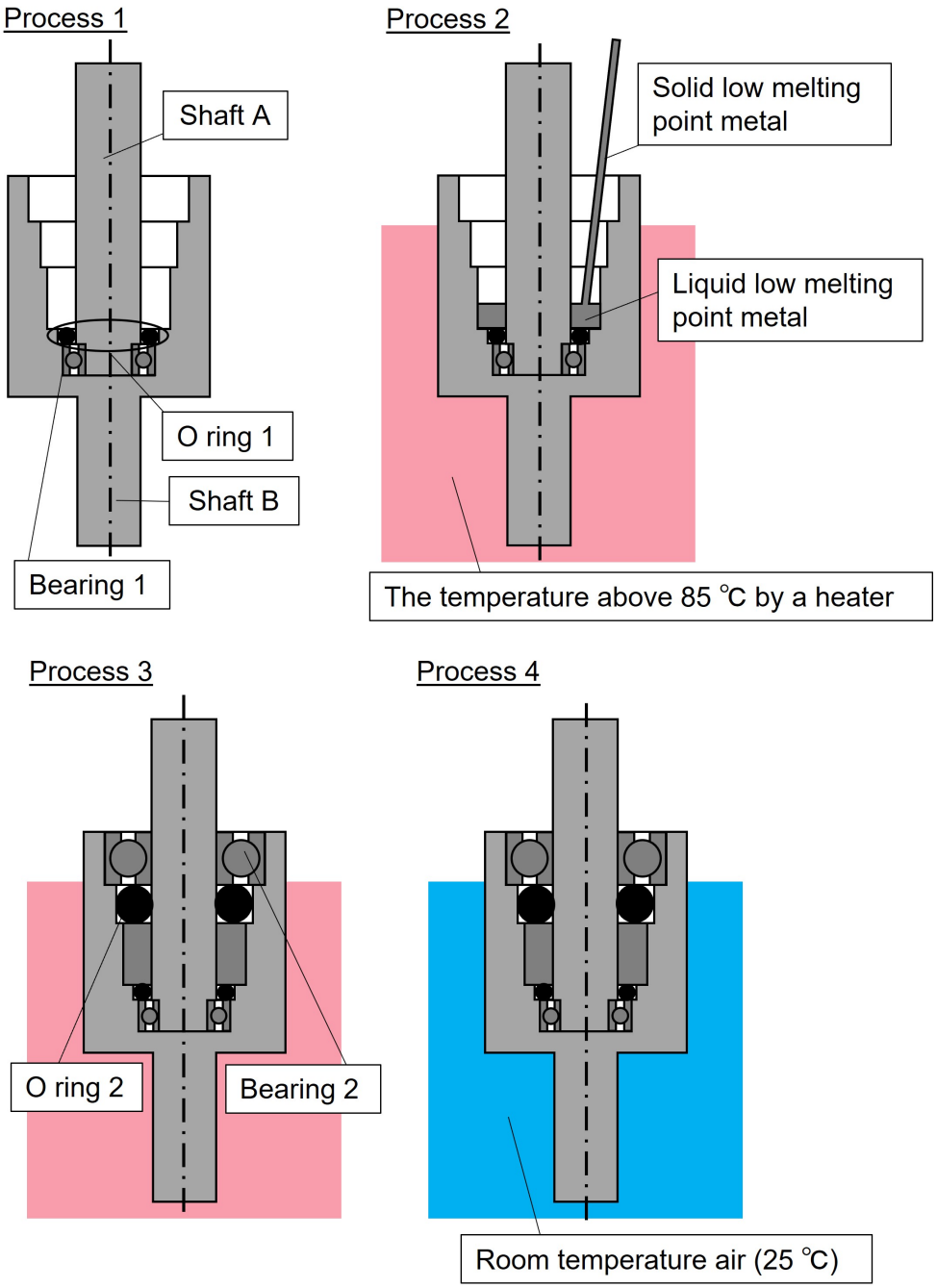

Figure 5.4 Assembly instructions for the self-healing rotary transmission element. In Process 1, insert bearing 1 into shaft B to fix the positional relationship between shafts A and B. In addition, an O-ring1 is installed to prevent low-melting-point metal from entering the bearing 1 side. In Process 2, a thin rod of low-melting-point metal is inserted into contact with the heated shaft B, melting the metal. In Process 3, the bearing 2 is installed while the O-ring 2 is installed to prevent the molten metal from flowing out. In Process 4, air cooling completes the assembly.

torque transmission is reconnected by self-healing the broken part using the melting–solidification phenomenon of the low-melting-point metal. Figure 5.5(c) depicts the condition when the heating during self-healing is insufficient. The low-melting-point metal is heated from the point where it contacts the shaft B, since the mechanism heats from the surface of the shaft B. Therefore, if the heating is insufficient, the low-melting-point metal in the keyway structure of shaft A does not reach its melting point, and the broken part is not healed. Hence, it does not self-heal, and torque transmission continues to be impossible.

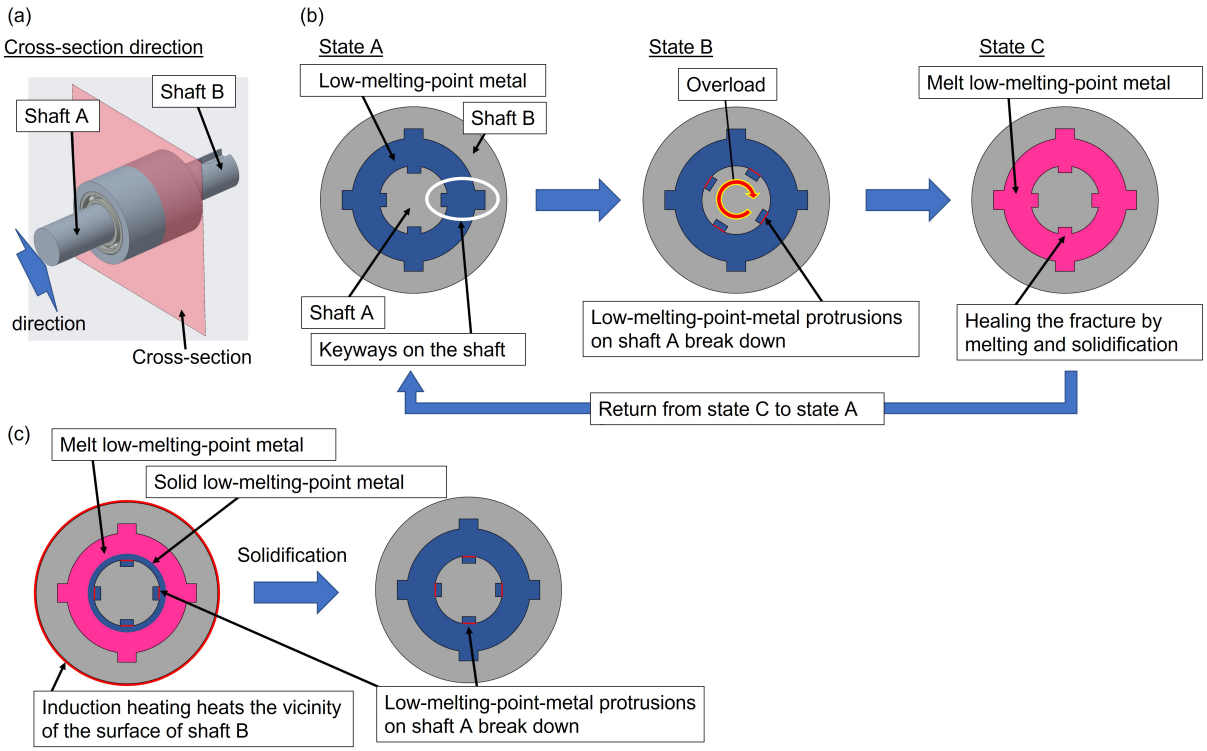

Figure 5.5 Principle of the self-healing torque transmission mechanism. (a) shows the cross-section and the direction of the figure shown in (b) and (c). (b) shows an overview of the operation of the proposed mechanism by dividing it into three states. State A shows the normal state, State B shows the breakdown of the internal low-melting-point metal due to overload, and State C shows the self-healing state. (c) shows what happens when the heating is insufficient during self-healing.

5.2.5 Transmission torque of the self-healing mechanism

The maximum transmission torque of the proposed mechanism is determined by two factors: the strength of the low-melting-point metal keyway structure and the friction generated between the shaft A and the low-melting-point metal. In other words, the proposed mechanism's transmittable torque is expressed by the following Equation

(5.1).

$$T_{all} = T_{key} + T_f \tag{5.1}$$

T_{all} is the transmittable torque, T_{key} is the torque value depending on the kayway structure, and T_f is the torque value generated by friction.

On shaft A, the proposed mechanism has four keyways. The low-melting-point metal enters the keyway grooves, and the shaft A and the low-melting-point metal are mechanically bonded. When an overload occurs, low-melting-point metal in the keyway structures breaks down, eliminating torque transmission by the T_{key} and slippage occurs between shaft A and shaft B. The value of T_{key} is determined by the critical cross-section area and the shear strength of the low-melting metal, which can be obtained by the following Equation (5.2).

$$T_{key} = nrA_{key}\tau_{max} \tag{5.2}$$

n is the number of keyway structures on the shaft A, r is the radius of the shaft A, A_{key} is the area of the critical cross-section per keyway structure, and τ_{max} is the shear strength of the low-melting-point metal.

In the proposed mechanism, a low-melting-point metal of bismuth alloy is used, and bismuth alloys containing more than 55% Bi have the property of expanding during solidification [127]. When melting and solidification occur in the mechanism, friction occurs between shaft A and the low-melting-point metal. The torque generated by this friction between shafts A and B is calculated by the following Equation (5.3).

$$T_f = rA_f P\mu' \tag{5.3}$$

A_f is the contact area of shaft A with the low-melting-point metal excluding keyway structures P is the pressure generated between the low-melting-point metal and shaft A, and μ' is the coefficient of kinetic friction. The proposed mechanism's load torque reaches its maximum value when the keyway structure is destroyed by the overload, and at this time there is a slight slip angle between shaft A and the low-melting-point metal, which is why the coefficient of kinetic friction is used instead of the coefficient of static friction.

5.3 Self-healing performance evaluation of rotary transmission element

The following three items should be evaluated as the performance of a self-healing rotary transmission element.

1. Value of the maximum transmission torque (transmittable torque) of the proposed mechanism
2. Self-healing efficiency of strength by self-healing (reproducibility of transmittable torque)
3. Energy absorption at the time of proposed mechanism breaking

The transmittable torque measures the amount of power that can be transferred, and the energy absorption measures the amount of energy that can protect the robot from collision or overload. The self-healing efficiency is an important factor in evaluating the mechanism's performance since it is closely related to the repeatability of the transmittable torque of the mechanism.

Therefore, the following three experiments were conducted to evaluate the performance of the rotary transmission element.

1. Measurement of transmittable torque
2. Measurement of transmission torque by friction
3. Measurement of energy absorption at the proposed mechanism breaking

In the transmittable torque measurement experiment, the maximum torque loaded on the mechanism was measured to confirm the value of the transmittable torque of the proposed mechanism. In addition, the change in the transmittable torque in the mechanism was measured to confirm the strength could be recovered by self-healing. At the same time, the relationship between the slip angle of shafts A and B and the transmission torque were also measured to investigate the characteristics of the torque transfer due to the mechanism. In the second experiment, the transmission torque by friction was measured to investigate the effect of friction on the transmittable torque of the proposed mechanism. The keyway structure of the proposed mechanism should

always generate the same transmission torque by self-healing. However, friction can be an unstable element. Therefore, the transmission torque due to friction and their stability were measured in order to confirm its effect on the reproducibility of the transmittable torque. The third experiment involved measuring the amount of energy absorption at the time the mechanism broke and examining how the amount of energy absorption changes as the rotating speed of the mechanism is changed.

The relationship between the slip angle of shafts A and B and the load torque of the proposed mechanism was measured in the evaluation experiments using the experimental device shown in Figure 5.6. The proposed mechanism was installed in the experimental device with two bearings such that the axes of rotation of shaft A and shaft B were coincident. In the experimental device, the motor and the torque sensor were connected to the shafts A and B of the proposed mechanism via couplings. Therefore, the torque could be applied to the proposed mechanism by a motor, and the torque could be measured by a torque sensor. The side of the torque sensor that was not connected to the proposed mechanism was connected to the experimental device, and it could not rotate against the device. Hence, an encoder attached to the motor could measure the slip angle between shaft A and shaft B. The minimum angle to be measured by the encoder was 0.001875 degrees. The torque sensor used is a DR-2477 from LORENZ Messtechnik GmbH. The experimental procedure is as follows: Step1-3.

Step 1 Initialize the slip angle and torque sensors of the experimental setup with the proposed mechanism installed but without applying any voltage to the motor.

Step 2 To generate a load torque on the suggested mechanism, the motor is rotated. The rotation speed control adjusts the rotation speed so that it does not exceed a certain value when the torque is loaded in order to keep the conditions at the time of fracture as constant as possible.

Step 3 Since the suggested mechanism's torque transmission is disrupted, the mechanism is heated to self-heal the low-melting-point metal parts. For 20 seconds, induction heating is performed at 12 V, 8.7 A, and 300 kHz. After heating, the mechanism is allowed to cool for at least 10 minutes at room temperature.

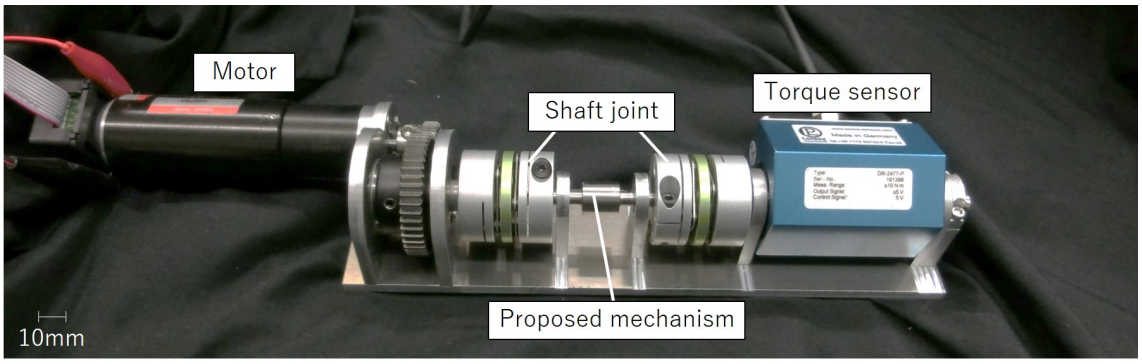

Figure 5.6 Experimental device for measuring torque and sliding angle. Torque and sliding angle are measured using an experimental instrument. Shaft couplings connect a motor and a torque sensor to the proposed mechanism. Because the motor is equipped with an encoder, the slip angle of the proposed mechanism can be measured. The torque sensor is completely fixed to the experimental device and does not move. Therefore, the motor torque and slip angle of the proposed mechanism can be measured.

5.3.1 Measurement of transmittable torque

Steps 1-3 were repeated 30 times to measure the stability of torque transmission performance and the relationship between the transmitted torque and the slip angle of the proposed mechanism shown in Figure 5.3. In step 2, the rotation speed of the motor's output shaft was set to 0.3 deg/s or less, and the rotation angle of the motor was set to 720 degrees or more in order to measure the effect of the slip angle on the transmission torque.

Figure 5.7 shows the values of the transmittable torque and Table 5.1 shows the mean, standard deviation, maximum and minimum values after 30 measurements. The transmittable torque is the value of the maximum torque at each measurement. The minimum and maximum transmittable torques were 2.95 N-m and 3.33 N-m respectively, and the average transmittable torque was 3.11 N-m with a standard deviation of 9.46×10^{-2} N-m. Even after multiple cycles of transmittable torque measurment with self-healing, the transmittable torque did not fall below 2.9 N-m. The standard deviation of the measurements from the 26th to the 30th was also less than 0.1 N-m. Therefore, there was no large fluctuation in the value of the transmittable torque.

Figure 5.8 shows the relationship between the slip angle and the torque applied to the mechanism during a single measurement. When the torque load applied by the motor starts, the torque increases and reaches its maximum value when the slip angle is between 0 and 10 deg. The low-melting-point metal inside the mechanism was

destroyed, and torque transmission became impossible, as shown in state B in Figure 5.5(b). Figure 5.8 shows that after kayway breakage, the torque decreases rapidly and finally reaches a constant value. In this condition, slippage occured between the low-melting-point metal and shaft A, and the torque was transmitted only by friction. In this experiment, the maximum torque was set as the transmittable torque, and Figure 5.8 also shows that the value of the transmittable torque was reached immediately after the slip angle occured. Table 5.2 shows the results of calculating the slip angle when the transmittable torque is measured at each measurement time. The average slip angle of transmittable torque during the 30 measurements was 5.83 °, with a minimum value of 2.15 °, a maximum value of 10.56 °, and a standard deviation of 2.01 °.

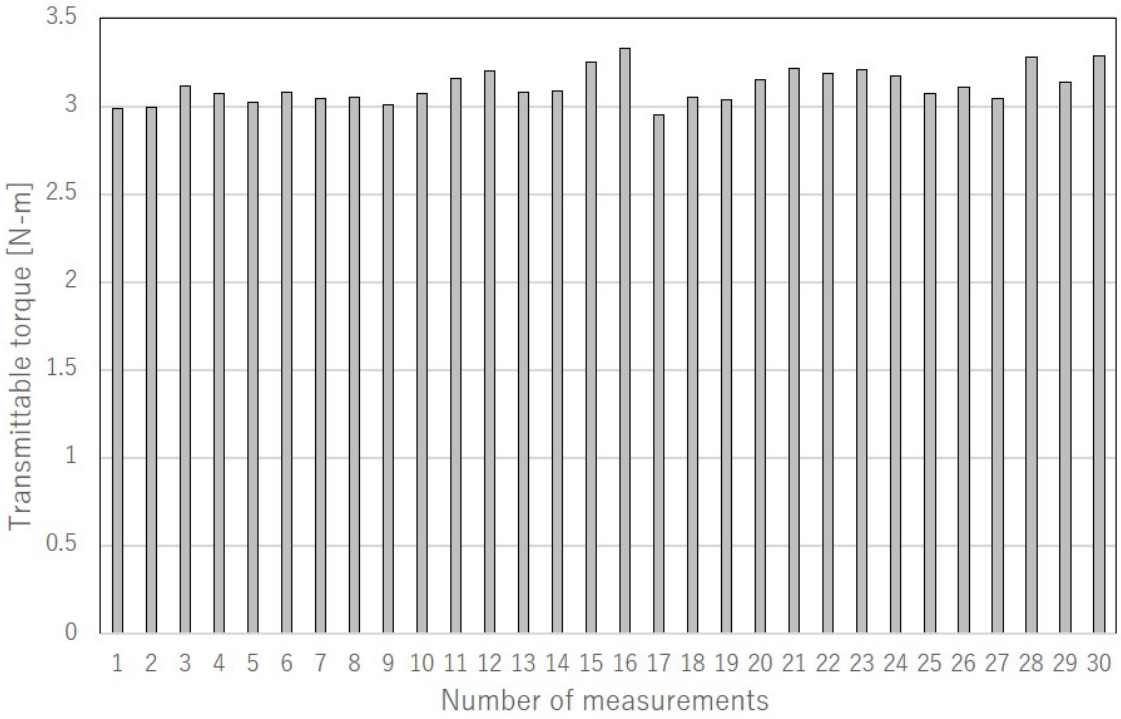

Figure 5.7 Relationship between the value of transmittable torque and the number of self-healing.

Table 5.1 Sliding angle when measuring the transmittable torque

The mean value [N]	3.11
The standard deviation [N]	9.46×10^{-2}
The maximum value [N]	3.33
The minimum value [N]	2.95

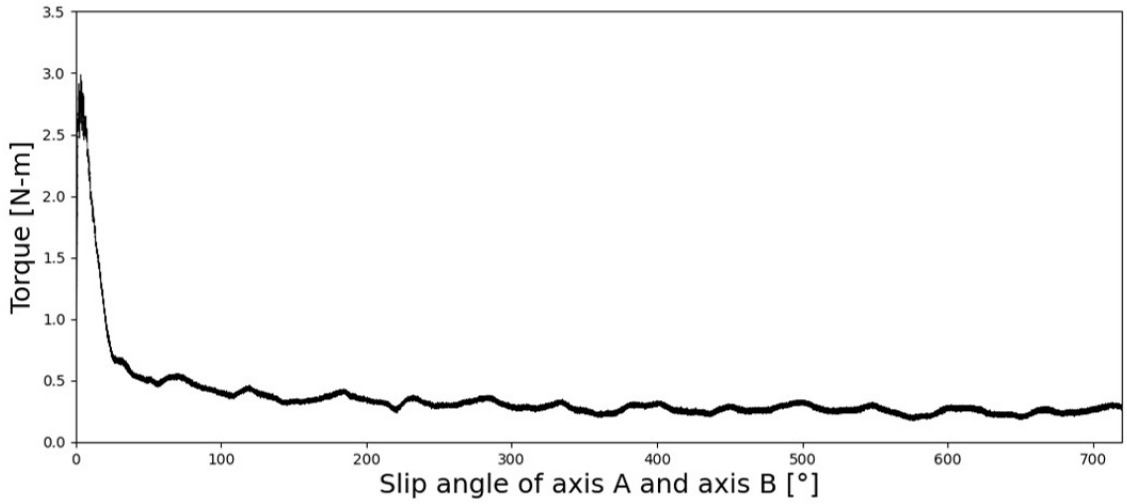

Figure 5.8 Relationship between torque applied to the mechanism and sliding angle.

Table 5.2 Sliding angle when measuring the transmittable torque

Average [°]	5.83
Standard deviation [°]	2.01
Minimum [°]	2.15
Maximum [°]	10.56

5.3.2 Measurement of transmission torque by friction

Figure 5.9 shows a mechanism without keyway structures on shaft A, prepared for an experiment to investigate the effect of transmission torque through friction on the transmittable torque. To quantify the relationship between the slip angle and the load torque, this experimental mechanism was connected to the experimental device shown in Figure 5.6. In step 2, the rotation speed of the output shaft of the motor was set to 7 deg/s or less, and the rotation angle of the motor was set to 720 degrees or more. The measurements were taken 35 times to investigate the trend of torque transmission change due to self-healing.

The results of 35 torque measurements are shown in Figure 5.10. The torque shown in Figure 5.10 is the average of the values from the minimum to the maximum slip angle that may reach the transmittable torque shown in Table 5.2, since this experiment is to verify the effect of friction torque on the transmittable torque.

The transmittable torque tended to increase when the number of self-healings was between 1 and 20. On the other hand, the transmission torque did not fall below 0.6 N-m, and there was no increasing trend after the 21st self-healing measurement. The

average torque from the 16th to the 35th measurements was 8.22×10^{-1} N-m, with a standard deviation of 1.25×10^{-1} N-m. The results of the average and standard deviation calculations for each of the five measurements are shown in Table 5.3. The result in Table 5.3 shows that the standard deviation gradually increased after the 16th measurement, when the torque was stable, at 0.6 N-m or higher.

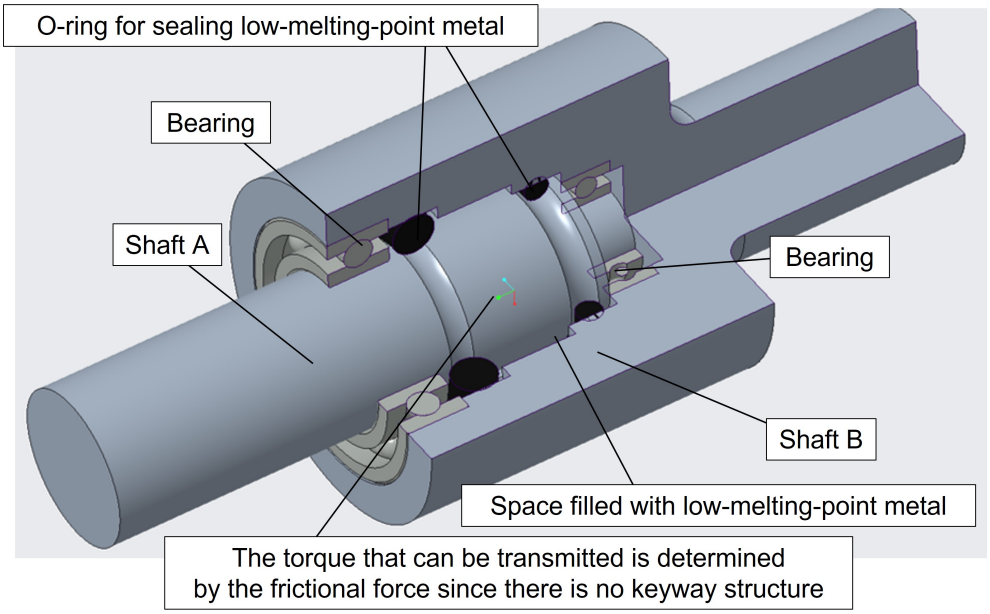

Figure 5.9 Proposal mechanism without keyway structure. The surface of shaft A is smooth to measure the transmission torque by friction. The other structures are identical to Figure 3 except for the surface of shaft A.

Table 5.3 Average values and standard deviation values of five frictional transmision torque measurements each

The number of self-healings	1-5	6-10	11-15	16-20	21-25	26-30	31-35
Average [$\times 10^{-1}$ N-m]	4.64	5.06	5.55	8.48	7.48	8.79	9.03
Standard deviation [$\times 10^{-2}$ N-m]	3.99	1.33	7.11	3.04	4.64	4.25	8.43

5.3.3 Measurement of energy absorption

During the torque interruption, the suggested mechanism is considered to absorb some of the energy required for the breakdown of the low-melting-point metal during the torque interruption. Therefore, by varying the rotation speed of the motor, this experiment measured the relationship between the transmission torque and slip angle and calculated the amount of energy absorption by the proposed mechanism when the torque transmission was interrupted. When the low-melting-point metal parts inside

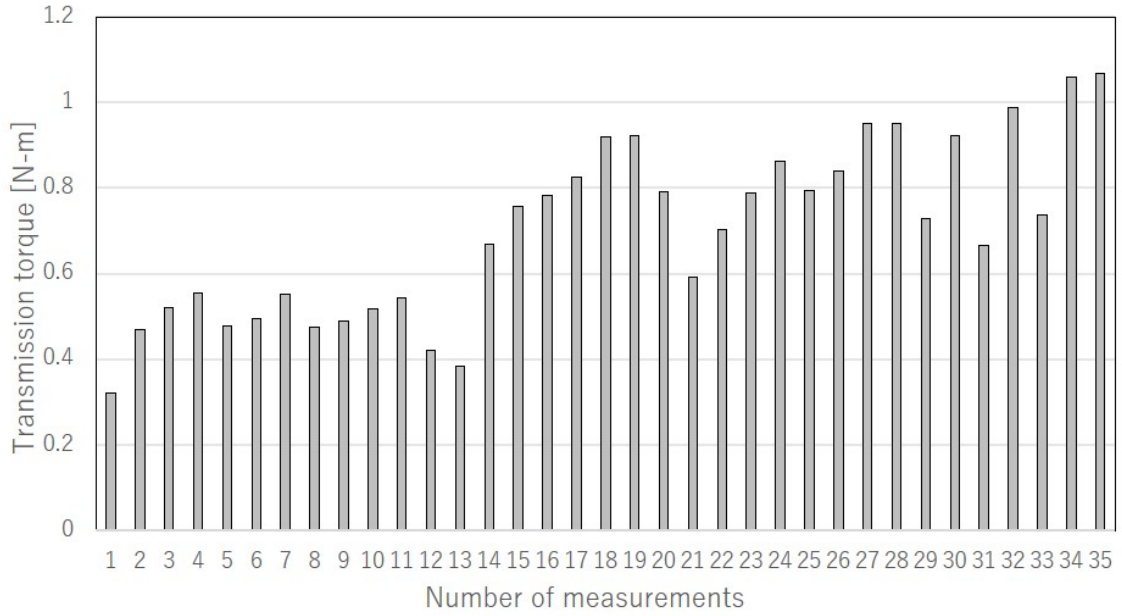

Figure 5.10 Relationship between the value of transmission torque caused by friction and the number of self-healing.

the proposed mechanism were destroyed, the motor was rotated at five different speeds. At each rotation speed, five measurements were taken.

The amount of the energy absorption was calculated using the following Equationb (5.4) based on the motor rotation angle and torque data.

$$Q = \int_0^{\theta_b} T(\theta) d\theta \tag{5.4}$$

Q is the amount of energy absorbed by the proposed mechanism, θ is the slip angle between the proposed mechanism's shaft A and shaft B, and $T(\theta)$ is the torque loaded on the proposed mechanism during the experiment. Figure 5.11 shows the explanation of θ_b. θ_b is the angle at which the keyway structures of the low-melting-point metal part inside the proposed mechanism completely break down. It is difficult to estimate the slip angle when the transmittable torque is measured. Therefore, when the critical cross-section of the keyway structures of the low-melting-point metal part with shaft A does not completely overlap with the critical cross-section of the keyway grooves on the shaft A, the keyway structures are regarded as completely destroyed, as shown in state B of Figure 5.11.

The amount of energy absorption of the proposed mechanism under overload is shown in figure 5.12. The horizontal axis of the Figure 5.12 shows the speed at which shafts A and B slip and rotate when the mechanism is loaded, and the vertical axis is

the amount of energy absorption. The energy absorption of the proposed mechanism increased as the rotational speed under load increased. However, the rate of increase in energy absorption was at most 5% compared to the average, and the overall standard deviation was 9.37×10^{-2} J.

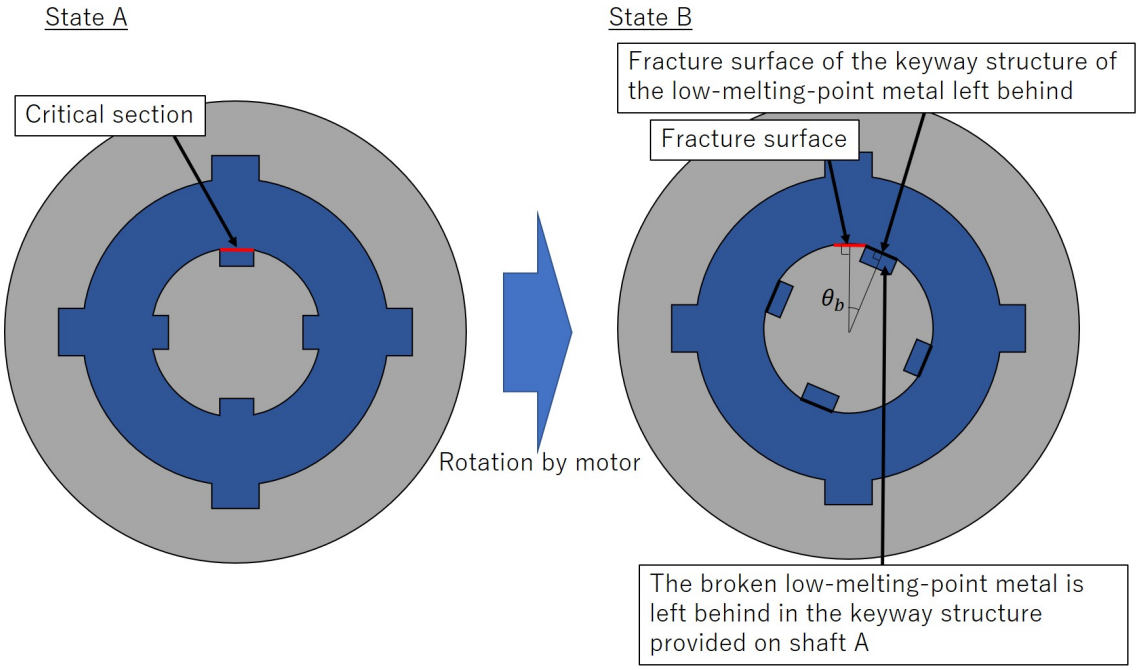

Figure 5.11 State when the keyway structure of a low-melting-point metal is completely destroyed. The angle at which the keyway structures completely break is determined geometrically because determining the angle from the experiment results of transmittable torque measurement was problematic. When the critical section area of the low-melting-point metal part and keyway grooves of shaft A completely cease to overlap, the keyway structures are considered destroyed.

5.4 Discussion

5.4.1 Transmission torque of friction and torque stability

Table 5.4 shows the average and standard deviation calculated from the transmittable torques shown in Figure 5.7 for each of the five self-healing times. The table shows that as the number of self-healings grew, the transmittable torque of the self-healing rotary transmission element increased marginally. In addition, Figure 5.10 shows that when the number of self-healing times increased, the transmission torque by friction increased to 1 N-m. Based on these results, it can be inferred that the cause of the increase in transmittable torque with the increasing number of self-healings was not a change in keyway structure strength but frictional transmission torque. The enlarged views of

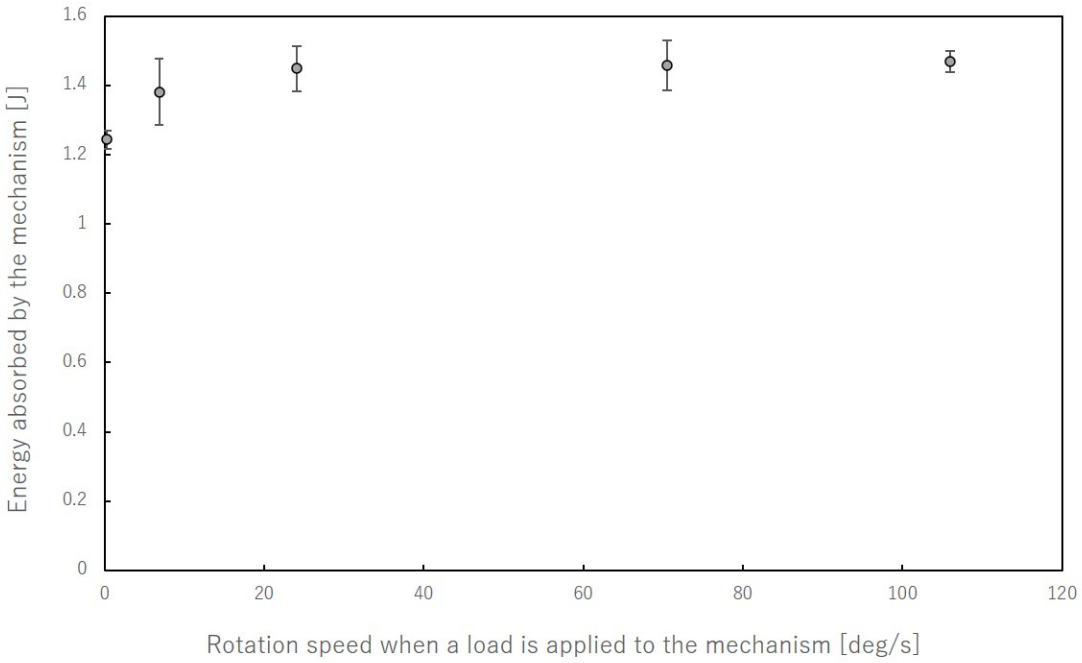

Figure 5.12 Energy absorbed by the mechanism when torque transmission is interrupted.

the surface of shaft A before and after the friction test are shown in Figure 5.13. Since the proposed mechanism was assembled without any modification after the parts were fabricated, the surface property of shaft A before the experiment was rather smooth (Figure 5.13B). However, the surface property was roughened after the experiment by sliding with the low-melting-point metal, resulting in the formation of unevenness (Figure 5.13C). The reason why the transmission torque by friction increased as the number of self-healings increases that the frictional force increases by the deterioration of the surface properties as the shaft is rubbed by friction. Next, the number of self-healing cycles until the transmission torque stops increasing is compared. It can be seen that more than 15 self-healings were required before the transmission torque reached a constant value in the experiment measurement of the transmission torque by friction from Table 5.3. On the other hand, the torque became a constant value after about 10 measurements of the transmittable torque, including the keyway structure from Table 5.4. This is because the cross-section where the keyway structures were destroyed had a worse surface than the other surface, and the areas around the shear failure were deformed by plastic deformation, which increased the pressure generated between shaft A and the low-melting-point metal. Therefore, the slippage distance required before the surface properties of shaft A affect the transmittable torque is smaller than when

only friction was measured.

The maximum difference in the transmittable torques values between the 30 measurements in Figure 5.7 is 3.74×10^{-1} N-m. This means that a torque difference of about 12% compared to the average value has occurred. This torque difference was caused by the above-mentioned transmission torque via the friction effect. The friction torque difference in Figure 5.10 was 6.83×10^{-1} N-m. Because the keyway structure section did not generate any transmission torque due to friction, the difference in transmission torque was larger than the difference in transmittable torque measured with the keyway structure. Therefore, the frictional transmission torque had a greater impact on the apparatus for measuring friction effect, which had more friction surfaces. The friction area of shaft A with the keyway structure was 54.3 mm^2, and the area of shaft A for friction torque measurement was 75.2 mm^2 each. Therefore, the effect of friction in the measurement of the transmittable torque is considered to be about 70% of that in the measurement of the transmission torque due to friction. Furthermore, the standard deviation value was larger for the 11th to 30th measurement than for the 1st to 10th measurement in Table 5.4. Table 5.3, which shows the transmission torque due to friction, also shows a tendency for the fluctuation of the torque value to increase as the number of self-healings increased. Therefore, the cause of the increasing fluctuation of the value of the transmittable torque with the increase in the number of self-healings could be attributed to the effect of the transmission torque due to friction. The value of the transmission torque by friction was about 0.9 N-m at most, which was about 1/3 of the transmittable torque. In addition, the frictional transmission torque fluctuation was about 0.6 N-m. Hence, the maximum transmittable torque fluctuation of the proposed mechanism is estimated to be ±9.5%.

Table 5.4 Average values and standard deviation values of five transmittable torque measurements each

The number of self-healings	1-5	6-10	11-15	16-20	21-25	26-30
Average [N-m]	3.04	3.05	3.15	3.10	3.17	3.17
Standard deviation [$\times 10^{-2}$ N-m]	4.79	2.67	6.58	12.8	5.02	9.73

5.4.2 Transmission torque and slip angle

Figure 5.14 shows an enlarged graph of the graph in Figure 5.8 when the slip angle is from 0 ° to 40 ° in order to confirm what happens when the slip angle is small in

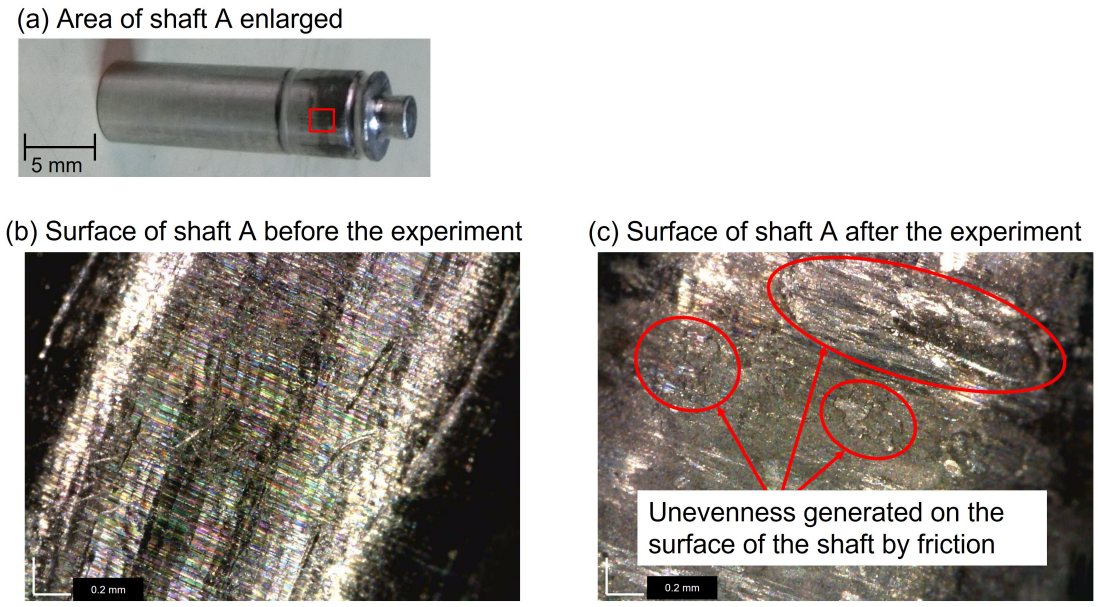

Figure 5.13 Enlarge surface of shaft A: (b) before the experiment, (c) after the experiment. The only irregularities in (b) are the cutting marks from machining, whereas in (c), the irregularities generated by rubbing against low-melting-point metal are visible.

the evaluation experiment of the self-healing rotary transmission element. The torque increases rapidly from 0 to 2 ° focusing on the slip angle between 0 and 10 °, and remained constant at around 2.75 N-m from 2 to 10 °. The reason for the sudden increase in the torque value from 0 ° to 2 ° is that the low-melting-point metal part in the mechanism and the keyway structure of shaft A started to be loaded, and the reason for the constant torque value from 2 ° to 10 ° is that the sliding angle increased while the keyway structure of the low-melting-point metal part gradually broke down. Bi-26In-17Sn which is used in the proposed mechanism is a ductile material which has caused the behavior of the torque value to become constant after a sudden increase in torque. The phenomenon that the value of the slip angle fluctuated between 2 ° and 10 ° when the transmittable torque was measured was caused by the fact that the measured torque reached its maximum value in the process of breaking the keyway structures of the low-melting-point metal part. Therefore, the fact that the sliding angle when the transmittable torque is measured is not perfectly constant is a characteristic of this mechanism. The torque value then gradually decreased until the slip angle reached around 25 °, due to the progressive breakdown of the keyway structures of the low-melting-point metal part. Furthermore, as the slip angle increased, the torque amount stayed constant because the friction generated in the mechanism caused the transmission torque.

Figure 5.15 shows the graph of the relationship between the slip angle of shaft A and shaft B and the torque measured in the experiment of measuring the transmission torque by friction to confirm the relationship between the transmission torque generated by friction and the slip angle, and Figure 5.16 shows an enlarged graph of the area where the slip angle is around 0 °. When the slip angle was around 0 °, the torque rose with nearly no slippage between shafts A and B, as shown in Figure 5.16. When the torque exceeded a particular threshold, slippage occurred between shaft A and the low-melting-point metal part, causing the transmission torque to drop. This is because a shift in the main factor of torque transmission from static friction force to dynamic friction force (Figure 5.16). The play of the transmission part of the experimental machine, such as the coupling and gear, generated a modest variation in the slip angle under static friction force. When torque transmission by dynamic friction force was continuously performed, the transmission torque steadily decreased (Figure 5.15). Each measurement corroborated the phenomenon that the torque decreased as the sliding angle between shafts A and B increased. The torque decreased is caused by low-melting-point metal powder that becomes the rotating body by the rubbing of the low-melting-point metal parts and shaft A. Figure 5.17 shows that the powder of low-melting-point metal was adhered to the shaft A after the experiment. Since the magnitude of the transmittable torque was recovered in each test, the powder seems to have melted during the heat of the self-healing mechanism and been integrated with the low-melting-point metal part.

5.4.3 Energy consumption

Although the amount of energy consumed by the proposed mechanism increased when the rotation speed was increased at the time of torque transmission interruption, the rate of increase was about 20% as a result of the torque interruption. The energy required for the breakdown of the keyway structures of the low-melting-point metal is absorbed. An enlarged view of the fracture surface of the keyway structure of the proposed mechanism is shown in Figure 5.18. The figure shows that large irregularities formed on the fracture surface and infers that very large plastic deformation occurred. In other words, during overload, the low-melting-point metal parts underwent ductile deformation, and most of the energy absorption occurred through plastic deformation.

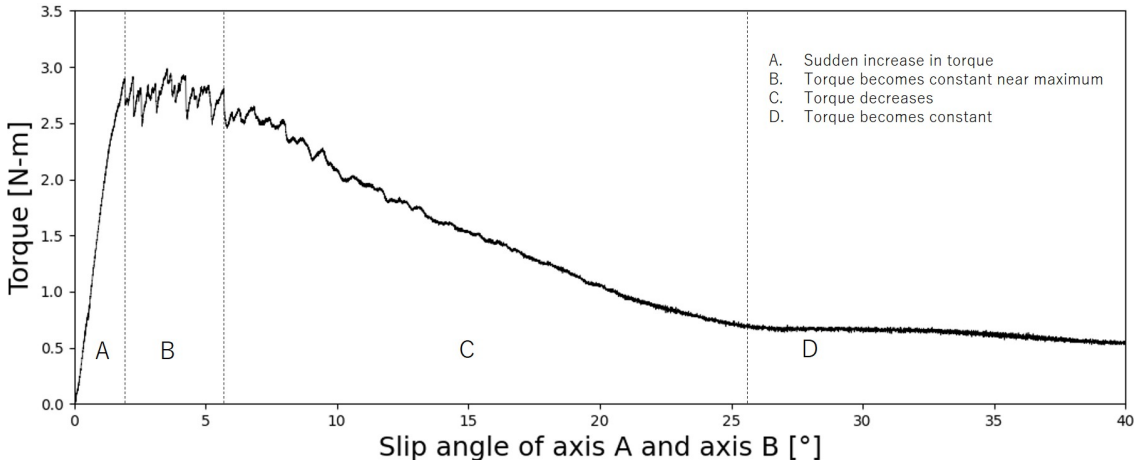

Figure 5.14 Relationship between transmission torque and slip angle of shaft A and B when the sliding angle is 0 ° to 40 °. When the slip angle is 0 ° to 2 °, the transmission torque is suddenly increase. When the slip angle is 2 ° to 5 °, the torque is constant value around 2.75 N-m. When the slip angle is 2 ° to 25 °, the torque gradualy decrease. When the slip angle is over 25 °, the torque is approximately constant value.

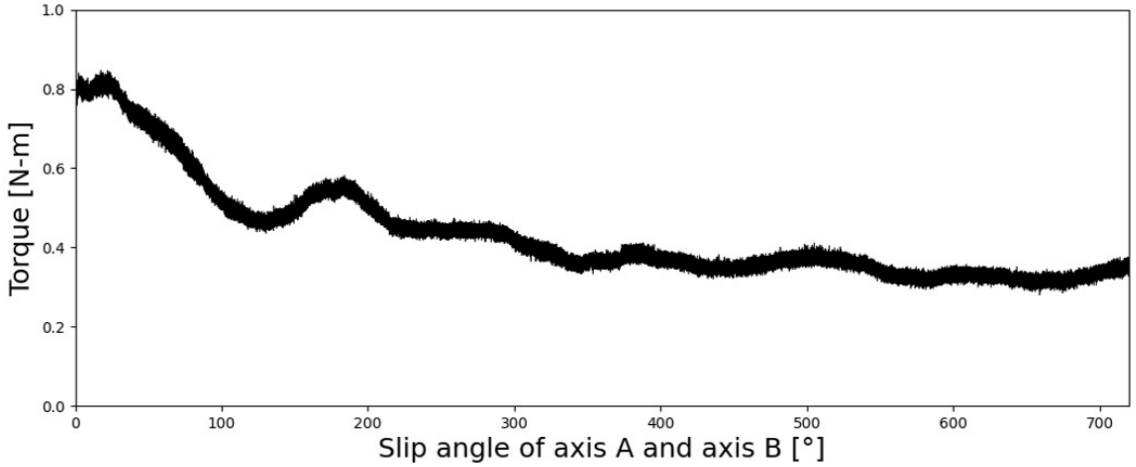

Figure 5.15 Relationship between frictional transmission torque and slip angle of shaft A and B when the sliding angle is 0 ° to 720 °. The torque is gradually decreasing and eventually becoming constant.

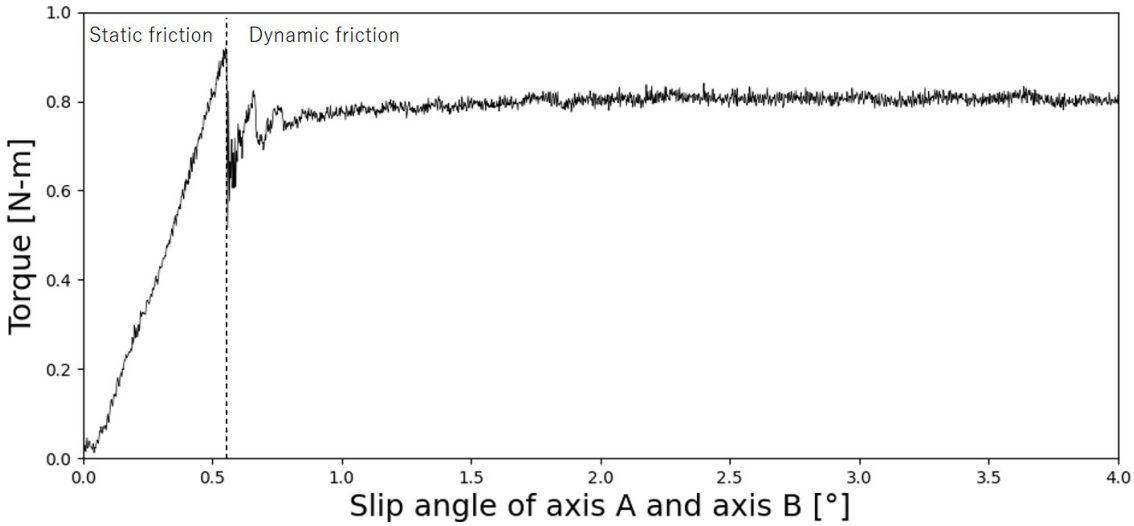

Figure 5.16 Relationship between transmission torque by friction and slip angle of shafts A and B when the sliding angle is 0 ° to 5 °. The transmission torque is caused by static friction at first, and the torque switches to dynamic friction when the slip angle exceeds a certain level.

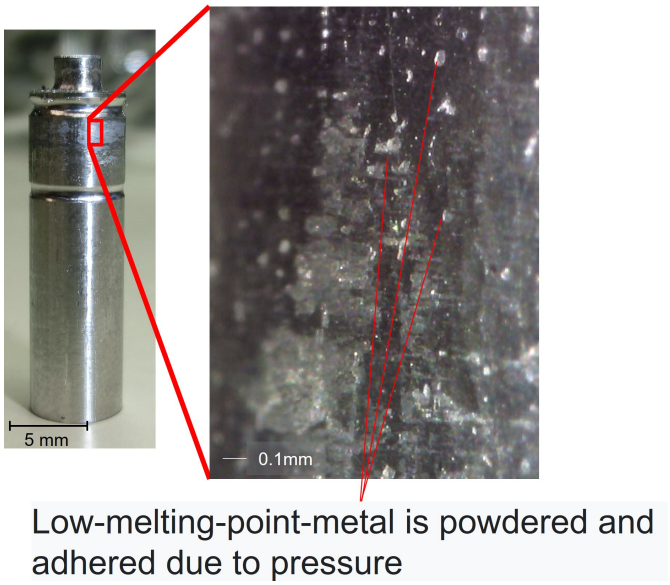

Figure 5.17 Low-melting-point metal powder adhering to shaft A. The left picture is shaft A, and the right picture is an enlarged view of the surface of shaft A.

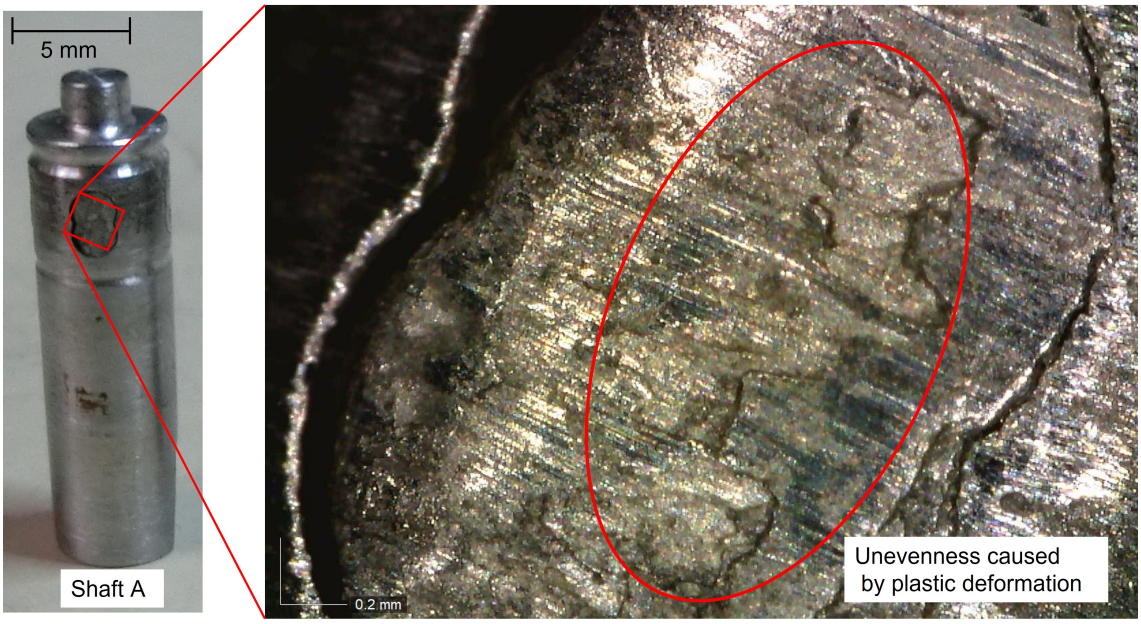

Figure 5.18 Fracture surface of keyway structure. The left picture is shaft A, and right picture is an enlarged view of the keyway structure. The fracture surface of the low-melting-point metal is uneven, indicating that a large plastic deformation has occurred.

5.4.4 Theoretical and real transmission torque

The parameters, such as the shear strength of Bi-26In-17Sn, a low-melting-point metal used in this dissertation, and the transmittable torque determined by the calculated keyway strength, are shown in Table 5.5. The value of T_{key} calculated by equation (5.2) using the parameters in Table 5.5 is 2.31 N-m, which is about two-thirds of the actual measured transmittable torque. Equation (5.3) which calculates T_f used the coefficient of dynamic friction to calculate the transmission torque due to friction. The maximum load torque of the proposed mechanism with the keyway structure occurred when shafts A and B had a slight slip angle, as shown in figure 5.14. Because the kinetic friction force is acting when measuring the transmittable torque, the use of the dynamic friction coefficient in Equation (5.3) is correct. However, the surface pressure generated on shaft A is difficult to measure, and the coefficient of dynamic friction varies depending on the surface properties of shaft A. Therefore, experiments must be conducted in order to confirm the transmission torque related to frictional force. Experiments in this dissertation revealed that the transmission torque due to friction was estimated to be 0.4 to 0.9 N-m.

Table 5.5 Parameters and calculated results of the transmission torque based on the keyway structure

n	4
r [mm]	3.0
A_{key} $[mm^2]$	5.22
τ_{max} [MPa]	42.0
T_{key} [N-m]	2.31

5.4.5 Supercooling of low-melting-point metal

The proposed mechanism uses the melting–solidification phenomenon of low-melting-point metals to perform self-healing. Because of the use of induction heating, the phase change from solid to liquid occurred quickly. On the other hand, the mechanism did not have a special cooling operation. In addition, when induction heating was done, the air around the proposed mechanism was heated, and the proposed mechanism was sealed by the resin guide and bearing for the heating coil installation, so that the proposed mechanism was insulated by an air layer. Therefore, the cooling of the proposed mechanism requires more time than usual.

Supercooling may occur when materials transition from the liquid to the solid phase. Supercooling is a phenomenon in which the temperature of materials decreases while they remain a liquid without changing phases, even when their temperature is below the freezing point. Metals undergo supercooling as well. In particular, the cooling of the low-melting-point metal inside the proposed mechanism was slow, indicating that this is a temperature change where supercooling is likely to occur. Supercooling has an effect on the ductility and strength of metallic materials. Therefore, supercooling has an effect on the performance of the proposed mechanism.

Bi-26In-17Sn, a eutectic alloy, is the low-melting-point metal used in this dissertation. Eutectic alloys are characterized by their resistance to undercooling because the concentration fluctuations in the liquid act as nucleation sites for solidification [128]. In addition, the proposed mechanism was designed with a low-melting-point metal surrounded by shafts A and B made of stainless steel (SUS303). Therefore, because they are impurities for the low-melting-point metal, shaft A and shaft B could be regarded as nucleation sites. Hence, undercooling is considered to be even less likely to occur. In summary, supercooling is expected to have little effect on the mechanism's performance, such as torque performance.

5.5 Conclusion

This chapter developed and evaluated a self-healing rotary transmission element based on the melting–solidification phenomenon. In the evaluation experiment, the transmittable torque and self-healing efficiency were measured using an experimental device. As a result, the transmittable torque was proven to be around 3 N-m, the self-healing time was only 20 s, and no reduction in transmittable torque occurred after multiple self-healing cycles. It was also confirmed that the transmittable torque of the mechanism was affected not only by the healing material's strength but also by the friction generated between the healing material and the structural parts. In addition, the fracture of the healing material of the low-melting-point metal resulted in an energy absorption of approximately 1.5 J. Furthermore, theoretical considerations of the transmittable torque shows that the transmittable torque of rotary transmission elements is proportional to the contact area of healing materials and structural materials, the strength of healing materials, and the diameter of the component made of the structural materials.

Chapter 6

Robot joint with self-healing rotary transmission elements

6.1 Introduction

The self-healing rotary transmission element established in the previous chapter, which utilizes the melting–solidification phenomenon of a low-melting-point metal, is adapted to a joint of a robot in this chapter. Because the developed rotary transmission element has no backlash and great rigidity, the rotary transmission element can be installed on high-precision robots. However, due to the melting–solidification phenomenon, the mechanism must be able to withstand the heat generated by self-healing. Therefore, the temperature immediately after the proposed mechanism's self-healing was measured, and the results were reflected in the design of the robot joint. In addition, the transmittable torque of the transmission element is as small as 3 N-m. Therefore, it was necessary to design a robot joint that could be driven even by the transmission element. As a result, the robot joint was designed to be able to output the required torque using a reduction mechanism.

6.2 Adaptation of a rotary transmission element in a robot joint

6.2.1 Effects of heat generated during self-healing

The temperature of the rotary transmission element after self-healing was measured in order to estimate the effects of the heat generated by induction heating on the sur-

rounding environment. Figure 6.1 shows two measurement points. The center surface of the structure that seals the low-melting-point metal of shaft B is the measuring point 1. The measurement point has the highest temperature of all the locations that can be measured since it is where induction heating occurs. The measurement point 2 is the surface of the output part of shaft A. This is the point where the rotary transmission element comes into contact with other mechanical elements, and therefore has the greatest impact on the surrounding mechanisms. A thermocouple was used to measure the temperature 10 seconds after the induction heating was applied. This 10-second period was necessary to remove the coil installation guide. The measurement results show that measurement point 1 had a temperature of 118 °C and measurement point 2 had a temperature of 94 °C. Since the heat resistance temperature of many mechanical components exceeds 100 °C, there is no need to demand special heat resistance performance in the robot design in order to adopt the suggested mechanism. However, some resin parts have low heat resistance. To employ these resin parts, it is necessary to take measures such as separating them from the proposed mechanism .

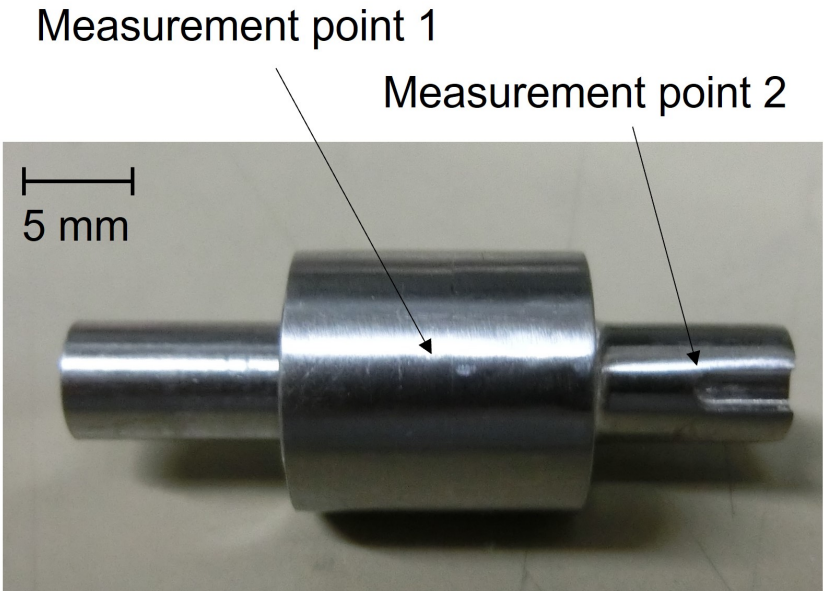

Figure 6.1 The rotary transmission element's temperature measurement sites. The figure shows the location of the temperature measured immediately after self-healing. Because it is directly heated by induction heating, temperature measuring point 1 is directly under the coil and is expected to be the most affected by the heat generated for self-healing. Measurement location 2 is chosen because it is the connecting point with the shaft joint and therefore has the most influence on the mechanical design.

6.2.2 Structure of a robot joint

Figure 6.2 shows a robot joint equipped with a rotary transmission element. The robot joint is connected by 270mm frames, and the distance from the joint rotation axis to the ends of the frames is 300 mm. The robot joint weighs around 2.5 kg. Figure 6.3 shows a picture of the mechanism with the joint area enlarged. The joint consists of a motor, a rotary transmission element, and a joint drive unit, all of which are connected via gears. Because an encoder is linked to the motor, the drive angle of the robot joint can be measured. The reduction ratio from the motor to the proposed mechanism is 2, and the reduction ratio between the proposed mechanism and the joint drive shaft is also 2. Therefore, the motor can generate the necessary torque to destroy the low-melting-point metal part inside the proposed mechanism. In addition, the proposed mechanism can be loaded with twice the transmittable torque to drive the joints. Shaft joints connect the proposed mechanism and the two gears. These shaft joints are used at temperatures of more than 100 °C to withstand the heat generated by the proposed mechanism during self-healing. A coil is wrapped around the proposed mechanism to perform self-healing by induction heating, and a Zero Volt Switch (ZVS) circuit is connected to the coil.

6.3 Evaluation of the self-healing robot joint

Figure 6.4 shows the evaluation experiment setting of the robot joint. One side of the frame of the robot joint was fixed on the base (Figure 6.4a). A weight installation component was mounted to the other end of the frame (Figure 6.4b). A weight of 1 kg was connected to this part that generated a maximum load of approximately 3 N-m on the robot joint. A microcontroller connected to a motor driver controlled the motor used to drive the joint, and the drive angle was controlled using Proportional-Integral-Differential (PID) control.

This evaluation experiment confirms that the robot joint equipped with the proposed mechanism can be driven and can self-heal its strength by utilizing the melting–solidification phenomenon of low-melting-point metals. The evaluation experiment was conducted in the four steps listed below.

Step 1 The weight is lifted by the motor until the robot joint reaches a posture that

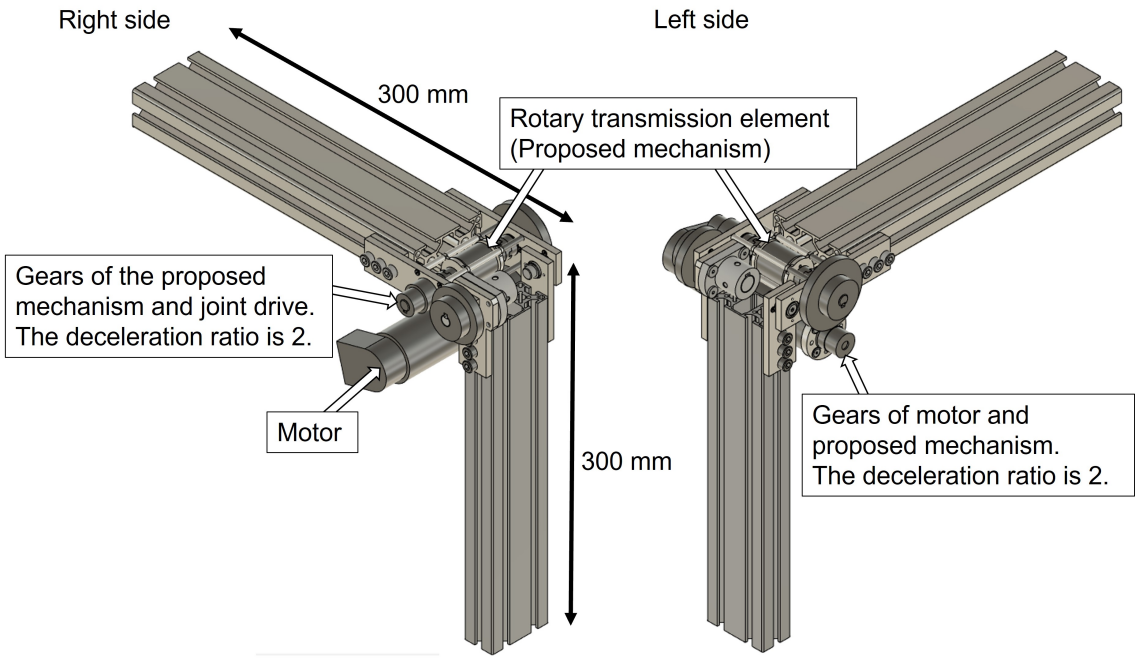

Figure 6.2 Robot joint that equipped with self-healing rotary transmission element. The figure is divided into two parts, one showing the right side of a robot joint and the other showing the left side. The proposed mechanism connects the input shaft to the motor through gears with a reduction ratio of 2, and the output shaft to the joint drive shaft via gears with a reduction ratio of 2. The joint is 300 mm from the tip of the robot frame, and the total weight of the robot joint is about 2.5 kg.

places the most load on the joint. This operation is repeated three times to confirm that the rotary transmission element can withstand the weight load. The robot joint is then fixed in the extended state by controlling the motor.

Step 2 Another weight of 2 kg is dropped on the tip of the robot joint, overloading and destroying the rotary transmission element. To ensure that the torque transmission mechanism has been completely cut off and the robot joint has been destroyed, use the motor to lift the weight in the same way as in Step 1. If the torque transmission of the rotary transmission element is cut off at this time, the robot joint cannot lift the weight.

Step 3 Power is applied to the ZVS circuit to generate inductive heating in the torque transmission mechanism in order to self-heal the mechanism's low-melting-point metal part. As in the self-healing mode, induction heating is performed for 20 seconds at 12V, 8.7A, and 300kHz. After heating, the rotary transmission element is left at room temperature for 30 minutes to dissipate the heat.

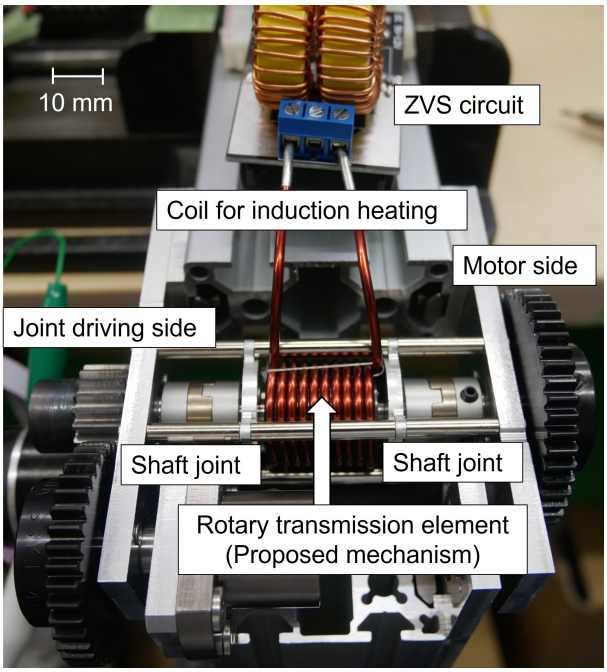

Figure 6.3 Detailed view of a robot joint. Shaft joints connect the input and output shafts of the rotary transmission element and gears. The shaft joint has a heat resistance temperature of more than 100 °C to withstand the heat generated during self-healing of the proposed mechanism. The proposed mechanism is covered by the coil in this figure. This coil is connected to the Zero Volt Switch (ZVS) circuit for induction heating.

Step 4 Perform exactly the same operation as in Step 1 to confirm if the rotary transmission element can withstand the load.

The evaluation experiment is shown in Figure 6.5. Step 4 is omitted because the robot joint works the same as in Step 1. The Figure 6.5a and 6.5b of Step 1 respectively show the joint in bending with no load on the rotary transmission element and the joint in extending with the most load on the mechanism. It was confirmed that the torque transmission mechanism did not break even when the joint was stretched and the load was applied, and that it followed the control of the motor. At this time, a current of about 650 mA was flowing in the motor. Figure 6.5a and b of Step 2 show the dropping of the weight and the driving of the motor after the destruction of the joint. When the weight dropped on the frame of the robot joint, the low-melting-point metal in the rotary transmission element was destroyed, and the power of the motor was not sufficiently transmitted to the joint. The weight attached to the frame could be lifted slightly, as shown in Figure 6.5b of Step 2, because the rotary transmission element could transmit a small torque by friction even when the low-melting-point metal part in the mechanism was broken. However, when the load torque was high,

slippage occurred between the input and output shafts of the rotary transmission element, and lifting the weight was no longer possible until the joint was fully extended, as it was in Step 1. The current flowing through the motor was also small, about 120 mA, indicating that after the mechanism was damaged, power transmission was interrupted. Step 3 in Figure 6.5 shows the rotary transmission element self-healing via electromagnetic induction. The rotary transmission element cannot transmit torque when the low-melting-point metal inside the mechanism becomes completely liquid due to electromagnetic induction. Therefore, the power transmission between the motor and the joint drive was completely released. When this state was reached, heat dissipation allowed the mechanism's low-melting-point metal to solidify, and self-healing was complete. In Step 4, it was confirmed that the self-healing worked effectively because the robot joint could bend and stretch. The evaluation experiment was exactly the same as in Step 1, and the current flowing to the motor is about 650 mA, the same as before the destruction, and the weight can be lifted to the position where the joint is stretched. The evaluation experiment confirmed that the self-healing mechanism in the robot joints can repair the function of a robot joint that is destroyed and becomes inoperable due to an overload and make it operable again through the self-healing process.

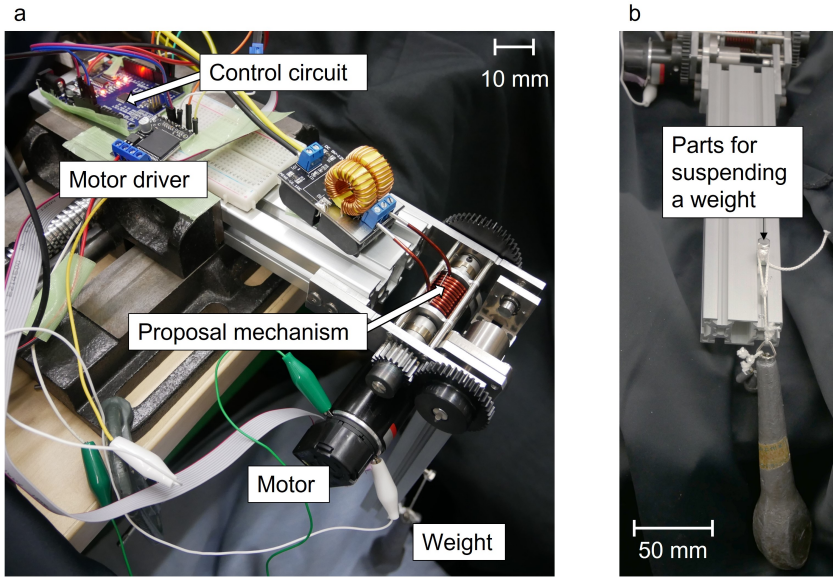

Figure 6.4 Evaluation experiment setting of the robot joint. The figure on the left shows one of the frames connected to the joint being clamped and fixed to the base. A ZVS circuit, a motor driver, and a control circuit are installed on this frame. The right figure shows the point of the opposite frame. A 1 kg weight is attached to the end of this frame, and as the joint stretches, a load is generated in the rotary transmission element.

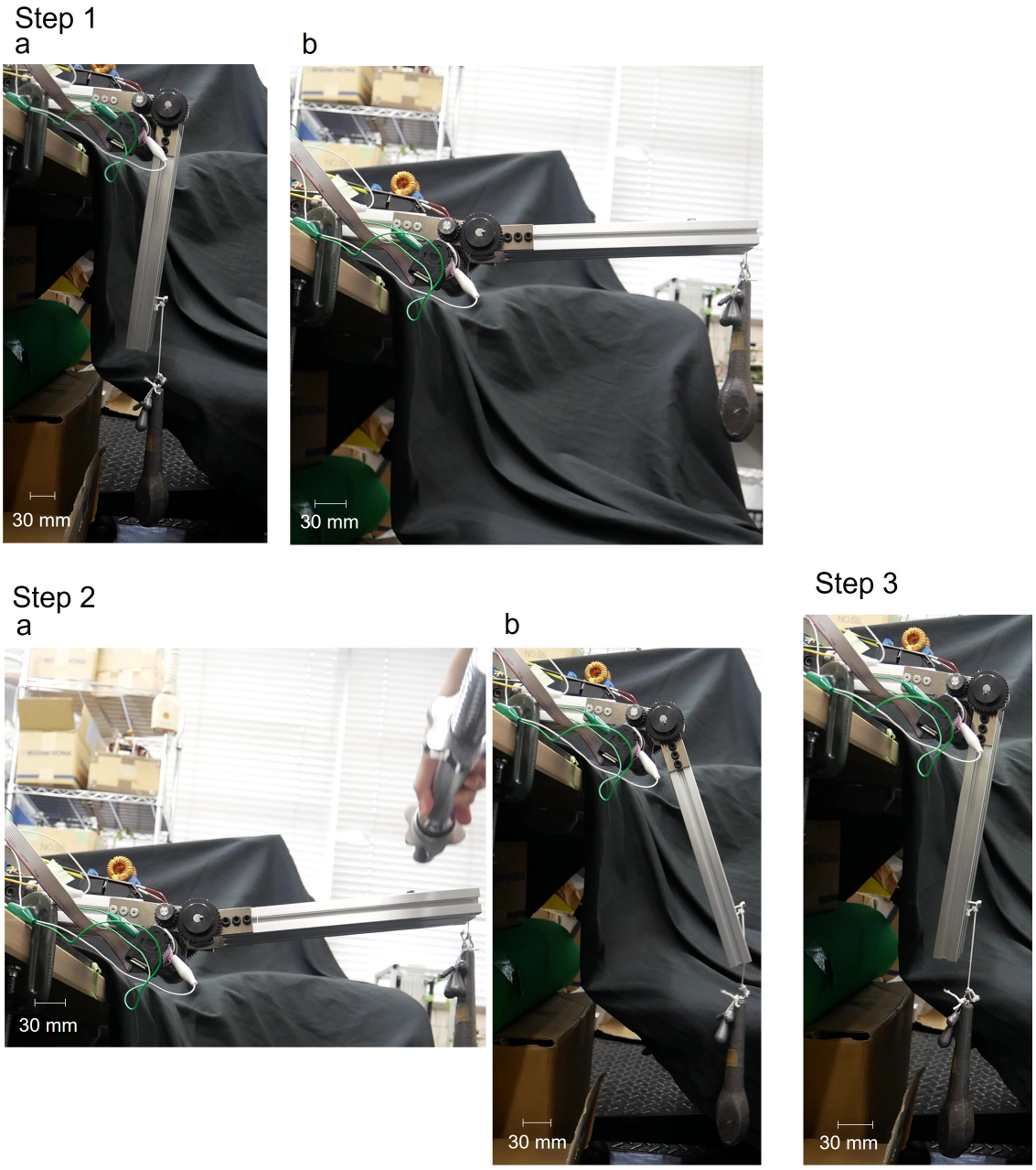

Figure 6.5 Evaluation experiment of the robot joint operation. Step 4 is omitted because it duplicates Step 1. Step 1 shows that the rotary transmission element is working properly and that the robot joint is stretched while lifting the weight. Step 2 shows the rotary transmission element being destroyed by dropping another weight and the attempt to extend the joint. After the rotary transmission element is destroyed, the weight is lifted only slightly due to the slight torque transmission by friction in case b. Step 3 shows the self-healing process. Even after the breakdown of the low-melting-point metal pieces, a small amount of torque transmission occurred due to friction. The input and output shafts are completely opened when the low-melting-point metal inside the mechanism melts and liquefies.

6.4 Operation continuity of the self-healing robot joint

By incorporating a self-healing rotary transmission element into a robot joint, it is confirmed that the joint could re-operate by self-healing even after it is destroyed by the overload. Due to the damage caused to transmission elements or actuators because of overloads and impact loads, normal robot joints require manual maintenance. However, by adding self-healing capability to the robot joints, the robot can heal the fracture and re-operate on its own. In other words, the self-healing capability enables the robot to continue operating without human intervention.

6.5 Conclusion

Based on the melting–solidification phenomenon of low-melting-point metals described in the previous chapter, this chapter developed a single-axis robot joint equipped with a self-healing rotary transmission element. The developed robot joint was used to conduct evaluation experiments on the joint flexion and extension, behavior due to overload, and self-healing function. Hence, it was possible to drive the joint equipped with the proposed transmission element. It was also confirmed that the joint function can self-heal even if the torque transmission mechanism of the joint is destroyed due to an overload and the joint becomes inoperable. Therefore, a self-healing rotary transmission element can be mounted to give the robot joint self-healing function.

Chapter 7

Conclusion

7.1 The achievements of this dissertation

This dissertation focuses on robot self-healing and develops a high-strength healing approach adaptable to robot systems based on the melting-solidification phenomenon. In addition, self-healing transmission elements were developed, and their self-healing performance was evaluated. Furthermore, the proposed mechanisms were mounted on robot systems to evaluate their self-healing capabilities. The achievements obtained in each chapter of this dissertation are listed below.

Chapter 1 summarized previous research aimed at achieving robotic systems that could continue to operate without human intervention and described the position of research on robot self-healing. This chapter also summarized research on self-healing materials and robot systems, pointed out the similarities between self-healing methods for materials and robot systems, and described the differences between the two methods. At the end of this chapter, it was shown that a self-healing method with high-strength was needed for the robot to self-heal.

Chapter 2 showed that providing self-healing performance to the transmission element was effective for self-healing robot. In addition, melting-solidification phenomena were proposed as a self-healing method for robot systems by organizing related research based on strength and self-healing efficiency. Moreover, the chapter concluded with an explicit description of design methodology for adapting melting-solidification phenomena to robot systems and the design of self-healing transmission elements.

Chapter 3 developed an actuator unit incorporating a linear transmission element with self-healing performance using the melting-solidification phenomenon and eval-

uated its self-healing performance. The reason for using an actuator unit instead of only a transmission element was that a linear transmission element required actuation for the self-healing process. In the first step of the evaluation experiments, the self-healing time that affected the self-healing efficiency was estimated by thermal simulation. Subsequently, self-healing cycles were repeated to measure the transfer force of the self-healing transmission element, and the transmittable force and self-healing efficiency were evaluated. These evaluation experiments showed that the self-healing linear transmission element could self-heal multiple times without loss of strength with the proper self-healing process.

Chapter 4 evaluated the self-healing performance of the single tendon-driven robot joint with the actuator unit developed in Chapter 3. A wire attachment mechanism and a length adjustment mechanism were additionally installed in order to attach the actuator unit to the tendon-driven mechanism. In the evaluation experiment, it was confirmed that the robot joint that broke because of an overload generated by a weight drop could self-heal. This evaluation experiment revealed that the linear actuation robot system had self-healing performance by adding self-healing capability to the transmission element.

Chapter 5 developed a rotary transmission element with self-healing performance using melting-solidification phenomenon and evaluated its self-healing performance. The self-healing time of the self-healing rotary transmission element was reduced by adopting induction heating for the self-healing process. In the evaluation experiments, transmittable torque and self-healing efficiency were evaluated by repeating torque measurements and self-healing cycles on an experiment device with an actuator. The results showed that the transmission element could self-heal after 30 self-healing cycles without deterioration of strength.

Chapter 6 evaluated the self-healing performance of a single robot joint with a self-healing rotary transmission element developed in Chapter 5. The robot joint design for installing the self-healing transmission element and the effect of temperature on the surrounding mechanical components during the self-healing process were discussed. In the evaluation experiment, it was shown that the robot joint broken by overload could re-operate by self-healing using induction heating for melting low-melting-point metal. This evaluation experiment showed that the rotary actuation robot system had self-healing performance by adding self-healing capability to the transmission elements.

7.2 Self-healing robot design theory using melting-solidification phenomenon

There were two mechanical design requirements to introduce self-healing into a robot system using the melting-solidification phenomenon, and two solutions were presented for each requirement. However, healing materials are assumed to be able to self-heal by re-forming the broken bonds of molecular atoms via the melting-solidification phenomenon.

Requirement1 Combining healing material with structural material since the entire mechanism cannot be composed of the healing material.

1. Utilize the atomic or molecular bonds that occur between healing and structural materials.

2. Utilize the mechanical bonding that occurs between healing and structural materials.

Requirement2 Preventing melted healing material from leaking out of the mechanism during self-healing.

1. Use healing materials with high viscosity during melting for self-healing.

2. Structurally seal the healing material.

The first requirement is discussed initially. By satisfying this requirement, mechanisms that use the melting-solidification phenomenon as a self-healing method are achievable, using two types of materials: the healing material that melts for self-healing and the structural material that constitutes the mechanism. When two different materials are used to build a mechanism, the strength of the mechanism is related to the strength of the two materials and the bonding force between them. In this scenario, the bonding force is usually the weakest. To create a high-strength self-healing mechanism, a high bonding force between the healing material and structural material is required. This dissertation used atomic or molecular bonding to formulate the force Equation (1) in the development of a linear transmission element in Chapter 3 and mechanical bonding to formulate the force as Equations (1), (2), and (3) in the development of a rotatory transmission element in Chapter 5. The binding force was expressed as

the product of area, such as the critical section and contact area, and material stress in these equations. This means that the strength of self-healing mechanisms using melting-solidification phenomena can be increased by expanding the area involved in bonding and enhancing the healing material's strength.

The second requirement is then discussed. This requirement is necessary to prevent defects from occurring in the healing material or in the bond between the healing material and the structural material due to leakage of the healing material and to achieve high self-healing efficiency. Experiments on the self-healing performance evaluation of the linear transmission element using thermoplastic resin showed that the method of using a material with high viscosity when melted for the healing material, which was mentioned as a solution to requirement 1, could prevent a rapid decrease in the self-healing efficiency. However, the experiments also showed that the healing material outflow could not be completely prevented. On the other hand, high self-healing efficiency was maintained when the resin was sealed using a thermal gradient during self-healing in Chapter 3. In addition, structurally sealing the healing material inside the rotatory transmission element mechanism by O-rings could maintain the self-healing efficiency close to 100% in Chapter 5. Therefore, the viscosity of the healing material during melting has a supplementary role in material leakage prevention, and it is necessary to structurally seal the healing material inside the mechanism to maintain the self-healing efficiency for self-healing using the melting-solidification phenomenon.

Self-healing robot systems must utilize structural and material properties, respectively, as shown in Chapter 2. In accordance with this theory, the following structural and material property design requirements must be satisfied to consist of self-healing robot systems using the melting-solidification phenomenon.

Structural design requirement

- The mechanism structurally seals healing materials to prevent the melting healing materials from leaking out during the self-healing process.

Material property design requirement

- Healing materials can self-heal by re-forming broken bonds between molecules or atoms through the melting-solidification phenomenon.
- Healing materials and structural materials can be bonded.

The transmission force of self-healing transmission elements using the phenomenon of melting and solidification was discussed by the formulation in this dissertation. As a result, the following were found for linear and rotary transmission elements, respectively.

- Transmission force of a linear transmission element is proportional to the contact area of the healing materials and structural materials and to the strength of the healing materials.
- The transmission torque of a rotary transmission element is proportional to the contact area of the healing materials and structural materials, the strength of the healing materials and the diameter of the part made of the structural materials.

Therefore, the transmission force of a self-healing transmission element is proportional to the fracture strength of healing materials. It can also be said that the transmission force of a self-healing linear transmission element is proportional to the square of its dimensions, while the transferable torque of a self-healing rotary transmission element is proportional to the cube of its dimensions.

7.3 Implications of this dissertation

The implications of this dissertation can be divided into three main categories. The first implication is to point out the differences in self-healing between materials and robot systems and to clarify that self-healing robot systems also need to recombine broken atomic or molecular bonds for healing mechanical properties. There are numerous reviews on self-healing materials and applications of self-healing materials. However, these reviews did not focus on self-healing robot systems; they summarized self-healing materials or applications whose self-healing methods were limited to specific methods. Therefore, this dissertation presented comprehensive analyses of research on

self-healing methods for various materials and self-healing robot systems and showed the commonalities. In addition, the dissertation also pointed out that some self-healing robot systems equate functional recovery with self-healing and the problems associated with this approach. Moreover, the requirements for self-healing robot systems, such as the need for strength restoration by healing bonds between atoms or molecules as with self-healing materials, were also presented. The clarification of these requirements for the consistence of self-healing robot systems is a logical contribution of this dissertation to the achievement of self-healing robots.

The second implication is to propose melting-solidification phenomena as a self-healing method that can be applied to robot systems and achieves both strength and self-healing efficiency and to clarify the design theory of a self-healing robot using melting-solidification phenomena. Chapter 2 summarized the related research on self-healing materials with a strength greater than 20 MPa and showed that the self-healing efficiency of most materials decreased with an increase in the number of self-healing cycles in research with multiple self-healing cycles. In addition, this dissertation focused on melting-solidification phenomena as a method that could maintain strength and self-healing efficiency after multiple self-healing cycles. Furthermore, design methods for installing self-healing materials by melting-solidification phenomena into robot mechanisms were proposed. In Chapters 3 and 5, self-healing transmission elements based on the proposed design method were developed, the theoretical equations of transmission force for each mechanism and the self-healing performance were evaluated, and it was demonstrated that the proposed design method can consist of self-healing robot systems. This design theory makes it possible to introduce self-healing using the melting-solidification phenomenon with high self-healing efficiency into robot systems and makes self-healing performance applicable to robot systems in general, which has only been applied to soft robots. Therefore, the proposal of a self-healing method using melting-solidification phenomenon that can maintain a high self-healing efficiency after multiple self-healing cycles and the design theory that makes self-healing by melting-solidification phenomena adaptable to robot systems have practical implications.

The third implication is to show self-healing transmission elements can be incorporated into robots to protect critical robot parts and provide self-healing capabilities to robot systems. It was known from previous research that clutches and mechanical fuses in robot joints could provide mechanical protection and prevented fatal damage [91]. Chapters 4 and 6 of this dissertation demonstrated that the self-healing transmission

elements could protect critical parts of the robot, as well as clutches and mechanical fuses, when the robot was overloaded by experiments using robot joints equipped with the developed self-healing transmission elements. In addition, the self-healing function of the transmission element enables the broken robot joints to self-heal and re-operate. The fact that these evaluation experiments showed a design method for installing self-healing performance in robots makes it possible to achieve robots that keep the robot operating with less maintenance and repair. This is the practical implication of this dissertation.

7.4 Limitations

As described above, this dissertation proposed and demonstrated a design theory for self-healing robot systems using melting-solidification phenomenon. This section discusses the limitations of this dissertation.

Self-healing mechanisms using the melting-solidification phenomenon are easy to miniaturize because of their simple structure, but they are not suitable for applications that require larger sizes. This is because the volume and weight of the healing material required increase rapidly with the increase in size of the mechanism because it is filled with the healing material. The use of clutches or mechanical fuses can make the design more compact if only disconnecting or connecting the transmitting power is required, because the internal structure can be more complex when the mechanism size is large. Therefore, while this dissertation method is suitable for miniaturization, it is not suitable for larger sizes.

Because the self-healing process of the melting-solidification phenomenon employs thermal energy, there are two limitations that occur due to temperature changes. The first limitation is the limited ambient temperature at which the self-healing mechanism of the melting-solidification phenomenon can be used. When the ambient temperature is higher than the temperature at the time of the self-healing process, the healing material is always in a liquefied state and cannot transmit force. On the other hand, when the ambient temperature is extremely low, the healing material cannot be heated sufficiently and the melting phenomenon does not occur, resulting in the failure of self-healing. These problems can be solved by adjusting the phase-change characteristics of the healing material. When a type of healing material is utilized, the range of am-

bient temperatures that can be accommodated is limited. The second is the limitation caused by the effect of the melting phenomenon of the healing material on the surrounding mechanical parts. The self-healing process heats up, raising the temperature around the self-healing mechanism. Measures such as inserting insulation between the transmission element and other elements and using components with a higher operating temperature than the melting point of the healing material were taken in this dissertation. However, this method was only effective because the melting points and glass transition temperatures of the healing materials used in this dissertation were below 100 °C. When the melting point of the healing material is high, further precautions are required. For example, when an aluminum-based material with a melting point exceeding 600°C is used as a healing material, the useful temperature range of most resin materials is exceeded. As a result of the melting-solidification phenomenon, resin materials cannot be used in the vicinity of the self-healing mechanism. Thus, there are limits due to the usable temperature of the mechanism that self-heals by the melting-solidification phenomenon and limits due to the effect of temperature change on the surroundings caused by the self-healing process.

7.5 Embodiment informatics and self-healing robot system

Embodiment informatics is a field that integrates machine technology with information and communication technology. Robotics is the study of the mechanical body as embodiment and the intelligence to move the body as information. Therefore, robotics can be said to be included in embodiment informatics. However, most of the research on robots to date has focused on either their bodies or their intelligence. For example, there is research that aims to accomplish a task no matter what kind of body a robot has by learning the robot's motion by moving multiple robot bodies through reinforcement learning [129], and research that learns to perform a task even if a part of the robot's body becomes inoperable [130]. These studies focus on intelligence in learning how to move the robot body to accomplish a task. On the other hand, as has been dealt with in this dissertation, research on robot bodies discusses new physical characteristics of robots but rarely discusses the intelligence of movements using these bodies. Thus, although robotics is included in embodiment informatics in that it focuses on either the physicality or intelligence of robots and deals with both, it

should essentially focus on both embodiment and information. When research on self-healing robot systems is viewed as embodiment informatics, "embodiment" includes proposals for self-healing using the melting and solidification phenomenon and the development of self-healing transmission elements, and "information" includes algorithms for detecting destruction by detecting anomalies and transitioning robot system state to a self-healing process. In other words, self-healing robot systems require research that focuses on both "embodiment" and "informatics" in this way, and thus belong to embodiment informatics.

7.6 Summary of this dissertation and prospects

In this dissertation, the melting-solidification phenomenon was proposed as a high-strength self-healing method and self-healing transmission elements were created and assessed. The results showed that self-healing using the melting-solidification phenomenon was capable of performing multiple self-healing cycles while maintaining high self-healing efficiency. In addition, the principles of the transmittable force of the transmission elements were clarified, the transmittable force was formulated, and a design policy for transmission elements with a higher transmittable force was also presented. Furthermore, for structural and material property design needs, the design theory of self-healing transmission elements based on the melting-solidification phenomenon was presented separately for structural and material property design requirements. Moreover, when the proposed transmission elements were placed on the robot systems, this dissertation demonstrated that the robot systems could acquire a self-healing function.

Although the robot system with a self-healing function using the phenomenon of melting and solidification proposed in this dissertation has many limitations, it is a widely applicable method in that it can add self-healing functions to the actuation part of conventional robot systems. This dissertation implies that industrial products such as heavy machinery using the mechanical fuses and robot arms using torque limiters can acquire self-healing functions by installing the proposed mechanism instead of mechanical safety devices. In addition, self-healing using melting-solidification phenomenon can be applied to more than just drive systems. Figure 7.1 shows an image of its development. For example, even if parts wear out, they can self-heal to their pre-wear state by melting while taking in the surrounding wear debris. If the robot frame is made of a self-healing material with a viscosity large enough that gravity does not

cause dripping when melted, multiple partial self-healing can be performed by applying thermal energy to the fractured area, no matter where the fracture or crack occurs. The ability to heal a broken part repeatedly also makes it possible to reseal an opened hermetically sealed container by the phenomenon of melting and solidification. Therefore, self-healing using the melting-solidification phenomenon can produce containers that can be opened and completely sealed multiple times. One of the ultimate goals is to achieve self-healing robot systems using the melting-solidification phenomenon and other self-healing methods.

Finally, the prospect of using the melting-solidification phenomenon to build self-healing robot systems that adapt to their operating environment and task is examined. Self-healing is a function of healing the broken part, and most self-healing methods only restore degraded mechanical properties or allow a system that has become inoperable to restart. However, self-healing using the melting-solidification phenomenon can not only self-heal the fractured part but also change the shape of the robot body. This means that in addition to the self-healing function, a robot system that adapts to tasks and operating environments by changing its body can also be achieved simultaneously. A system image of an adaptive robot system is shown in Figure 7.2 as a cycle diagram of the process by which the robot system adapts to the task and operating environment.

Situation judgment

Analyze the task and operating environment. The robot system's behavior and the results of performing tasks are also evaluated.

Decision of physical demands

Determine a better body shape based on the results of the analysis and evaluation performed in the situational judgment.

Body generation

The body of the robot is generated by melting-solidification phenomena according to the determined body shape.

Performing tasks

The robot system executes the task.

The robot system gets increasingly flexible to its operating environment and task by repeating steps 1-4. Self-healing methods that allow a material to alter shape freely,

such as the melting-solidification phenomenon, may enable a robot system that can adapt to tasks and the environment and evolve.

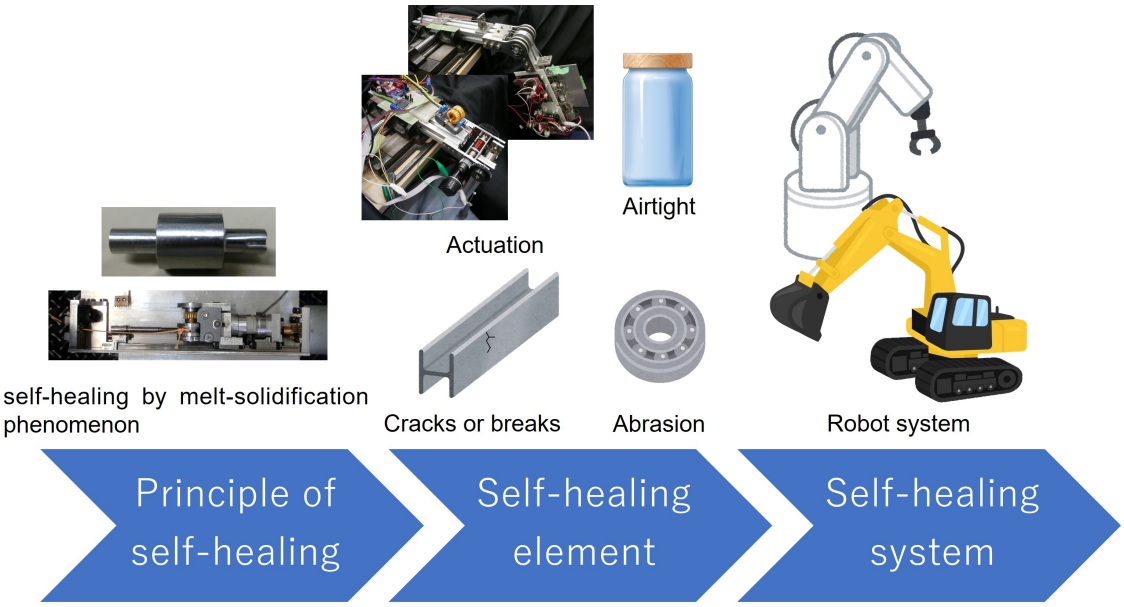

Figure 7.1 Development of self-healing using the melting-solidification phenomenon. The development of a self-healing robot system can be divided into three steps: investigation of self-healing principles, development of self-healing elements, and achievement of a self-healing system. The self-healing principle was investigated in this dissertation, and self-healing elements were developed.

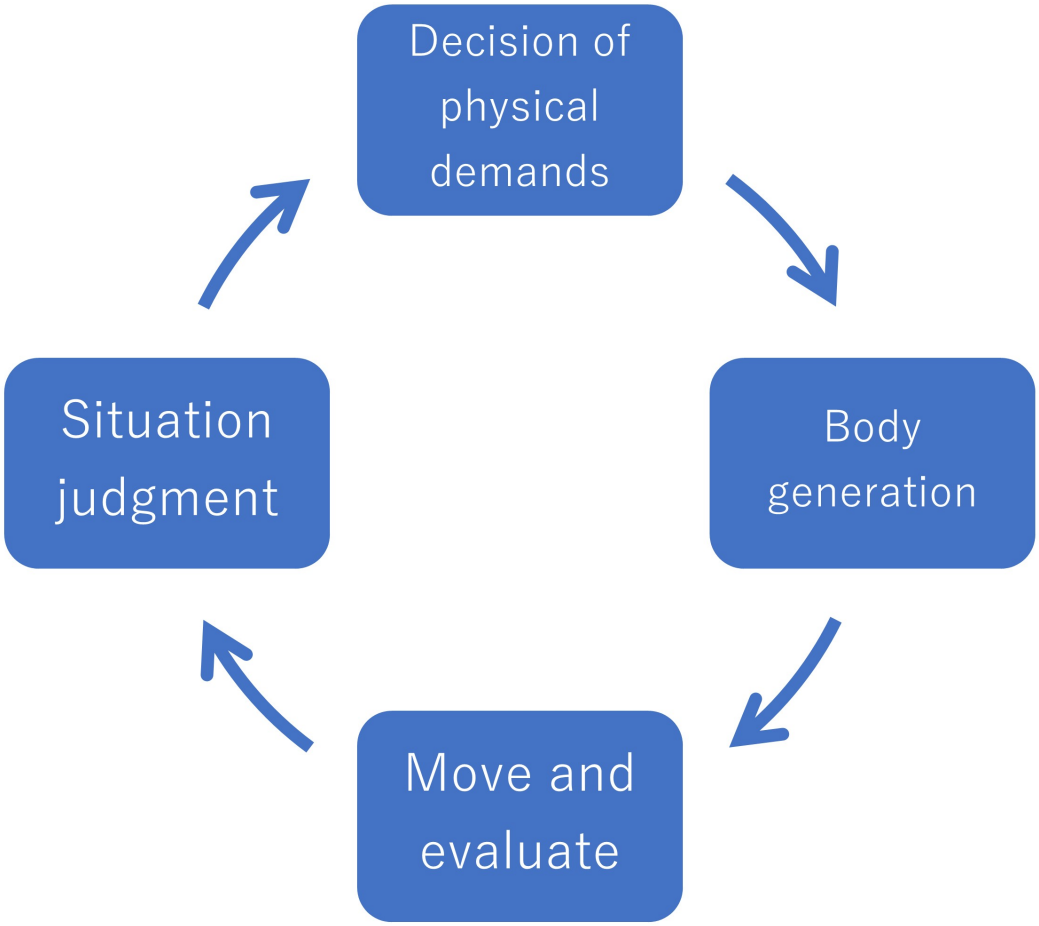

Figure 7.2 Cycle diagram of the process of an adaptive robot system using the melting and solidifying phenomenon.

References

[1] Anne Jurkat, Rainer Klump and Florian Schneider, Tracking the Rise of Robots: The IFR Database, Journal of Economics and Statistics, 2021.

[2] Francesco Chiacchio, Georgios Petropoulos, David Pichler, The impact of industrial robots on EU employment and wages: A local labour market approach, Bruegel Working Paper, No. 2018/02, Bruegel, Brussels, 2018.

[3] Luzius Brodbeck, Simon Hauser and Fumiya Iida, Morphological Evolution of Physical Robots through Model-Free Phenotype Development, PLoS One, Vol. 10, No. 6, 2015.

[4] T. Matsumaru, Design and control of the modular robot system: TOMMS, Proceedings of 1995 IEEE International Conference on Robotics and Automation, pp. 2125-2131, 1995.

[5] Hongxing Wei, Youdong Chen, Jindong Tan and Tianmiao Wang, Sambot: A Self-Assembly Modular Robot System, ambot: A Self-Assembly Modular Robot System, in IEEE/ASME Transactions on Mechatronics, Vol. 16, No. 4, pp. 745-757, 2010.

[6] Simon Kalouche, David Rollinson and Howie Choset, Modularity for Maximum Mobility and Manipulation: Control of a Reconfigurable Legged Robot with Series-Elastic Actuators, 2015 IEEE International Symposium on Safety, Security, and Rescue Robotics (SSRR), pp. 1-8, 2015.

[7] Shinichi Fujisawa, Atsushi Takami, Yuuki Takayama, Shuhei Kuraoka, Ryo Matoba and Ryo Yamaguchi, Robot Production Factory with Robots, K.H.I. technical review, Vol. 178, pp. 18-21, 2017.

[8] Brian T. Kirby, Burak Aksak, Jason D. Campbell, James F. Hoburg, Todd C. Mowry, Padmanabhan Pillai and Seth Copen Goldstein, A modular robotic system

using magnetic force effectors, IEEE/RSJ International Conference on Intelligent Robots and Systems, pp. 2787-2793, 2007.

[9] Trudy Kortes, In-Space Robotic Manufacturing and Assembly (IRMA), 2016 Committee Meeting, NASA Headquarters, 2016.

[10] Maximo A. Roa, Korbinian Nottensteiner, Armin Wedler and Gerhard Grunwald, Robotic Technologies for In-Space Assembly Operations, Advanced Space Technologies in Robotics and Automation, 2017.

[11] B. J. Blaiszik, S. L. B. Kramer, S. C. Olugebefola, J. S. Moore, N. R. Sottos, and S. R. White, Self-Healing Polymers and Composites, Annual Review of Materials Research, Vol. 40, pp. 179-211, 2010.

[12] Seppe Terryn, Glenn Mathijssen, Joost Brancart, Guy Van Assche, and Bram Vanderborght, Towards the first developments of Self-Healing Robotics: thermoreversible Diels-Alder polymer networks in compliant actuators, Proceedings of the International Conference on Self-Healing Materials, 2015.

[13] Dingwei Zhao, Mi Feng, Ling Zhang, Bin He, Xinyan Chen, and Jian Sun, Facile synthesis of self-healing and layered sodium alginate/polyacrylamide hydrogel promoted by dynamic hydrogen bond, Carbohydrate Polymers Vol. 256, 2021.

[14] Zhang, X., and He, J., Hydrogen-Bonding-Supported Self-Healing Antifogging Thin Films. Scientific Reports, Vol. 5, Article number 9227, 2015.

[15] Antoinette B. South and L. Andrew Lyon, Autonomic Self-Healing of Hydrogel Thin Films, A Journal of the German Chemical Society Angewandte Chemie International Edition, Vol. 49, pp. 767-771, 2010.

[16] Changyou Shao, Huanliang Chang, Meng Wang, Feng Xu, and Jun Yang, High-Strength, Tough, and Self-Healing Nanocomposite Physical Hydrogels Based on the Synergistic Effects of Dynamic Hydrogen Bond and Dual Coordination Bonds, ACS Applied Materials and Interfaces, Vol.9, pp. 28305–28318, 2017.

[17] Tough, Swelling-Resistant, Self-Healing, and Adhesive Dual-Cross-Linked Hydrogels Based on Polymer–Tannic Acid Multiple Hydrogen Bonds, Macromolecules, Vol. 51, pp.1696-1705, 2018.

[18] Chuanhui Xu, Wei Zhan, Xiuzhen Tang, Fang Mo, Lihua Fu, and Baofeng Lin, Self-healing chitosan/vanillin hydrogels based on Schiff-base bond/hydrogen bond hybrid linkages, Polymer Testing, Vol. 66, pp. 155–163, 2018.

[19] Ting Li, Zhining Xie, Jun Xu, Yunxuan Weng, and Bao-Hua Guo, Design of a self-healing cross-linked polyurea with dynamic cross-links based on disulfide bonds and hydrogen bonding, European Polymer Journal, Vol. 107, pp. 249-257, 2018.

[20] Florian Herbst, Diana Dohler, Philipp Michael, and Wolfgang H. Binder, Self-Healing Polymers via Supramolecular Forces, Macromolecular Rapid Communications, Vol. 34, pp. 203-220, 2013.

[21] Antonella Campanella, Diana Dohler, and Wolfgang H. Binder, Self-Healing in Supramolecular Polymers, Macromolecular Rapid Communications, Vol. 39, pp. 1700739- 1700739, 2018.

[22] Charles E. Diesendruck, Nancy R. Sottos, Jeffrey S. Moore, and Scott R. White, Biomimetic Self-Healing, Angewandte Chemie, Vol. 54, pp. 10428–10447, 2015.

[23] D. Therriault, R. F. Shepherd, S. R. White, J. A. Lewis, Fugitive Inks for Direct-Write Assembly of Three-Dimensional Microvascular Networks, Advanced Materials, Vol. 17, pp. 395-399, 2005.

[24] H. R. Williams, R. S. Trask, and I. P. Bond, Self-healing composite sandwich structures, Smart Materials and Structures, Vol. 16, pp. 1198–1207, 2007.

[25] S.M. Bleay, C.B. Loader, V.J. Hawyes, L. Humberstone, and P.T. Curtis, A smart repair system for polymer matrix composites, Composites Part A: Applied Science and Manufacturing, Vol. 32, pp. 1767-1776, 2001.

[26] Ivana Radovic, Aleksandar Stajcic, Andjela Radisavljevic, Filip Veljkovic, Maria Cebela, Vojislav V. Mitic, and Vesna Radojevic, Solvent effects on structural changes in self-healing epoxy composites, Materials Chemistry and Physics, Vol. 256, Article number 123761, 2020.

[27] Christopher J. Hansen, Willie Wu, Kathleen S. Toohey, Nancy R. Sottos, Scott R. White, and Jennifer A. Lewis, Self-Healing Materials with Interpenetrating Microvascular Networks, Advanced Materials, Vol. 21, pp. 4143-4147, 2009.

[28] K.S. Toohey ,N.R. Sottos ,S.R. White, Characterization of Microvascular-Based Self-healing Coatings, Experimental Mechanics, Vol. 49, pp. 707-717, 2009.

[29] Kathleen S. Toohey, Christopher J. Hansen, Jennifer A. Lewis, Scott R. White, and Nancy R. Sottos, Delivery of Two-Part Self-Healing Chemistry via Microvascular Networks, Advanced Functional Materials, Vol. 19, pp. 1399-1405, 2009.

[30] Jason F. Patrick, Kevin R. Hart, Brett P. Krull, Charles E. Diesendruck, Jeffrey S. Moore, Scott R. White, and Nancy R. Sottos, Continuous Self-Healing Life Cycle in Vascularized Structural Composites, Advanced Materials, Vol. 26, pp. 4302-4308, 2014.

[31] Sang-Ryoung Kim, Bezawit A. Getachew, and Jae-Hong Kim, Toward microvascular network-embedded self-healing membranes, Journal of Membrane Science, Vol. 531, pp. 94-102, 2017.

[32] S. R. White, J. S. Moore, N. R. Sottos, B. P. Krull, W. A. Santa Cruz, R. C. R. Gergely, Restoration of Large Damage Volumes in Polymers, Science, Vol. 344, pp. 620-623, 2019.

[33] A. R. Hamilton, N. R. Sottos, and S. R. White, Pressurized vascular systems for self-healing materials, Journal of the Royal Society Interface, Vol. 9, pp. 1020-1028, 2012.

[34] Diane Gardner, Daniel Herbert, Monica Jayaprakash, Anthony Jefferson, and Alison Paul, Capillary Flow Characteristics of an Autogenic and Autonomic Healing Agent for Self-Healing Concrete, Journal of Materials in Civil Engineering, Vol. 29, Issue 11, 2017.

[35] Mohamed Gibril Bah, Hafiz Muhammad Bilal, and Jingtao Wang, Fabrication and application of complex microcapsules: a review, Soft Matter, Vol. 3, pp. 570-590, 2020.

[36] B.J. Blaiszik, M.M. Caruso, D.A. McIlroy, J.S. Moore, S.R. White, N.R. Sottos, Microcapsules filled with reactive solutions for self-healing materials, Polymer, Vol. 50, pp. 990-997, 2009.

[37] Hafeez Ullah, Khairun Azizi M Azizli, Zakaria B Man, Mukhtar B Che Ismail, and Muhammad Irfan Khan, The Potential of Microencapsulated Self-healing Materials

for Microcracks Recovery in Self-healing Composite Systems: A Review, Polymer Reviews, Vol. 56, pp. 429–485, 2016.

[38] Khaled Abid Althaqafi, Julian Satterthwaite, and Nikolaos Silikas, A review and current state of autonomic self-healing microcapsules-based dental resin composites, Dental Materials, Vol. 36, pp. 329-342, 2020.

[39] Fariba Safaei, Saied Nouri Khorasani, Hadi Rahnama, Rasoul Esmaeely Neisiany, and Mohammad Sadegh Koochaki, Single microcapsules containing epoxy healing agent used for development in the fabrication of cost efficient self-healing epoxy coating, Progress in Organic Coatings, Vol. 114, pp. 40-46, 2018.

[40] Zhao Yang, Zhang Wei, Liao Le-ping, Wang Si-jie, and Li Wu-jun, Self-healing coatings containing microcapsule, Applied Surface Science, Vol. 258, pp. 1915-1918, 2012.

[41] Yanjuan Tian, Mulian Zheng, Peng Li, Jinhao Zhang, Ruizhe Qiao, Cheng Cheng, and Hailei Xu, Preparation and characterization of self-healing microcapsules of asphalt, Construction and Building Materials, Vol. 263, Article number 120174, 2020.

[42] Tim S. Coope, Ulrich F.J. Mayer, Duncan F. Wass, Richard S. Trask, and Ian P. Bond, Self-Healing of an Epoxy Resin Using Scandium(III) Triflate as a Catalytic Curing Agent, Advanced Functional Materials, Vol. 21, pp. 4624–4631, 2011.

[43] E. N. Brown, S. R. White, and N. R. Sottos, Microcapsule induced toughening in a self-healing polymer composite, Journal of Materials Science, Vol. 39, pp. 1703–1710, 2004.

[44] Reaz A. Chowdhury, Mahesh V. Hosura, Md. Nuruddin, Alfred Tcherbi-Narteh, Ashok Kumar, Veera Boddu, and Shaik Jeelani, Self-healing epoxy composites: preparation, characterization and healing performance, Journal of Materials Research and Technology, Vol. 4, pp. 33-43, 2015.

[45] Qi Li, Siddaramaiah, Nam Hoon Kim, David Hui, and Joong Hee Lee, Effects of dual component microcapsules of resin and curing agent on the self-healing efficiency of epoxy, Composites Part B: Engineering, Vol. 55, pp. 79-85, 2013.

[46] J.Y.Wang, H.Soens, W. Verstraete, and N. De Belie, Self-healing concrete by use of microencapsulated bacterial spores, Cement and Concrete Research, Vol. 56, pp. 139-152, 2014.

[47] Qw Zhan, Jl Zhou, Sg Wang, Yl Su, By Liu, Xn Yu, Zh Pan, and Cx Qian, Crack self-healing of cement-based materials by microorganisms immobilized in expanded vermiculite, Construction and Building Materials, Vol. 272, Article number 121610, 2021.

[48] Iee Lee Hia, Eng-Seng Chan, Siang-Piao Chai, and Pooria Pasbakhsh, A novel repeated self-healing epoxy composite with alginate multicore microcapsules, Journal of Materials Chemistry A, Vol. 6, pp. 8470-8478, 2018.

[49] Febby Krisnadi, Linh Lan Nguyen, Ankit, Jinwoo Ma, Mohit Rameshchandra Kulkarni, Nripan Mathews, and Michael D. Dickey, Directed Assembly of Liquid Metal–Elastomer Conductors for Stretchable and Self-Healing Electronics, Advanced Materials, Vol. 32, pp. 2001642-2001642, 2020.

[50] Tomoya Koshi, and Eiji Iwase, Self-healing metal wire using electric field trapping of metal nanoparticles, Japanese Journal of Applied Physics, Vol. 54, Article number 06FP03, 2015.

[51] X. G. Zheng, Y.-N. Shi, and K. Lu, Electro-healing cracks in nickel, Materials Science & Engineering A, Vol. 561, pp. 52–59, 2013.

[52] X. G. Zheng, Y.-N. Shi, and K. Lu, Evaluating the Performance of 2-Mercapto-5-Benzimidazolesulfonic Acid in Controllable Electro-Healing Cracks in Nickel, Journal of The Electrochemical Society, Vol. 162, pp. D222-D228, 2015.

[53] Christopher P. Kabb, Christopher S. O'Bryan, Christopher C. Deng, Thomas E. Angelini, and Brent S. Sumerlin, Photoreversible Covalent Hydrogels for Soft-Matter Additive Manufacturing, ACS Applied Materials & Interfaces, Vol. 10, pp. 16793-16801, 2018.

[54] Hendrik Frisch, David E. Marschner, Anja S. Goldmann, and Christopher BarnerKowollik, Wavelength-Gated Dynamic Covalent Chemistry, Angewandte Chemie International Edition, Vol. 57, pp. 2036 -2045, 2018.

[55] Yuanlai Fang, Xiaosheng Du, Zongliang Du, Haibo Wang, and Xu Cheng, Light- and heat-triggered polyurethane based on dihydroxyl anthracene derivatives for self-healing applications, Journal of Materials Chemistry A, Vol. 5, pp. 8010-8017, 2017.

[56] Mariapaola Staropoli, Andreas Raba, and Claas H. Hövelmann, Melt dynamics of supramolecular comb polymers: Viscoelastic and dielectric response, Journal of Rheology, Vol. 61, pp. 1185-1196, 2017.

[57] Hongping Xiang, Jingfeng Yin, Guanghong Lin, Xiaoxuan Liu, Minzhi Rong, and Mingqiu Zhang, Photo-crosslinkable, self-healable and reprocessable rubbers, Chemical Engineering Journal, Vol. 358, pp. 878-890, 2019.

[58] Ying Wanga, Qiang Liua, Jinhui Lia, Lei Linga, Guoping Zhanga, Rong Suna, and Ching-Ping Wongc, UV-triggered self-healing polyurethane with enhanced stretchability and elasticity, Polymer, Vol. 172, pp. 187-195, 2019.

[59] Yuye Zhu, Kangli Cao, Min Chen, and Limin Wu, Synthesis of UV-Responsive Self-Healing Microcapsules and Their Potential Application in Aerospace Coatings, ACS Applied Materials & Interfaces, Vol. 11, pp. 33314-33322, 2019.

[60] Wanchun Guo, Yin Jia, Kesong Tian, Zhaopeng Xu, Jiao Jiao, Ruifei Li, Yuehao Wu, Ling Cao, and Haiyan Wang, UV-Triggered Self-Healing of a Single Robust SiO2 Microcapsule Based on Cationic Polymerization for Potential Application in Aerospace Coatings, ACS Applied Materials & Interfaces, Vol. 8, pp. 21046-21054, 2016.

[61] Leyang Lv, Peiyan Guo, Gang Liu, Ningxu Han, and Feng Xing, Light induced self-healing in concrete using novel cementitious capsules containing UV curable adhesive, Cement and Concrete Composites, Vol. 105, pp. 103445, 2020.

[62] Ying-Ling Liu, and Tsai-Wei Chuo, Self-healing polymers based on thermally reversible Diels–Alder chemistry, The Royal Society of Chemistry, Vol. 4, pp. 2194–2205, 2013.

[63] N. I. Khan, S. Halder, S. B. Gunjan, T. Prasad, A review on Diels-Alder based self-healing polymer composites, International Conference on Mechanical, Materials and Renewable Energy, Vol. 377, Article Number 012007, 2018.

[64] Pengfei Du, Xuanxuan Liu, Zhen Zheng, Xinling Wang, Thomas Joncheray, and Yuefan Zhang, Synthesis and characterization of linear self-healing polyurethane based on thermally reversible Diels–Alder reaction, The Royal Society of Chemistry, Vol. 3, pp. 15475-15482, 2013.

[65] T. S. Coope, D. H. Turkenburg, H. R. Fischer, R. Luterbacher, H. van Bracht, and I. P. Bond, Novel Diels-Alder based self-healing epoxies for aerospace composites, Smart Materials and Structures, Vol. 25, Article number 084010, 2016.

[66] J. B. Ferguson, Benjamin F. Schultz, and Pradeep K. Rohatgi, Self-Healing Metals and Metal Matrix Composites, The Journal of The Minerals, Metals & Materials Society, Vol. 66, pp. 866–871, 2014.

[67] Afsaneh Dorri Moghadam, Benjamin F. Schultz, J. B. Ferguson, Emad Omrani, Pradeep K. Rohatgi, and Nikhil Gupta, Functional Metal Matrix Composites: Self-lubricating, Self-healing, and Nanocomposites-An Outlook, Vol. 66, pp. 872–881, 2014.

[68] Biao Zhang, Wang Zhang, Zhiqian Zhang, Yuan-Fang Zhang, Hardik Hingorani, Zhuangjian Liu, Jun Liu, and Qi Ge, Self-Healing Four-Dimensional Printing with an Ultraviolet Curable Double-Network Shape Memory Polymer System, ACS Applied Materials & Interfaces, Vol. 11, pp. 10328-10336, 2019.

[69] Juan Gallego, Miguel A. del Val, Verónica Contreras, Antonio Páez, Heating asphalt mixtures with microwaves to promote self-healing, Construction and Building Materials, Vol. 42, pp. 1-4, 2013.

[70] Lu Huang, Ningbo Yi, Yingpeng Wu, Yi Zhang, Qian Zhang, Yi Huang, Yanfeng Ma, and Yongsheng Chen, Multichannel and Repeatable Self-Healing of Mechanical Enhanced Graphene-Thermoplastic Polyurethane Composites, Advanced Materials, Vol. 25, pp. 2224–2228, 2013.

[71] Guanghao Li, Peishuang Xiao, Shengyue Hou, Yi Huang, Rapid and efficient polymer/graphene based multichannel self-healing material via Diels-Alder reaction, Carbon, Vol. 147, pp. 398-407, 2019.

[72] Jinhui Li, Qiang Liu, Derek Ho, Songfang Zhao, Shuwen Wu, Lei Ling, Fei Han, Xinxiu Wu, Guoping Zhang, Rong Sun, and Ching-Ping Wong, Three-Dimensional

Graphene Structure for Healable Flexible Electronics Based on Diels-Alder Chemistry, ACS Applied Materials and Interfaces, Vol. 10, pp. 9727-9735, 2018.

[73] E. Acome, S. K. Mitchell, T. G. Morrissey, M. B. Emmett, C. Benjamin, M. King, M. Radakovitz, and C. Keplinger, Hydraulically amplified self-healing electrostatic actuators with muscle-like performance, Science, Vol. 359, pp. 61–65, 2018.

[74] Shane K. Mitchell, Xingrui Wang, Eric Acome, Trent Martin, Khoi Ly, Nicholas ellaris, Vidyacharan Gopaluni Venkata, and Christoph Keplinger, An Easy-to-Implement Toolkit to Create Versatile and High-Performance HASEL Actuators for Untethered Soft Robots, Advanced material, Vol. 6, Article Number 1900178, 2019.

[75] Philipp Rothemund, Nicholas Kellaris, Shane K. Mitchell, Eric Acome, Christoph Keplinger, HASEL Artificial Muscles for a New Generation of Lifelike Robots-Recent Progress and Future Opportunities, Advanced material, Vol. 33, Article Number 2003375, 2021.

[76] Maura R. O'Neill, Eric Acome, Shannon Bakarich, Shane K. Mitchell, Julia Timko, Christoph Keplinger, and Robert F. Shepherd, Rapid 3D Printing of Electrohydraulic (HASEL) Tentacle Actuators, Advanced Functional materials, Vol. 30, Article Number 2005244, 2020.

[77] Kosuke Nagaya, Sigeo Ikai, Manabu Chiba, Xujing Chao, Tire with Self-Repairing Mechanism, JSME International Journal Series C Mechanical Systems, Machine Elements and Manufacturing, Vol. 49, Issue 2, pp. 379-384, 2006.

[78] Peter L. Stang, Joel V. Van Ornum, Self-sealing vehicle tire and sealant composition, US3935893A, 1974.

[79] Wei Tang, Chao Zhang, Yiding Zhong, Pingan Zhu, Yu Hu, Zhongdong Jiao, Xiaofeng Wei, Gang Lu, Jinrong Wang, Yuwen Liang, Yangqiao Lin, Wei Wang, Huayong Yang, and Jun Zou, Customizing a self-healing soft pump for robot, nature communications, Vol. 12, Article number 2247, 2021.

[80] Seppe Terryn, Joost Brancart, Dirk Lefeber, Guy Van Assche, and Bram Vanderborght, Self-healing soft pneumatic robots, Science Robotics, Vol. 2, pp.1-12, 2017.

[81] Seppe Terryn, Glenn Mathijssen, Joost Brancart, and Bram Vanderborght, and Dirk Lefeber, Investigation of self-healing compliant actuators for Robotics, Proceedings IEEE International Conference on Robotics and Automation 2015, pp. 258-263, 2015.

[82] Seppe Terryn, Glenn Mathijssen, Joost Brancart, Tom Verstraten, Guy Van Assche, and Bram Vanderborght, Toward Self-Healing Actuators: A Preliminary Concept, IEEE Transactions on Robotics, Vol. 32, pp. 736-743, 2016.

[83] Seppe Terryn, Joost Brancart, Ellen Roels, Guy Van Assche, and Bram Vanderborght, Room Temperature Self-Healing in Soft Pneumatic Robotics, IEEE ROBOTICS & AUTOMATION MAGAZINE, pp. 44-55, Dec 2020.

[84] Mary M. Caruso, David A. Delafuente, Victor Ho, Nancy R. Sottos, Jeffrey S. Moore and Scott R. White, Solvent-Promoted Self-Healing Epoxy Materials, Macromolecules, Vol. 40, No. 25, pp. 8830-8832, 2007.

[85] Ali Faghihnejad, Kathleen E. Feldman, Jing Yu, Matthew V. Tirrell, Jacob N. Israelachvili, Craig J. Hawker, Edward J. Kramer and Hongbo Zeng, Adhesion and Surface Interactions of a Self-Healing Polymer with Multiple Hydrogen-Bonding Groups, Advanced Functional Materials, Vol. 24, pp. 2322–2333, 2014.

[86] Saul Utrera-Barrios, Raquel Verdejo, Miguel A. Lopez-Manchado and Marianella Hernandez Santana, Evolution of self-healing elastomers, from extrinsic to combined intrinsic mechanisms: a review, Materials Horizons, Vol. 7, No. 11, pp. 2882-2902, 2020.

[87] R. V. Siva Prasanna Sanka, Balaji Krishnakumar, Yves Leterrier, Shyam Pandey, Sravendra Rana and Véronique Michaud, Soft Self-Healing Nanocomposites, frontiers in Material, Vol. 6, No. 137, 2019.

[88] Nand Jee Kanu, Eva Gupta, Umesh Kumar Vates, Gyanendra Kumar Singh, Self-healing composites: A state-of-the-art review, Composites Part A: Applied Science and Manufacturing, Vol. 121, pp. 474-486, 2019.

[89] Zhanhua Wang, Xili Lu, Shaojie Sun, Changjiang Yu and Hesheng Xia, Preparation, characterization and properties of intrinsic self-healing elastomers, Journal of Materials Chemistry B, Vol. 7, No. 32, pp. 4876-4926, 2019.

[90] Haicheng Jiang, Lijie Duan, Xiuyan Ren and Guanghui Gao, Hydrophobic association hydrogels with excellent mechanical and self-healing properties, European Polymer Journal, Vol. 112, pp. 660–669, 2019.

[91] S Haddadin, et al, Robot Collisions: A Survey on Detection, Isolation, and Identification, IEEE Transactions on Robotics, Vol. 33, No. 6, 2017.

[92] Peter R. N. Childs, Mechanical Design Engineering Handbook, Butterworth-Heinemann, pp. 600-655. 2019.

[93] Adrianus Johannes Josephus Van Der Horst and Arnold Aalders, A mechanical fuse, a neck cord comprising a mechanical fuse and a method of connecting a mechanical fuse to a neck cord, European Patent Office EP2556269B1, 2010.

[94] David Tunno and Stuart Larsen, RETROFITTABLE CABLE MECHANICAL FUSE, US 2011/0027007 A1, 2007.

[95] S Chidambaram, Ashok Kamaraj, R Saravana Kumar and V Karthik4, Shear Fracture and Industrial Overload Failure of Mechanical Fuse Shear Pin, International Conference on Mechanical, Materials and Renewable Energy 2018.

[96] Yan Song, Yuan Liu, Tao Qi and Guo Liang Li, Towards Dynamic but Supertough Healable Polymers through Biomimetic Hierarchical Hydrogen-Bonding Interactions, Angewandte Chemie International Edition, Vol. 57, Issue 42, pp. 13838-13842, 2018.

[97] Jie Liu, Jun Liu, Sheng Wang, Jing Huang, Siwu Wu, Zhenghai Tang, Baochun Guo and Liqun Zhang, An advanced elastomer with an unprecedented combination of excellent mechanical properties and high self-healing capability, Journal of Materials Chemistry A, Vol. 5, Issue 48, pp.25660-25671, 2017.

[98] Guo Haiyun, Fang Xu, Zhang Ling, Sun Junqi, Facile Fabrication of Room-Temperature Self-Healing, Mechanically Robust, Highly Stretchable, and Tough Polymers Using Dual Dynamic Cross-Linked Polymer Complexes, ACS Applied Materials & Interfaces, Vol. 11, Issue 36, pp. 33356-33363, 2019.

[99] Maochen Liu, Jiang Zhong, Zijian Li, Jinchuang Rong, Kun Yang, Jiyong Zhou, Liang Shen, Fei Gao, Xuelong Huang and Haifeng He, A high stiffness and self-healable polyurethane based on disulfide bonds and hydrogen bonding, European Polymer Journal, Vol. 124, No. 109475, 2020.

[100] Jin Hu, Ruibin Mo, Xiang Jiang, Xinxin Sheng, Xinya Zhang, Towards mechanical robust yet self-healing polyurethane elastomers via combination of dynamic main chain and dangling quadruple hydrogen bonds, Polymer, Vol. 183, No. 121912, 2019.

[101] Yue Lai, Xiao Kuang, Ping Zhu, Miaoming Huang, Xia Dong and Dujin Wang, Colorless, Transparent, Robust, and Fast Scratch-Self-Healing Elastomers via a Phase-Locked Dynamic Bonds Design, Advanced Materials, Vol. 30, Issue 38, 2018.

[102] Shiwen Yang, Shuang Wang, Xiaosheng Du, Zongliang Du, Xu Cheng, Haibo Wang, Mechanically robust self-healing and recyclable flame-retarded polyurethane elastomer based on thermoreversible crosslinking network and multiple hydrogen bonds, Chemical Engineering Journal, Volume 391, No. 123544, 2020.

[103] Pengfei Du, Meiyin Wu, Xuanxuan Liu, Zhen Zheng, Xinling Wang, Thomas Joncheray and Yuefan Zhang, Diels–Alder-based crosslinked self-healing polyurethane/urea from polymeric methylene diphenyl diisocyanate, Journal of Applied Polymer Science, Vol. 131, Issue 9, pp. 2014.

[104] Yiting Zhong, Xinling Wang, Zhen Zhenga and Pengfei Du, Polyether–maleimide-based crosslinked self-healing polyurethane with Diels–Alder bonds, Journal of Applied Polymer Science, Vol. 132, Issue 19, 2015.

[105] Yunseon Heo and Henry A. Sodano, Self-Healing Polyurethanes with Shape Recovery, Advanced Functional Materials, Vol. 24, Issue 33, pp. 5261-5268, 2014.

[106] Naoko Yoshie, Shunsuke Saito, Nobuhiro Oya, A thermally-stable self-mending polymer networked by Diels–Alder cycloaddition, Polymer, Vol. 52, Issue 26, pp. 6074-6079, 2011.

[107] Lu, Xili Fei Guoxia, Xia Hesheng and Zhao Yue, Ultrasound healable shape memory dynamic polymers, Journal of Materials Chemistry A, Vol. 38, Issue 38, pp. 16051-16060, 2014.

[108] Yang Li, Lu Xili, Wang Zhanhua and Xia Hesheng, Diels–Alder dynamic crosslinked polyurethane/polydopamine composites with NIR triggered self-healing function, Polymer Chemistry, Vol. 9, Issue 16, pp. 2166-2172, 2018.

[109] Pu W, Fu D, Wang Z, Gan X, Lu X, Yang L, Xia H., Realizing Crack Diagnosing and Self-Healing by Electricity with a Dynamic Crosslinked Flexible Polyurethane Composite, Advanced Science News, Vol. 5, No. 5, 2018.

[110] Du Pengfei, Wu Meiyin, Liu Xuanxuan, Zheng Zhen, Wang Xinling, Sun Peiyu, Joncheray Thomas and Zhang Yuefan, Synthesis of linear polyurethane bearing pendant furan and cross-linked healable polyurethane containing Diels–Alder bonds, New Journal of Chemistry, Vol. 38, Issue 2, pp. 770-776, 2014.

[111] Pengfei Du, Haiyan Jia, Qinghua Chen, Zhen Zheng, Xinling Wang and Denglong Chen, Slightly crosslinked polyurethane with Diels–Alder adducts from trimethylolpropane, Journal of Applied Polymer Science, Vol. 133, No. 39, 2016.

[112] Shen Yu, Rongchun Zhang, Qiang Wu, Tiehong Chen and Pingchuan Sun, Bio-Inspired High-Performance and Recyclable Cross-Linked Polymers, Advanced Materials, Vol. 25, Issue 35, pp. 4912-4917, 2013.

[113] Yu-mi Ha, Young-O Kim, Seokhoon Ahn, Seoung-ki Lee, Jae-suk Lee, Min Park, Jae Woo Chung, Yong Chae Jung, Robust and stretchable self-healing polyurethane based on polycarbonate diol with different soft-segment molecular weight for flexible devices, European Polymer Journal, Vol. 118, pp. 36-44, 2019.

[114] Sang-Hyub Lee, Se-Ra Shin, Dai-Soo Lee, Self-healing of cross-linked PU via dual-dynamic covalent bonds of a Schiff base from cystine and vanillin, Materials & Design, Vol. 172, No. 107774, 2019.

[115] Hamed Daemi, Sareh Rajabi-Zeleti, Haritz Sardon, Mehdi Barikani, Ali Khademhosseini and Hossein Baharvand, A robust super-tough biodegradable elastomer engineered by supramolecular ionic interactions, Biomaterials, Vol. 84, pp. 54-63, 2016.

[116] Wen-Xing Liu, Chi Zhang, Huan Zhang, Ning Zhao, Zhi-Xiang Yu and Jian Xu, Oxime-Based and Catalyst-Free Dynamic Covalent Polyurethanes, Vol. 139, No. 25, pp. 8678-8684, 2017.

[117] William F. Smith and javad Hashemi, Foundations of Materials Science and Engineering Fifth Edition in SI Units, Mc Graw Hill Education, pp. 627, 2011.

[118] P. A. Davidson, Introduction to Magnetohydrodynamics, Cambridge University Press, pp. 543, 2016.

[119] Katsuhiko Nakamae, Interfacial Aspect of the Resin-metal Adhesion, Journal of the Surface Finishing Society of Japan, Vol. 66, No. 8, pp. 338-341, 2015.

[120] Ashby, M. F. Materials selection in mechanical design, Butterworth-Heinemann, pp. 56–61, 2005.

[121] Aditya V. Natu ,Ankit R. Sharma ,Nitinkumar R. Anekar, "Variation of Adhesive Strength in Single Lap Joint (SLJ) with Surface Irregularities", American Journal of Mechanical Engineering. Vol. 7, pp. 61-6, 2019.

[122] Sun-Lai Chang, Jyh-Jone Lee, and Home-Che Yen, "Kinematic and compliance analysis for tendon-driven robotic mechanisms with flexible tendons", Mechanism and Machine Theory, Vol. 40, pp. 728-739, 2005

[123] Shunsuke Nagahama, Junichi Tanabe, Shigeki Sugano, "Development of a dipping wire method to improve the abrasion resistance of a plastic wire", 2016 IEEE International Conference on Robotics and Biomimetics (ROBIO), 2016

[124] Shota Miyake, Shunsuke Nagahama, Shigeki Sugano, "Development of a tendon-driven mechanism with liquid circulation system for improving wear resistance", 2017 IEEE International Conference on Robotics and Biomimetics (ROBIO), 2017.

[125] Werner Friedl, Maxime Chalon, Jens Reinecke, Markus Grebenstein, "FAS A flexible antagonistic spring element for a high performance over", 2011 IEEE/RSJ International Conference on Intelligent Robots and Systems, 2011.

[126] J. Acero, J. M. Burdio, L. A. Barragán, D. Navarro, R. Alonso J. R. García, F. Monterde, P. Hernández, S. Llorente and I. Garde, The domestic induction heating appliance: an overview of recent research, 2008 Twenty-Third Annual IEEE Applied Power Electronics Conference and Exposition, pp. pp. 651-657, 2008.

[127] Brian Knapp, Actinium to Fluorine (A to F) - Elements S. v. 16 (Hardback), Atlantic Europe Publishing Co Ltd, pp. 28, 2001.

[128] Toshio Itami, Hirokatsu Aoki, Takeru Shibata, Motoshige Ikeda, Koichi Hotozuka, "The estimation of concentration fluctuations in liquid Ag–Si and Au–Si alloys", Journal of Non-Crystalline Solids, Vol. 353, pp. 3011-3016, 2007.

[129] Sudeep Dasari, Frederik Ebert, Stephen Tian, Suraj Nair, Bernadette Bucher, Karl Schmeckpeper, Siddharth Singh, Sergey Levine and Chelsea Finn, "RoboNet: Large-Scale Multi-Robot Learning", Conference on Robot Learning (CoRL) 2019.

[130] Antoine Cully, Jeff Clune, Danesh Tarapore and Jean-Baptiste Mouret, "Robots that can adapt like animals", Nature, Vol. 521, pp. 503-507, 2015.

Acknowledgment

Many people helped me in writing my doctoral dissertation, and I was able to finish it. I would like to take this opportunity to express my deepest appreciation to the people.

First, I would like to appreciate Prof. Sugano for serving as the principal referee. Prof. Sugano guided my research for a very long time. I first met Prof. Sugano when I founded ROBOSTEP (Waseda's Robocon club) in my second year of undergraduate school, before I joined his lab. I really appreciated that he listened to me without making fun of me, who still did not understand engineers or researchers, and was my club advisor. The club grew and became an organization for students who are still serious about competing in the Robocon. I then joined Sugano Laboratory and started my research, leading to the writing of my bachelor's thesis, master's thesis, and even my doctoral dissertation. Thanks to Prof. Sugano's advice on my research, I have been able to advance my research from now.

Next, I would like to thank Prof. Takanishi, Prof. Ogata, Prof. Miyashita, and Prof. Iwata for serving as a referee for my doctoral dissertation. The professors pointed out areas where I was lacking in my dissertation and presentation, and even gave me concrete suggestions. I was able to revise my dissertation and presentation based on these details, which allowed me to survive the review process. I really appreciate it.

In my research life, Dr. Nagahama, a former assistant professor at Waseda University and current lecturer at Kyoto University of Advanced Science and Technology, has been very helpful in guiding me on my research policy and content from my graduation thesis to my doctoral dissertation. Dr. Nagahama discussed the details of my research with me at first, and when it came to presentation, he taught me from scratch, as I had no understanding of research presentation at all. I still remember the first time I wrote a paper in Japanese, and he looked at it until there was not a single sentence without a single correction. I was shocked at the time, but without that correction, I might not have been able to write a proper paper. Furthermore, the way Dr. Nagahama conducted his research allowed me to get a close-up look at what a researcher should be like, and he was a role model for me and someone I should aspire to be like. I would like to take this opportunity to express my appreciation.

During my time in the laboratory life, I was very much indebted to my seniors

and juniors in the WAMOEBA group. I have many memories with them outside of research, such as going out to eat. However, if it had been a place to just do research, I might have failed because I could not stand the rigidity. I was able to enjoy my research life because I had them to research with and to play with from time to time. Thank you so much.

I am also indebted to my grandmother, parents, and wife for their support in private life. My grandmother supported me in life from my undergraduate days to my master's degree. In particular, she continued to support me while I was involved in the Robocon, which had been one of my goals all through university. Thanks to her, I was able to live my undergraduate life without regrets. In addition, my parents supported me not only financially but also in my personal life until the first to second year of my PhD course. Now that I am doing my own housework and living with my wife, I realize once again that I have had a lot of the hard parts done for me in the past. My parents have always thought of me and told me things whenever I felt like I was mentally breaking down, or when I was getting on a roll. In addition, my wife has supported me for about eight years since we started dating, especially during the last two years of my doctoral program while we lived together. Thanks to the many times she listened to me explain my doctoral dissertation, I was able to structure and phrase my dissertation in a way that readers could understand easily. I would like to thank my grandmother, parents, and wife for supporting my life. Thank you so much.

A doctoral degree is not the goal, but the beginning of being a researcher or a cutting-edge roboticist. In the future, I will do my best to give back to the world what I have received so far and to be a person who supports others. Thank you for everything.

ResearchAchievements

Related Research Papers

- Shota Miyake, Shunsuke Nagahama, Shigeki Sugano, Performance evaluation of self-healable torque transmission mechanism using phase change of low-melting-point-metal and application to robot joints,Smart Materials and Structures, VOL. 31, NO. 1, Dec. 2021
- Shota Miyake, Shunsuke Nagahama, Shigeki Sugano,Development of self-healing linear actuator unit using thermoplastic resin, International journal of Advanced Robotics, VOL. 33, NO. 23, pp.1235-1247, Apr. 2019
- Shota Miyake, Shunsuke Nagahama, Shigeki Sugano, "Development of a tendon-driven mechanism with liquid circulation system for improving wear resistance", Proceedings of IEEE International Conference on Robotics and Biomimetics 2017, pp.1670-1675, Macau, China, Dec. 2017

Other Research Papers

- Satoshi Hosono, Tamon Miyake, Shota Miyake, Emi Tamaki, Feedback Method of Force Controlled by Electrical Muscle Stimulation Based on Infrared Optical Sensing, Frontiers in Virtual Reality, Vol. 3, Jul 2022

Lectures

- Shota Miyake, Shunsuke Nagahama, Shigeki Sugano, Development of Rotary Clutch using Phase Change of Low Melting Point Metal, The International Chemical Congress of Pacific Basin Societies 2021, Dec. 2021
- 三宅章太・長濱峻介・菅野重樹、低融点金属の相変化を利用したクラッチの伝達力に及ぼす摩擦の影響に関する研究、ロボティクス・メカトロニクス 講演会- 2021 (robomech2021)、Jun. 2021
- 三宅章太・長濱峻介・菅野重樹、誘導加熱による低融点金属の相変化を利用したクラッチの再結合手法の提案，日本機械学会第 26 回関東支部講演会、Mar. 2020
- 三宅章太・長濱峻介・菅野重樹、低融点金属の相変化を用いた回転型クラッチの開発、第 37 日本ロボット学会学術講演会 (RSJ2019)、Sep. 2019

- 三宅章太・長濱峻介・菅野重樹、自己修復機能を有する腱駆動アクチュエータユニットの修復性の向上に関する研究、ロボティクス・メカトロニクス 講演会-2019、 Jun. 2019
- Shota Miyake, Design for applying soft materials to mechanical systems, 1st Workshop on Active Matter for Soft Robotics, Tokyo, Japan, Mar. 2019
- 三宅章太・長濱峻介・菅野重樹、自己修復する腱駆動アクチュエータユニットの開発、第 36 回 日本ロボット学会学術講演会 (RSJ2018)、sep. 2018
- 三宅章太・長濱峻介・菅野重樹、液体循環により耐摩耗性を向上させた腱駆動機構の開発」, 第 18 回 計測自動制御学会システムインテグレーション部門講演会 (SICE SI 2017)、 Dec. 2017
- 三宅章太・長濱峻介・菅野重樹、ワイヤーへの液体潤滑剤の供給機能を有する腱駆動機構の開発、ロボティクス・メカトロニクス 講演会- 2017 (robomech2017)、May 2017